Doctoral Dissertation (Shinshu University)

Geometrical and mechanical analysis of fabric drape

March 2021

YANG, LIU

Table of contents

Table of figures

Table of tables

Chapter 1

General introduction

Chapter 1 General introduction

1.1 Background

“A piece of fabric may be supported in some parts and not supported in other parts. Such a fabric will be subjected to force from the supports and to the force of gravity. The description of the fabric deformation produced by these forces may be called the drape of the fabric.”[1]

The drape of fabric is a physical deformation but lead to the aesthetic recognition of human sense, which resulted that this subject is complicated but interesting to many researchers. The research range today including not only the analysis of the deformation of fabrics in the laboratory, but also the aesthetic evaluation to the garments in my daily life.

The drape of fabric is connected to the drape for garment for the factors such as luster and color. However, the drape of garment is more complicated than the drape for fabric in drape tests because of parameters such seams and ease allowance[2, 3]. Thus, in this present work, the drape is more focused on a narrow range with only the fabric deformation.

In the aspect of the analysis of the deformation of fabrics, the work in this research field starts in 1930s. Peirce[4], Chu et al.[5], and Cusick[1] laid the foundation in this area by proposing methods to evaluate drape quantitatively. Based on their research, many researchers, such as Hearle et al.[6], Morooka and Niwa[7], Postle and Postle[8], and Hu and Chan[9], investigated the relationship between drape and mechanical properties of fabrics. The mechanical properties of fabric, such as bending rigidity and shear stiffness, are usually measured with standardized apparatus such as Kawabata Evaluation System (KES)[10] or Fabric Assurance by Simple Testing (FAST)[11]. According to these researches,

it is found that bending rigidity and shear stiffness are the main mechanical properties affecting fabric drape.

Besides, many researchers focused on the simulation of the drape on computer, which is a highly interesting topic for the fashion industry today. The applicant of garment simulation considering the fabric drape started by Thalmann's group[12, 13]. After the work of them, many developments with consideration of the mechanical properties of fabrics were made to improve the accuracy and the efficiency of simulation of fabric. Some researchers used finite element method with measured or assumed mechanical properties[14-16]. Other researchers used particle method with a spring-mass model by approximating the mechanical properties measured with the standardized apparatus[17-20].

Even though great efforts have been made to drape simulation, some geometrical and mechanical issues on drape, such as the effect of the dimension on drape and the shear deformation on drape, are still unclear. These questions limited the improvement of the accuracy of drape simulation.

This study focused on the geometrical effect of fabric dimension and mechanical effects of bending and shear deformation of fabric as determined by the Fabric Research Laboratories (FRL) drape test[5]. On the one hand, for fabric drape in FRL drape test, an evaluation index called drape coefficient (DC) is used to evaluate the drapability of fabric. A piece of circular fabric is sandwiched by two circular support disks. The radii of the disks are smaller than the fabric's. Holding the combination in horizontal, then the unsupported part of the fabric falls under weight. The DC is then determined by the areas in the projection to the FRL drape. Many researchers investigated the effects mechanical properties of fabric on drape following different testing standards, which use different dimensions. They also used a strip cantilever for calculating drape analytically. However, the effects of dimension on drape were less noted. Because the DC is related to the dimension, there is a necessity to discuss the impact of dimension. Moreover, for a precise numerical simulation of drape, it is necessary to analyze the drape shape with a model considering the uneven shape of drape. On the other hand, it is well-recognized that bending rigidity and shear stiffness affect the drape. For bending rigidity, its effect on drape has been investigated and been analytically discussed. But for shear stiffness, due

to the lack of measurement of shear deformation on FRL drape, its effect on drape is still vague. It is also not clear that how the bending rigidity and shear stiffness jointly affect the drape deformation.

1.2 Purpose of this study

To answer the geometrical and mechanical questions on drape listed above, the objectives of this study are:

1) To clarify the effects of dimension in the drape test and the limits of the fabric DC under various combinations of the fabric and support disk radii

2) To explore the shear deformation on drape in the view of location and degree

3) To explain how the bending and shear properties affect drape

1.3 Thesis outline

In this study, an extensive analysis on geometrical and mechanical properties of fabric drape was conducted.

Chapter 1 introduced the background to this research, as well as the purpose and methodology of this study.

Chapter 2 exposed a literature review of previous studies on the general theories regarding drape and its relationship with the mechanical properties of fabric. Related researches on simulation of drape are also presented and summarized in this chapter.

In Chapter 3, the effects of fabric dimension on drape deformation are analyzed using a model of a circular segment cantilever for infinite shear stiffness (upper limit) and the deflection of strip cantilevers in radial directions for zero shear stiffness (lower limit). The drape shapes are determined by nondimensional parameters K and K' in addition to the parameters m and m', which are given by the ratio of the fabric radius and segment

cantilever length. K and K' are given by the segment cantilever length for the upper limit and by the differences between the radii of the fabric and support disk for the lower limit, with weights, and bending rigidity. Drape coefficient (DC) limits of fabrics are theoretically obtained using the model in three cases according to the relationship of m and m'. Even for different fabrics, the drape shapes are similar for the same m and K, or m' and K' in each case. The effects of dimension on fabric drape are therefore clarified theoretically. Obtained limits are experimentally verified for eight woven fabrics and one sheet.

In Chapter 4, a measuring method of shear deformation in drape using three-dimensional scanning was proposed. Using the proposed method, the local shear angles in FRL drape for various woven fabrics were measured. The effects of the relative positions of the node to the center grainlines that cross at the fabric center, and the bending and shear properties of fabric on the shear angles were investigated.

Finally, the conclusion of this thesis is described in Chapter 5, and the suggestion for future research is also given.

References

1. Cusick GE. *A study of fabric drape*. University of Manchester, Institute of Science and Technology, 1962.

2. Sanad R, Cassidy T, Cheung V, et al. Fabric and Garment Drape Measurement - Part 2. *Journal of Fiber Bioengineering and Informatics* 2013; 6: 1-22. DOI: 10.3993/jfbi03201301.

3. Sanad RA and Cassidy T. Fabric objective measurement and drape. *Textile Progress* 2016; 47: 317-406. DOI: 10.1080/00405167.2015.1117243.

4. Peirce FT. 26—the "Handle" of Cloth as a Measurable Quantity. *Journal of the Textile Institute Transactions* 1930; 21: T377-T416. DOI: 10.1080/19447023008661529.

5. Chu CC, Cummings CL and Teixeira NA. Mechanics of elastic performance of textile materials: Part V: A study of the factors affecting the drape of fabrics—the development of a drape meter. *Textile Research Journal* 1950; 20: 539-548.

6. Hearle JW, Grosberg P and Backer S. *Structural mechanics of fibers, yarns, and fabrics Volume 1*. New York: Wiley-Interscience, 1969.

7. Morooka H and Niwa M. Relation between drape coefficients and mechanical properties of fabrics. *Journal of the Textile Machinery Society of Japan* 1976; 22: 67-73.

8. Postle JR and Postle R. Fabric bending and drape based on objective measurement. *International Journal of Clothing Science and Technology* 1992; 4: 7-15.

9. Hu J and Chan Y-F. Effect of Fabric Mechanical Properties on Drape. *Textile Research Journal* 1998; 68: 57-64. DOI: 10.1177/004051759806800107.

10. Kawabata S. *The standardization and analysis of hand evaluation*. 2nd ed. Osaka: The Textile Machinery Society Japan, 1980.

11. De Boos AG and Tester DH. *SiroFAST: Fabric Assurance By Simple Testing: a system for fabric objective measurement and its application in fabric and garment manufacture*. 1994. CSIRO Division of Wool Technology.

12. Lafleur B, Magnenat-Thalmann N and Thalmann D. Cloth animation with self-collision detection. *Modeling in computer graphics*. Springer, 1991, pp.179-187.

13. Carignan M, Yang Y, Thalmann NM, et al. Dressing animated synthetic actors with complex deformable clothes. *ACM Siggraph Computer Graphics* 1992; 26: 99-104.

14. Imaoka H, Okabe H, Tomiha T, et al. Prediction of three-dimensional shapes of garments from two-dimensional paper patterns. *Sen'i Gakkaishi* 1989; 45: 420-426.

15. Kang TJ and Yu WR. Drape Simulation of Woven Fabric by Using the Finite-element Method. *Journal of the Textile Institute* 1995; 86: 635-648. DOI: 10.1080/00405009508659040.

16. Teng J, Chen S and Hu J. A finite-volume method for deformation analysis of woven fabrics. *International Journal for Numerical Methods in Engineering* 1999; 46: 2061-2098.

17. Breen DE, House DH and Wozny MJ. A particle-based model for simulating the draping behavior of woven cloth. *Textile Research Journal* 1994; 64: 663-685.

18. Mitsui S, Komai D, Dai X, et al. Particle Model Reflecting Non-linearity and Anisotropy of the Mechanical Properties of Cloth and Its Collision and Repulsion Mechanism. *The Journal of the Institute of Image Information and Television Engineers* 2000; 54: 1762-1770. DOI: 10.3169/itej.54.1762.

19. Dai X, Furukawa T, Mitsui S, et al. Drape formation based on geometric constraints and its application to skirt modelling. *International Journal of Clothing Science and Technology* 2001; 13: 23-37. DOI: 10.1108/09556220110384842.

20. Dai X, Li Y and Zhang X. Simulating anisotropic woven fabric deformation with a new particle model. *Textile research journal* 2003; 73: 1091-1099.

Chapter 2

Literature review

Chapter 2 Literature review

2.1 Bending rigidity of fabric

2.1.1 Introduction

Bending rigidity, also called flexural rigidity, is defined as the pure moment required to bend a fixed non-rigid structure by one unit of curvature. It is used to express the resistance to bending deformation in the elastic region.

In theory of strength of materials, common materials such as steel, are considered as elastic, linear, homogeneous, isotropic with a continuum body. The bending deformation of continuum body is usually considered as continuous tensile and in-plane compressive deformation on the cross section. Based on this hypothesis, the Hooke's law to one dimension can be applied. Therefore, the bending rigidity B can be obtained from

$$B = E \cdot I \tag{2.1}$$

where E is Young's modulus, I is the cross-section moment of inertia. The bending rigidity of those materials is usually measured by three-point bending or four-point bending test based on small deformation theory.

However, not like common materials, fabrics are made of a large of fibers that have considerable freedom of motion relative to each other within the fabric structure. Because of the inter-fiber friction associated with the fiber movement[1], fabrics are not continuous, non-linear, and anisotropic. Its deformation is very large with hysteresis phenomenon. These lead to that fabric cannot be treated as a continuum body when analyzing the deformation of fabric. Moreover, the moment of inertia of area I of fabric is impossible

to obtain. Thus, measuring bending rigidity *B* is equivalent to measuring *EI* for fabric. To obtain the bending rigidity of fabric, pure bending test is used.

Peirce's work[2] in 1930 initiated the researches on the measurement of bending rigidity of fabric. He proposed an objective measurement of bending rigidity using a cantilever. This method tests the fabric in pure bending. Besides of the cantilever method, other methods, such as a heart loop method proposed by Peirce[2] and Clark method[3], are conventional methods used for the measurement of fabric bending rigidity. In addition, he also first recognized the importance of the relationship between the moment and curvature of a fabric, which gave a hint for researchers to develop measuring method considering the non-linearity of fabrics.

2.1.2 Measurement of bending rigidity

Conventional methods such as the cantilever method, loop method and Clark method, are based on the fabric deformation under its own weight. A typical commercial instrument based on this principle is Fabric Assurance by Simple Testing (FAST)[4].

Other methods focus on the moment-curvature relationship as shown in Figure 2.1 and measure forces, moments or energy to describe bending deformation of fabric. A typical commercial instrument based on this principle is Kawabata Evaluation System (KES)[5].

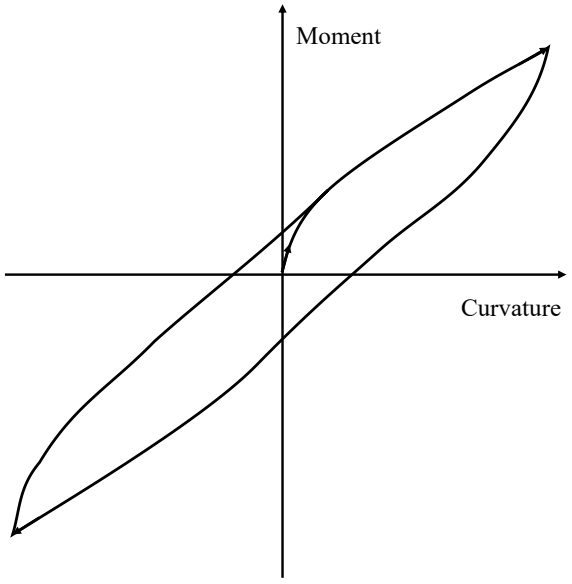

Figure 2.1 A typical moment-curvature relationship of fabric

2.1.2.1 Measuring fabric deformation under its own weight

In the Bernoulli–Euler law for a moment-curvature relationship:

$$\frac{1}{\rho} = -\frac{M}{E \cdot I} \tag{2.2}$$

where ρ is the radius of curvature, M is the bending moment at any point of a cantilever, and $E \cdot I$ is the bending rigidity. Thus, the bending rigidity can be calculated by measuring bending moment and the radius of curvature.

In the work of Peirce[2] to evaluate fabric handle, he introduced the objective measurement of the bending rigidity of woven fabrics using a cantilever as shown in Figure 2.2.

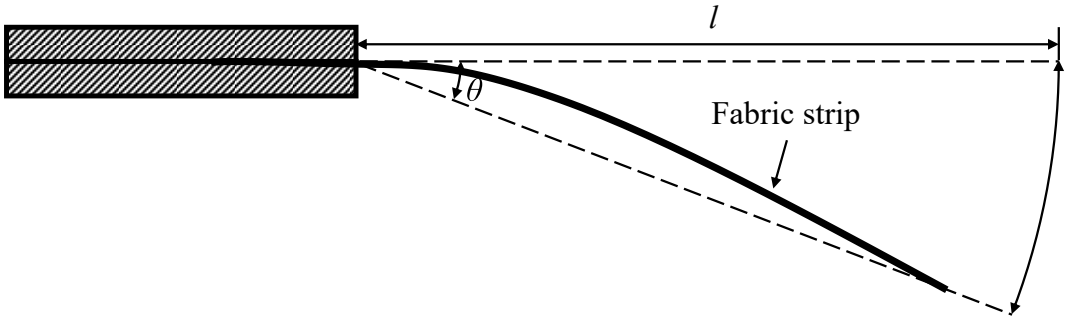

Figure 2.2 Schematic diagram of Peirce's cantilever principle

He introduced bending length c, which refers to the length of fabric that bends under its own weight to a definite extent. The bending length is given as

$$c = l \cdot f_1(\theta) \text{ , where } f_1(\theta) = \left(\frac{\cos\frac{\theta}{2}}{8\tan\theta}\right)^{\frac{1}{3}} \tag{2.3}$$

where l is the overhanging length of fabric, θ is the angle of fabric deflection.

As for the method to obtaining θ, an instrument named Flexometer developed by the British Cotton Industry Research Institution was employed as shown in Figure 2.3. A 1-in.×6 in. fabric strip is prepared. The strip bends under its own weight as a cantilever and is projected to a platform. The angle θ between the horizontal and platform is measured.

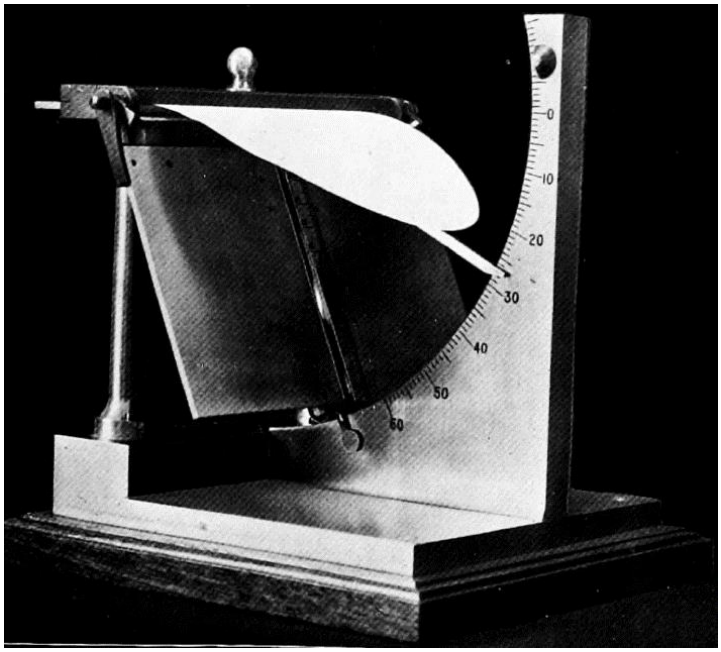

Figure 2.3 Flexometer (Source: Pierce, 1930[2])

Fabric bending rigidity is the bending moment for unit curvature per unit width of strip, and the weight per unit area of the fabric is denoted by w, then the bending rigidity of the fabric can be obtained from.

$$B = w \cdot c^3 \tag{2.4}$$

In 1951, Abbott[6] compared the measuring methods to bending rigidity existing at that time, including cantilever, hear loop, and Schiefer's Flexometer[7] (Another instrument to measure the flexural work, flexural resilience, and bending rigidity. Different from Flexometer mentioned above). The results showed by cantilever and Schiefer's Flexometer are the closet to subjective evaluation. Abbott[8] also pointed out that for cantilever test, when θ was 41°, the bending length c was one-half the fabric length l. With more experiment conducted, researchers found using θ as 41.5° was more accurate than 41°. Then the Administrative Committee on Standard and the American Society for Testing Material[9] accepted using 41.5° cantilever method as preferred method for the measurement to the stiffness of woven fabrics. Shirley stiffness tester (Figure 2.4) was then developed. Not like Flexometer using a fixed sample size and an unfixed angle of deflection, Shirley stiffness tester uses a fixed angle (41.5°) and sample with a fixed width

(1 in.) and an unfixed length.

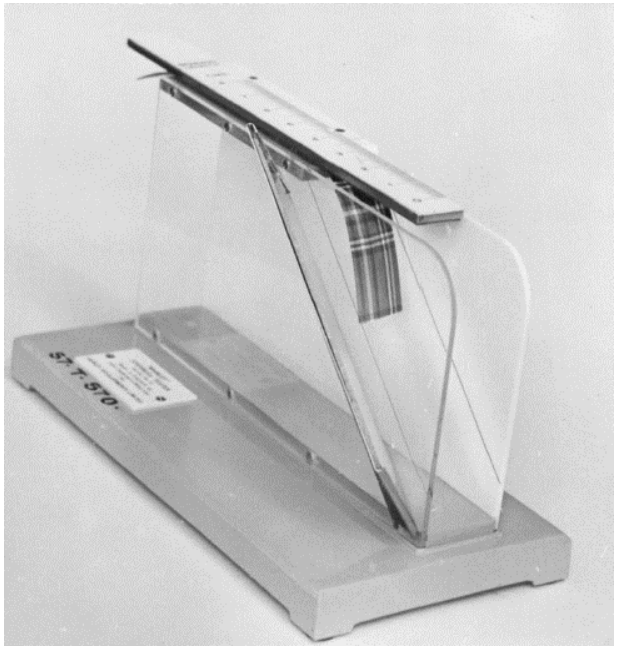

Figure 2.4 Shirley stiffness tester (Source: Cusick, 1965[10])

FAST-2 bending meter[4] follows the same principle of cantilever test. An advanced feature of this instrument is that it shows the measured bending length on its monitor directly.[11]

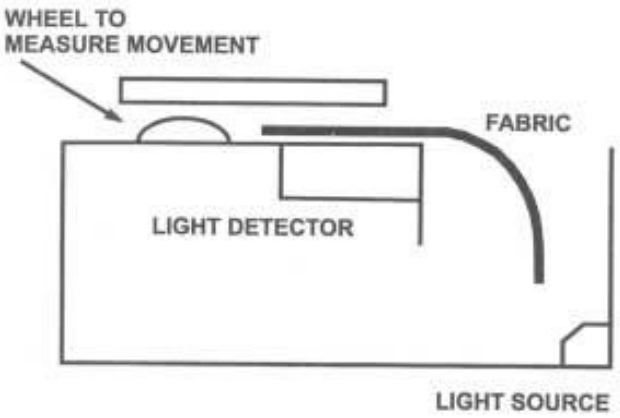

Figure 2.5 Schematic diagram of FAST-2 bending meter (Source: De Boos and Tester, 1994[4])

2.1.2.2 Measuring the moment-curvature relationship in fabric

Inspired by Peirce[2], Eeg-Olofsson[12] proposed an instrument as shown in Figure 2.6 to record moment-curvature relationship of fabric in 1959. The fabric sample is held by two vertical clamps: a fixed clamp C_1 and a clamp C_2 floating on mercury. Then the sample is bent to an arc of circle while recording following a chosen time-schedule the bending moment and the curvature. The bending rigidity of fabric is then obtained directly from the moment-curvature relationship with Equation (2.2).

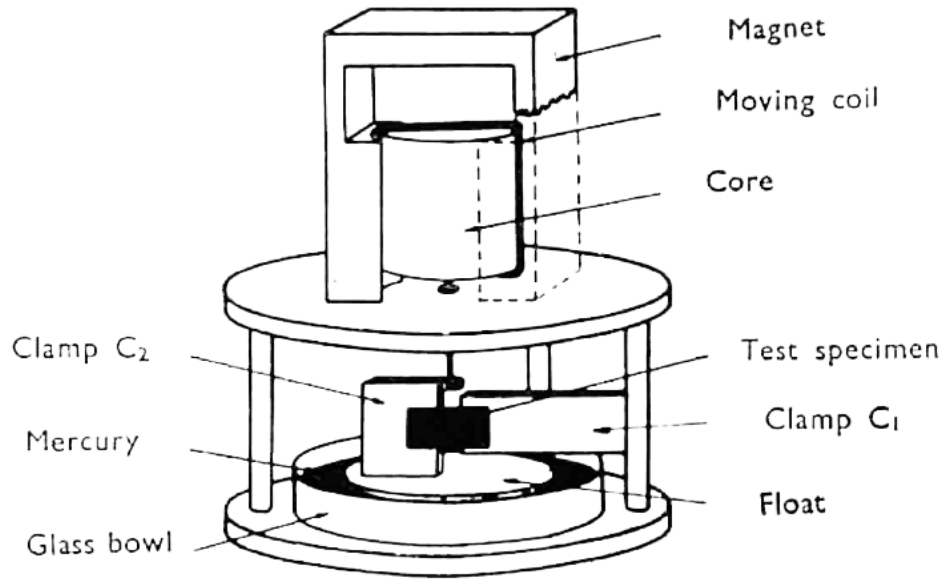

Figure 2.6 Eeg-Olofsson's instrument (Source: Eeg-Olofsson, 1959[12])

Besides, Livesey and Owen[13] proposed a relatively simple mechanism to measure pure bending of very small fabric samples. Owen[14] and Abbott and Grosberg[15] adapted the tester of Livesey and Owen to a tensile tester, which lead that it is possible to obtain the bending-hysteresis relationship directly. Owen[16] further improved his tester with an ability to obtain bending moment and curvature directly.

In 1957, Isshi[17] initially devised a bending tester capable of measuring bending properties of fibers, yarns and fabrics. Isshi's bending tester could be considered as an embryonic model of KES-FB 2.

Figure 2.7 shows the principle of Isshi's bending tester. A fabric sample is mounted by two clamps: a fixed clamp at O and a moving clamp Q with a fixed angle pointer. Both clamps are attached with one torsion spring. A slight ration occurs at the torsion spring of O due to the bending of the sample. However, through a linkage system of the tester, the rotation of the spring at O is revised to be nullified by the other spring. The deflection of the second spring can be recorded and is directly related the bending moment of the clamp.

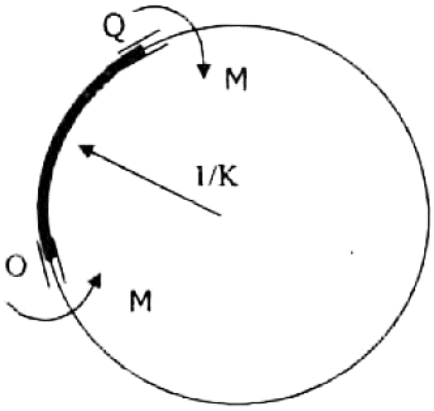

Figure 2.7 Principle of Isshi's bending tester (Source: Ghosh and Zhou, 2003[1])

Popper and Backer[18] modified Isshi's bending tester with a synchronous motor in order to obtain moment-curvature relationship continuously. The moment exerted on the sample is measured by a transducer, the output signal of which is used directly for recording.

KES developed by Kawabata[5] is a widely used commercial measuring instrument for mechanical properties of fabrics. KES-FB 2 pure bending tester is a further modification of Isshi's and Popper and Backer's work and focuses on the measurement of bending properties of fabric. Figure 2.8 shows the measuring principle of KES-FB 2 pure bending tester. Pure bending when the curvatures in the range of -2.5 cm^{-1} ~ 2.5 cm^{-1} is obtained at a constant curvature changing rate of 0.5 cm^{-1} per second. Bending rigidity B is defined as the slope of the moment-curvature for curvature in the range of 0.5 cm^{-1} ~ 1.5 cm^{-1} (B_f) or in the range of -0.5 cm^{-1} ~ -1.5 cm^{-1} (B_b). Another bending property of fabric named bending hysteresis $2HB$, representing the recovery ability of fabric, can also be measured by KES-FB 2. The bending hysteresis $2HB$ is defined as the mean value of the hysteresis width in the range of curvature of 0.5 cm^{-1} ~ 1.5 cm^{-1} ($2HB_f$) or -0.5 cm^{-1} ~ -1.5 cm^{-1}

($2HB_b$).

To summary, the characteristic values from KES-FB 2 are:

B: Bending rigidity per unit length (unit: gf·cm^2·cm^{-1})

2*HB*: Moment of hysteresis per unit length (unit: gf·cm·cm^{-1})

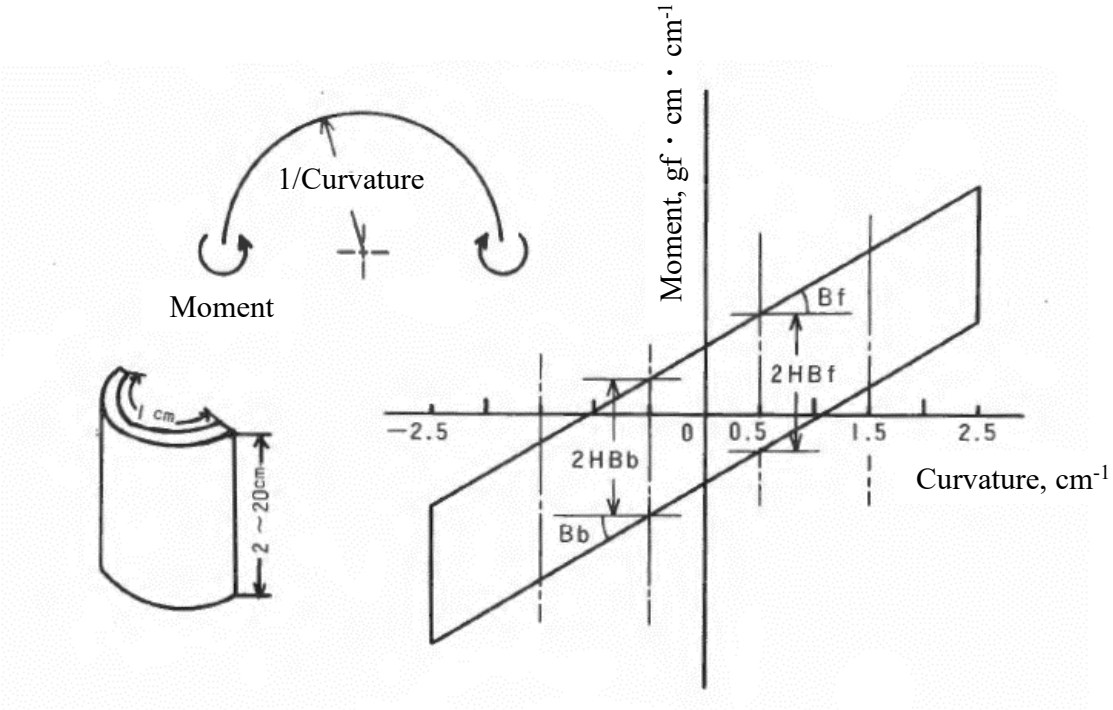

Figure 2.8 KES-FB2 pure bending test method

(Adapted form source: Kawabata, 1980[5])

2.2 Shear property of fabric

2.2.1 Introduction

Together with bending deformation, shear deformation is essential but important in determining the fabric deformation.

The first definition of shear strain is considered to be given by Love[19] and Jagger[20]. Pure shear strain and simple shear strain are two modes of shear deformation of materials. Pure shear strain, as shown in Figure 2.9(a), is the deformation of a body by uniform extension in one direction and contraction in a perpendicular direction, so that its areas remains constant.[21] Simple shear strain, as shown in Figure 2.9(b), is the deformation in which parallel planes in a body remain parallel and maintain a constant distance, while translating relative to each other.

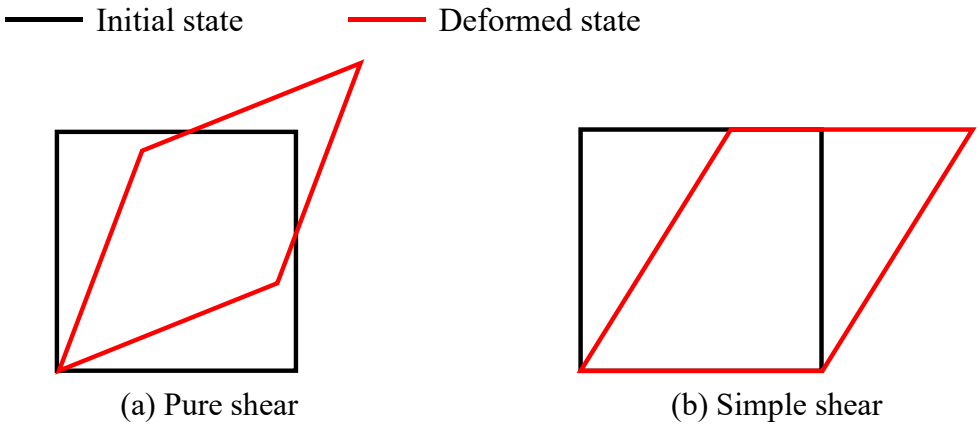

Figure 2.9 Two modes of shear deformation

Shear modulus *S*, or modulus of rigidity, is defined as the ratio of shear stress to the shear strain and used to describe the material's response to shear stress. For common material such as steel, the shear modulus can be obtained from

$$S = \frac{E}{2(1+v)} \tag{2.5}$$

where *S* is the shear modulus, *E* is the young's modulus, and *v* is the Poisson's ratio.

However, fabric presents a more complicated shear deformation and do not behave in this simple manner because of the nonlinearity and anisotropy of fabric. Because of these problems, the above three parameters of fabric are interconnected.

Initiated by Peirce[2], a considerable amount of work has been done for investigating fabric shear. Here most important works are listed. Mack and Taylor[22] suggested that when a fabric is fitted on a surface, the deformation of the fabric can be considered to be composed by shearing angles of warp and weft threads. Lindberg et al.[23] tested various

fabrics in shear and summarized the procedure of shear deformation of fabric: 1) shearing without yarn sliding; 2) shearing with low friction at cross-over points of warp and weft yarns and 3) shearing with the increasing friction. Skelton[24] showed the definition of shear stiffness *G* of fabric as

$$G = \frac{\text{Shearing couple / Unit area}}{\text{Unit shear angle}} = \frac{\text{Force/ Unit length}}{\text{Unit shear angle}} \quad \textbf{(2.6)}$$

Kawabata et al.[25] proposed a linear approximation using a friction resistance item and an elastic resistance item to obtain the relationship between the shear force and shear angle. Comparing with Skelton's complete theoretical analysis, the coefficients in the work of Kawabata et al. were determined by experiments.

Other works of researchers such as Asvadi and Postle[26], Mohammed et al.[27], and Sun and Pan[28] also contributed to the understanding of shear deformation of fabrics. However, most of the researches mentioned above focus on the two-dimensional shear deformation. For three-dimensional (3D) shear deformation of fabric such as drape and wrinkles, it is noted that Amirbayat and Hearle[29] conducted a detailed analysis of formation of three-fold buckling and simulated the complicated deformation in computer.

2.2.2 Measurement of shear property

The experimental approaches to shear behavior of woven fabrics can be characterized as three types: the bias extension test as shown in Figure 2.10 (a), the shear frame test as shown in Figure 2.10 (b), and the KES-FB1 shear test as shown in Figure 2.10 (c).

The bias extension test employs the principle of uniaxial extension (45° direction to the warp) to determine the in-plane shear properties of fabrics. FAST – 3 extensibility meter[4] is also designed following this measuring principle. The measuring procedure is simple and quick so that to be favored by many researchers[30-34]. However, the deformation of the fabric obtained from this approach includes not only shear but also tension, which makes it difficult to isolate pure shear deformation of the fabric.

The shear frame test uses the shearing of a fabric clamped by a square frame hinged at the frame corners. The sample is usually required at a size of 20 cm×20 cm. The picture frame is pulled apart at two corners with a diagonal force at a constant rate in a tensile testing machine[27, 35, 36].

KES-FB1 shear test[5] follows the principle of test methods which were used to testing the shear properties for low shear angles[10, 37-39]. Nowadays, as a representative of these methods, KES-FB 1 is widely used in the textile industry. As shown in Figure 2.11, the fabric sample is prepared with a size of 20 cm ×5 cm and clamped along the two opposite long edges. The clamped edges are moved to generate shear deformation of the fabric. To keep the clamped edges apart, a tension is also applied with 10gf·cm^{-1}. The shear stiffness G in defined as the slope of the obtained F-ϕ curve as shown in Figure 2.11. The shear hysteresis is expressed by two characteristic values: 2HG, the hysteresis at shear angle ϕ=0.5°, and 2HG5, the hysteresis at ϕ=5°.

The relationship among the three tests are investigated by many researchers.[27, 40, 41]. It is found that the pure shear obtained from the shear frame test is higher than the other two methods.

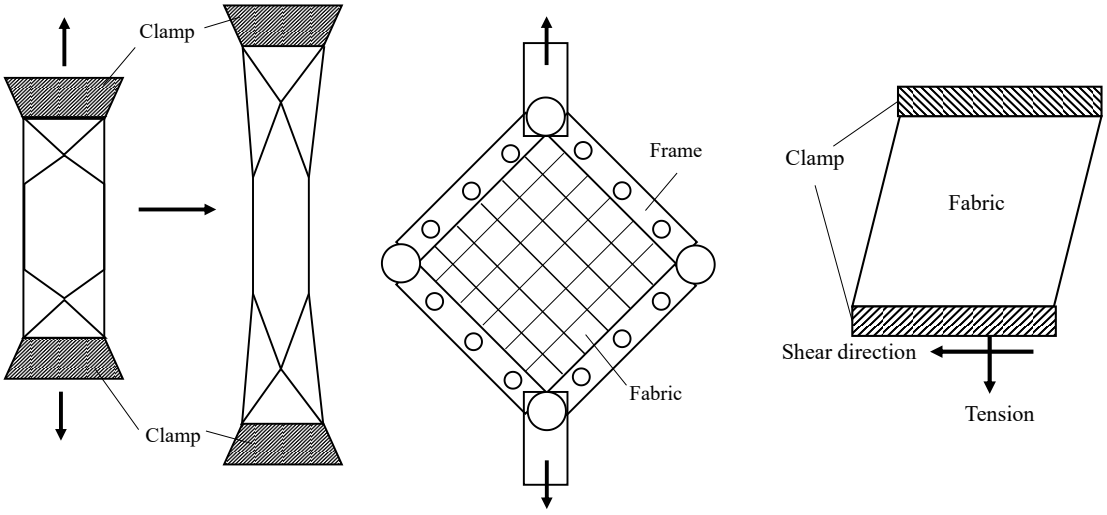

(a) The bias extension test (b) The shear frame test (c) KES-FB1 shear test

Figure 2.10 Three types of shear tests

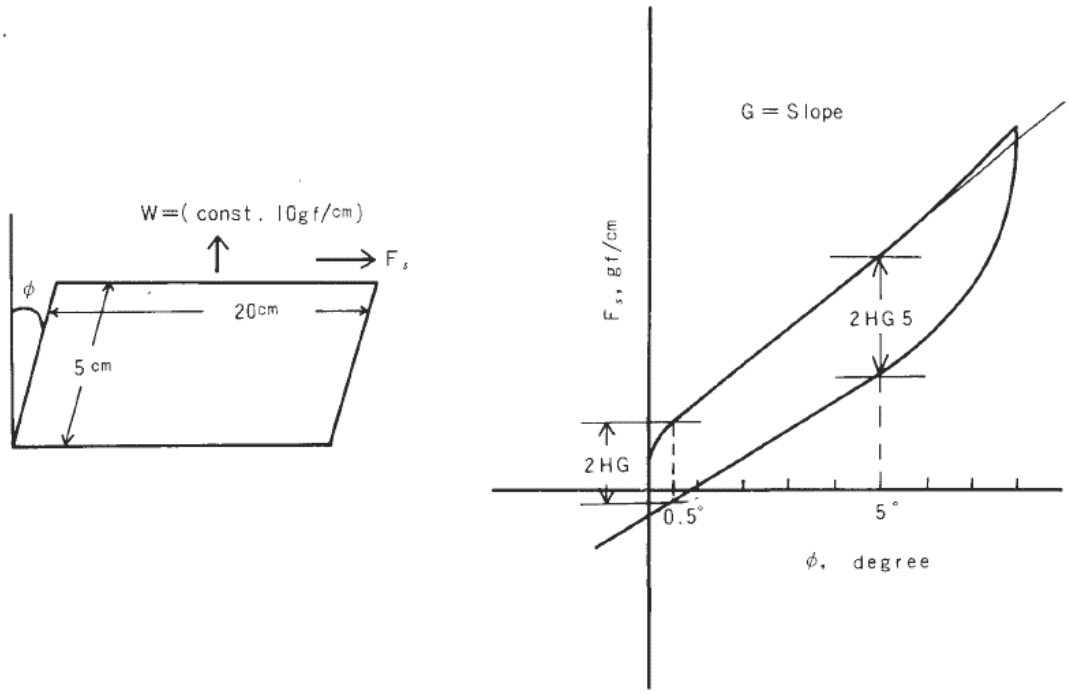

Figure 2.11 KES-FB1 shear test method (Source: Kawabata, 1980[5])

2.3 Drape of fabric

2.3.1 Measurement of drape

The study of drape starts since 1930s. Peirce[2] was one of the pioneers to conduct the initial studies of drape. He connected the fabric handle and the mechanical properties of fabrics, laying the foundation for future research. He also recognized the importance of the objective measurement of fabrics.

After the work of Peirce, Chu et al.[42] were the pioneers who established drape measurements using an Fabric Research Laboratories (FRL) drape meter as shown in Figure 2.12. In their procedure, a fabric is clamped between two disks and then lifted. Under the drape, a light source under the drape is used to obtain the projection shadow of the fabric drape. Then, the projection shadow is captured with a pen. The diameters of the

drape meter are 4 inches (10.16 cm) and 5 inches (12.7 cm) for the discs and 10 inches (25.4 cm) for the circular fabric. They then introduced the drape coefficient (DC), defined as the percentage of the annular-ring area covered by the vertical projection of the draped sample, to compare various drape profiles according to Equation (2.7).

$$\begin{aligned} \text{DC}\ (\%) &= \frac{\text{Vertical projection area of the annular ring of draped fabric}}{\text{Area of the flat annular ring of fabric}} \times 100\% \\ &= \frac{S-\pi r^2}{\pi R^2-\pi r^2} \times 100\% \end{aligned} \tag{2.7}$$

Here S is the area of the shadow, r is the radius of the disks, and R is the radius of the fabric. According to this definition, it is easy to understand that the DC is affected by the radius of the fabric and the support disk, and the projection area of the drape.

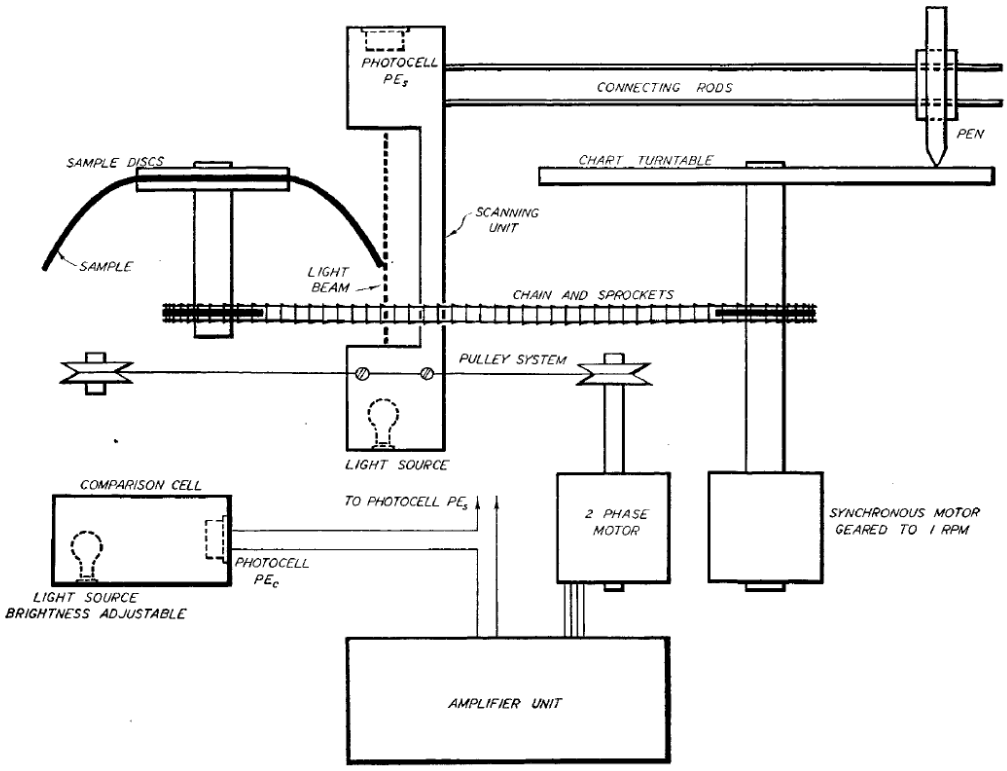

Figure 2.12 Drapemeter of Chu et al. (Source: Chu et al., 1950[42])

Following the research results of Chu et al., Cusick [10, 43] further simplified the drape meter following the same principle of the FRL drape meter as shown in Figure 2.13. A

parallel light source is used to obtain the projection shadow of the drape on a paper ring. Then the projection shape is trace on the paper ring. According to Cusick's method, the definition of DC in Equation (2.7) is rewritten as

$$\text{DC}\ (\%) = \frac{\text{Weight of the paper with traced projection shadow of drape}}{\text{Weight of the paper ring}} \times 100\% \qquad \textbf{(2.8)}$$

By testing a large range of fabrics on different support sizes, Cusick [10, 43] found that the most suitable combination for a drape test is a 15-cm-radius sample and 18-cm-diameter support disk. However, these settings are not suitable for measuring limp fabrics. In 1986, Cusick [44] recommended that a 12-cm-radius fabric and a-18 cm-radius fabric also be used. Today, BS5058[45] follows the rule of Cusick's drape meter and suggests that the DC should be obtained using fabric samples of 15, 12, or 18 cm radius and support discs of 9 cm radius.

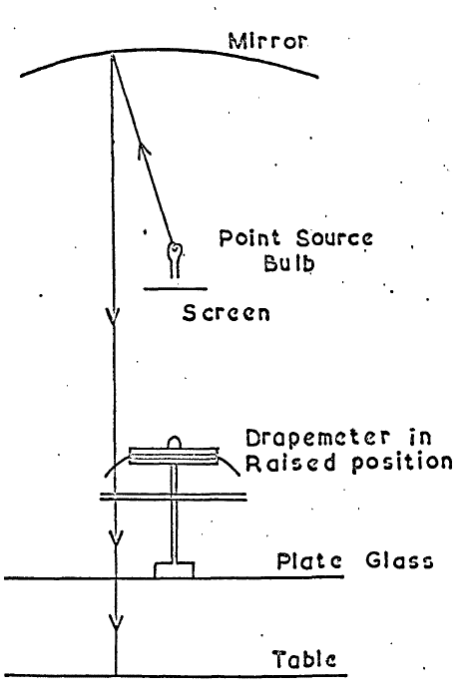

Figure 2.13 Cusick's drapemeter (Source: Cusick, 1965[43])

Collier [46] found that the bending rigidity is the main property affecting the DC for a 5-inch-diameter support disk, while the thickness and bending rigidity affect the DC together for a 3-inch-diameter support disk. JIS L 1096 [47] suggests measuring the DC using a combination of 25.4-cm-diameter samples and 12.7-cm-diameter support disks as

shown in Figure 2.14, following the method of Chu et al.

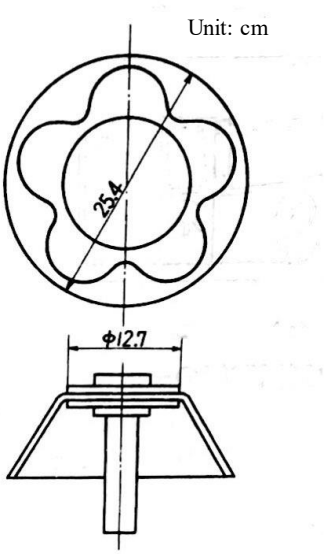

Figure 2.14 Measurement of the DC in JIS L 1096 (Source: JIS L 1096: 2010[47])

In addition to the radius of the fabric and the disks, the number of the node n is also found to be related to the drape[48]. Bhatia and Phadke[49] found that the DC increases as n decreases. Behera and Mishra[50] showed that there is a negative correlation between n and B.

With the development of digital image technologies, researchers[51-53] simplified the calculation of DC by counting the number of pixels of drape in projection photographs rather than weighing the weight of the paper ring. Thus, the definition of DC in Equation (2.7) is can be expressed as

$$\mathrm{DC}\ (\%) = \frac{\dfrac{\text{Total pixels of projected drape area}}{\text{Pixels per cm}^2} - \pi r^2}{\pi R^2 - \pi r^2} \times 100\% \qquad \textbf{(2.9)}$$

Besides the traditional DC, many researchers have used new indicators to describe the fabric drape objectively. Yang and Matsudaira[54-56] defined new dynamic drape coefficients, namely the revolving drape-increase coefficient D_r, the revolving drape coefficient D_r at 200 r/min D_{200}, and the dynamic drape coefficient for swinging motion D_d. Mizutani et al.[57] developed a new instrument for describing the mechanism of drape generation. They also proposed a new indicator determined by the projection shadow of

drape to evaluate the complicity of drape shape. Yu et al.[58] introduced a new indicator called total drape angle (TDA) based on 3D scanned fabric drape. This indicator is determined by the area of draped fabric and the degree of the drape angle. Thus, it is understanded that not only the two-dimensional projected shadow of the drape, but also the 3D drape shape is necessary for the understanding to the drape mechanism.

2.3.2 Effect of mechanical properties of fabric on drape

Many empirical studies proved that the mechanical properties affect the fabric drape.

Chu et al.[48] described the effect of Young's modulus (E) , the cross-section moment of inertia (I), and fabric weight (w) on drape as

$$\mathrm{DC}\ (\%) = f(EI/w) \tag{2.10}$$

where the product of EI is B as mentioned in Equation (2.1).

In addition, the work of Cusick[10, 43] showed that the shear stiffness of fabric also affect the DC in addition to bending properties. He derived a regression equation for predicting DC as

$$\mathrm{DC}\ (\%) = 35.6c - 36.1c^2 - 2.59A + 0.0461A^2 + 17.0 \tag{2.11}$$

where:

c = the bending length measured with the Shirley Stiffness Tester and obtained from

$$c = \frac{1}{4}(c_1 + c_2 + 2\,c_b),$$

where:

c_1 = bending length in the weft direction

c_2 = bending length in the warp direction

c_b = bending length in the 45°-bias direction

A = the shearing angle at a stress of 2 g-wt·cm/cm^2.

Morooka and Niwa[59] measured the DC and mechanical properties of 138 samples of woven fabrics and showed that the value of $(B/w)^{1/3}$ is strongly related with the DC. Niwa and Seto[60] confirmed this result with experimental data for 145 ladies' dress fabrics. Moreover, they proposed a prediction model as

$$\text{DC}(\%) = -22.66+291.8\sqrt[3]{\frac{B}{w}}+387.71\sqrt[3]{\frac{2HB}{w}}-3.71\sqrt[3]{\frac{G}{w}}+30.53\sqrt[3]{\frac{2HG}{w}} \quad \textbf{(2.12)}$$

Collier[46] found that B, G, $2HG$, and $2HG5$ had high correlations with the DC. The work of Jeong[61] and Jeong and Phillip[62] suggested that the variation in drape is determined by the fabric cover factor, fabric structure, shear stiffness, and other mechanical properties. Nagai, Suda and Inagawa [63-68] showed that the FRL drape figures of different fabrics are predicted using a similarity using a non-dimensional parameter $k = l/c$, where l is the fabric length.

Even though many mechanical properties are shown to be related to the drapability of fabric, the bending rigidity and the shear stiffness are recognized as the two main mechanical properties.

2.3.3 Summary

The factors that affect the FRL drape mechanism can be summarized as following:

- The geometrical factors of drape:

  (i) The radius of the fabric and the support disks

  (ii) The projected area of the drape

  (iii) The node number of the drape

  (iv) The 3D shape of the drape

Factor (i) is the input parameter of the drape, which are controllable in the FRL drape test.

Factors (ii), (iii), and (iv) are the output of the drape, which are related to the unmanageable drape shape.

- The mechanical properties of the fabric: bending rigidity and shear stiffness

2.4 Simulation of drape

Since the mechanical properties of fabrics affect the drape, researchers attempted to quantify the effects.

2.4.1 Numerical analysis to drape

For numerical calculation to drape taking into account bending rigidity, in 1937, Bickley[69] first numerically integrated the deflection of Peirce's rectangular cantilever model. He derived the shape of the cantilever of equal length for various angle between the tangent at the end of the overhanging fabric and the horizontal, considering the effect of bending length *c*, which is related to fabric length and bending rigidity. Inspired by his work, Cusick[10] first calculated DC under the conditions of infinite and zero shear stiffness. The conditions for the radius of the fabric and support disks were 15 cm and 9 cm, respectively. However, because of the weight distribution in drape is different, using the deflection of rectangular cantilever can lead to unprecise calculation results. Nevertheless, no additional research using other calculation model to DC after Cusick has been noted.

Since shear stiffness is another property affecting the drape, some researchers focused on analysis of fabric in the view of shear. In the work of Weissenberg[70] and Chadwick et al.[71], a trellis model was described for the analysis of fabric mechanical problems. In this model, the fabric is assumed to be a continuum which is composed of small cells (trellises), consisting of two sets of parallel rigid rods mutually pinpointed where they cross. The cells can expand and contract in certain directions without change in length or form of the rods. By analyzing the relationship of stress-strain in the cells, complicated fabric behavior can be simplified. They also applied this model for analyzing the simple pulls in fabric in various direction including 45° and verified the proposed model by experimental evidence obtained from angle changes of trellises drawn on the fabric samples.

2.4.2 Drape modelling

With the development of information technologies, modelling the drape on computer also raised interests of researchers. One of the methods to model fabric drape is the finite element method (FEM). FEM is the most widely used numerical method solving problems of engineering and mathematical models. The basic idea of FEM is to divide a body into finite elements, reconnect the elements at nodes, and obtain an approximate solution as shown in Figure 2.15[72].

For researchers in textile community, FEM is preferred in the drape simulation since the mechanical properties can be applied for model construction. The first successful trial of drape simulation using FEM could be the work of Imaoka's group. In 1985, Okabe et al.[73, 74] developed a 3D computer-aided-design system for simulation of skirt drape using FEM. Imaoka et al[75] improved the system and managed to simulate garments having different simple styles with drape; e.g., skirts and blouses. As for the simulation for drape of fabric, Collier et al.[76] used a geometric non-linear FEM to predict drape. They treated the fabric as an orthotropic shell membrane. In their model, tensile moduli in the two principal planar direction and Poisson's ratio were required parameters to construct the drape model. Gan et al.[77] used similar FEM to Collier et al. but considered the fabric as orthotropic and linearly elastic. Chen and Govindaraj[78] proposed a FEM model for drape simulation taking into account four measured fabric characteristics: Young's modulus in the warp and weft directions, shear modulus and Poisson's ratio. Kang and Yu[79] calculated drape deformation using the FEM with the measured or estimated tensile and shear modulus, bending rigidity, and Poisson's ratio. Teng et al.[80] and Hu et al.[81] simulated fabric drape behavior over circular pedestals and compared the simulated drape shape with the experimental shape. Even though by using FEM, the drape can be reproduced on computer with fabric mechanical properties, it requires huge and complicated computation. Moreover, it is difficult to integrate large nonlinear deformation and highly variable collisions into finite elements, which reduces the ability of the finite-element model to cope with complicated geometrical problems.

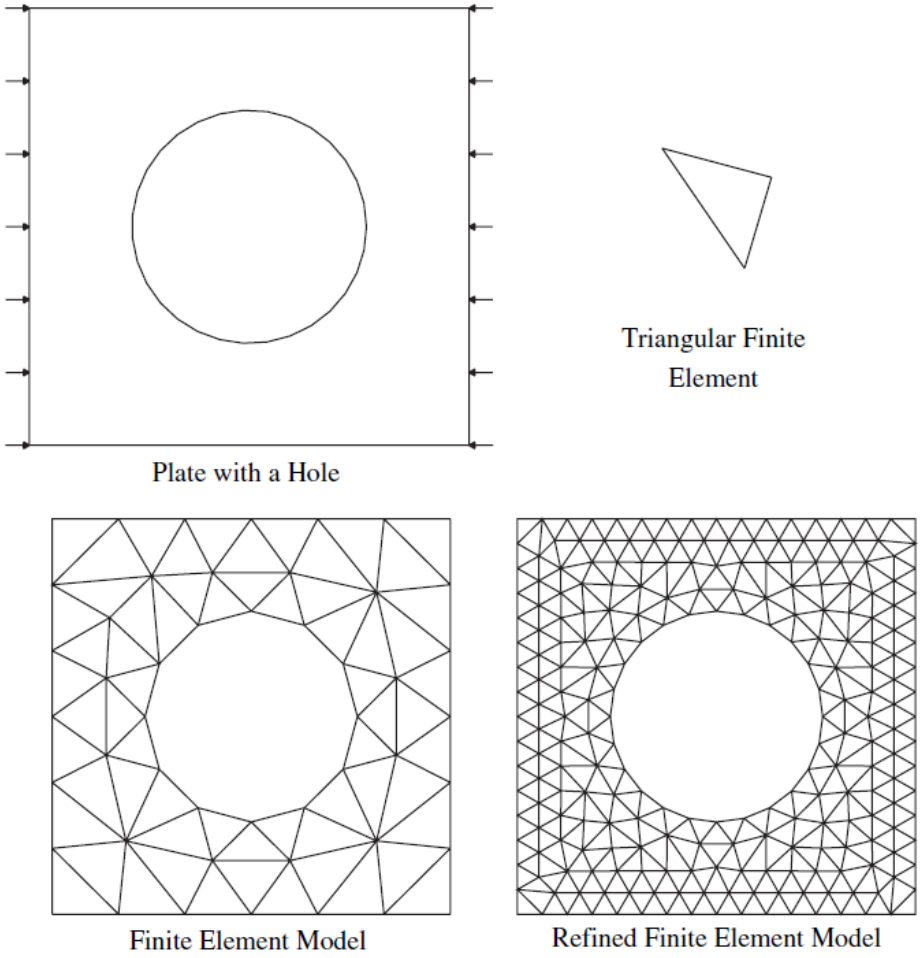

Figure 2.15 Geometry, loads and finite element meshes

(Source: Fish and Belytschko, 2009[72])

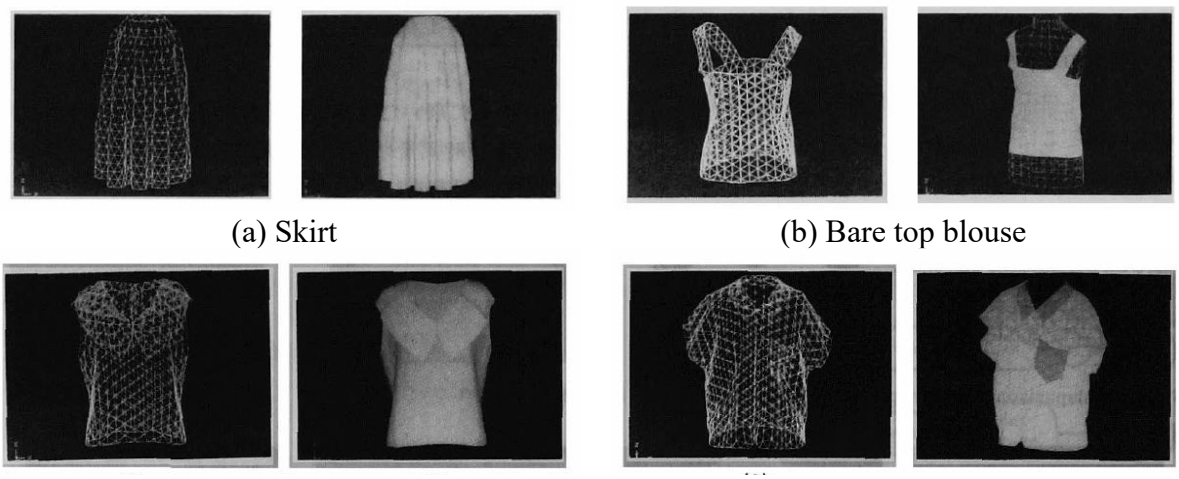

(a) Skirt (b) Bare top blouse

(c) Long collared blouse (d) Short collared blouse with a pocket

Figure 2.16 Garments simulated using the apparel CAD system of Imaoka et al.[75]

Another method called a particle method using a mass-spring model is an easier alternative to simulate fabric drape for modeling and animation. In the particle-spring model as shown in Figure 2.17, particles connected by linear springs to form square elements on the surface. These elements are allowed to have in and out of plane distortion for fabric deformation and the springs are used to simulate the mechanical properties of the fabric[82].

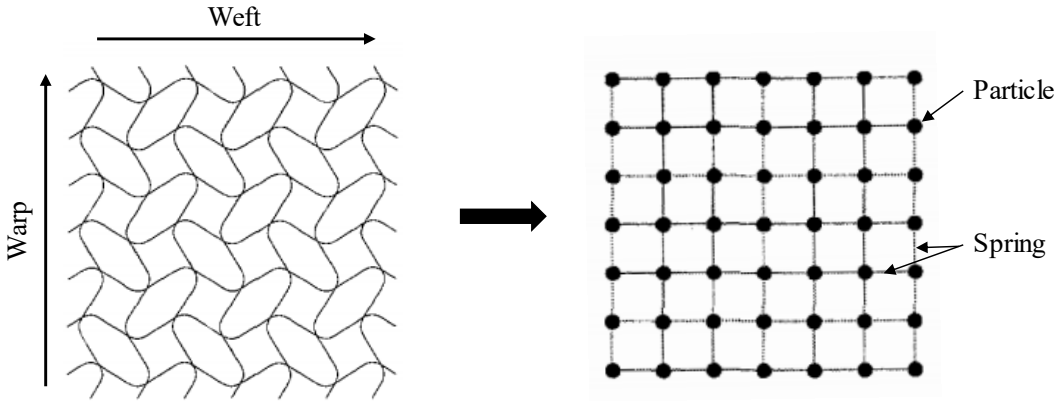

(a) plain weave (b) particle representation

Figure 2.17 Particle representation of a plain weave(Source: Breen et al.[83], 1992)

Weil[84] uses a geometric approach that first approximates the folds in a constrained piece of square cloth with catenary curves. Terzopoulos and Fleischer[85] and Aono[86] created 3D fabric-liked structures that can bend, fold, wrinkle, and tear. Based on the fundamental research, in 1991, Lafleur et al.[87] successfully simulated clothing in animation as shown in Figure 2.18 with the particle model. By now, researchers on computer-graphic community managed to simulate the shape and the complex deformation of the fabric. However, the mechanical properties of fabric itself were not fully considered.

Breen et al.[83, 88, 89] improved the particle method with more accurate drape simulation. They used KES mechanical curves and converted them to necessary energy functions for simulation. Their simulation results showed great similarity to actual drape intuitively as shown in Figure 2.19.

The work of Breen et al. inspired the researchers in both computer-graphic community

and textile community to improve the simulation accuracy. For computer-graphic community, Eberhardt et al.[90] used a Lagrange dynamics reformulation of the basic energy equations in the model of Breen et al., which improved the computation time and making the simulation results more precise. Volino et al.[91] investigated pleating, buckling, and creasing, and developed a set of techniques for solving collisions in the fabric itself, which allowed the simulation of deformable surfaces in various mechanical situations. For textile community, Mitsui et al.[92] improved Breen's particle model by considering the nonlinearity and anisotropy of fabric mechanical properties. A precise collision and repulsion mechanism were included in their model. They compared their results with Breen's method in bending and shear recovering forces. Dai et al.[93, 94] simulated drape considering the bending and shear properties, fabric twist, and force and displacement relationships of various types of deformation. Their results showed agreement for the shape and essential features. In addition to improve the accuracy in the view of mechanical properties of fabrics, Fan et al.[95] proposed a method using a fuzzy-neural network system based on drape images to predict the drape of lady's dress in the view of the drape shape. Comparing with conventional drape simulation methods based on fabric mechanics, this approach enabled to obtain the predicted drape as an image with a very fast computation rate, even though the image was not exactly the actual drape image of the garment.

Figure 2.18 'FlashBack': early virtual garments used context-dependent simulation of simplified cloth models (Source: Volino et al., 2000[96])

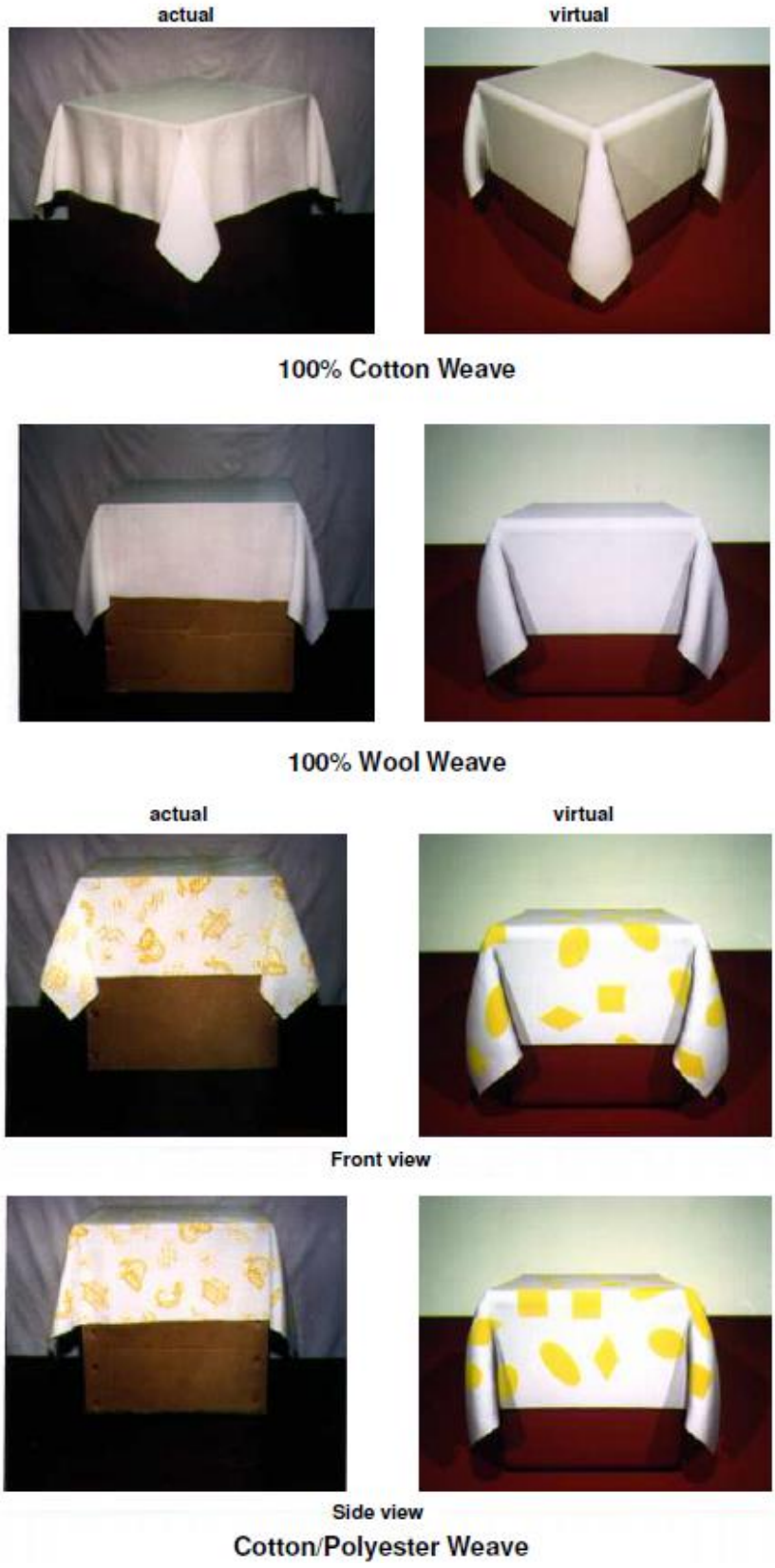

Figure 2.19 The comparison between actual and simulated fabric drape (Source: Breen et al., 1994[88])

2.4.3 Summary

Numerical analysis of drape is a kind of fundamental drape simulation. For bending deformation in drape, cantilever model is a traditional method to calculate the deflection of drape. Bending length, weight, and the fabric length are the parameters for the model construction. For shear deformation in drape, a trellis model is an alternative analyzing method.

Drape modelling in computer can be achieved by two methods: FEM and particle model. FEM is preferred by textile researchers since it based on the strength of textile materials. However, using FEM to simulate drape requires large computation time. Particle model is proposed by computer-graphic researchers. It starts from the idea of simulating the shape of fabric deformation. Even though had been improved by considering the mechanical properties of fabric, the accuracy of the simulation results cannot be evaluated due to the lack of measuring method to the local deformation in 3D drape.

References

1. Ghosh T and Zhou N. Characterization of fabric bending behavior: A review of measurement principles. *Indian Journal of Fibre & Textile Research* 2003; 28: 471-476.

2. Peirce FT. 26—the "Handle" of Cloth as a Measurable Quantity. *Journal of the Textile Institute Transactions* 1930; 21: T377-T416. DOI: 10.1080/19447023008661529.

3. Clark JdA. Determining the rigidity, stiffness, and softness of paper. *Paper Trade J* 1935; 100: 41-44.

4. De Boos AG and Tester DH. *SiroFAST: Fabric Assurance By Simple Testing: a system for fabric objective measurement and its application in fabric and garment manufacture*. 1994. CSIRO Division of Wool Technology.

5. Kawabata S. *The standardization and analysis of hand evaluation*. 2nd ed. Osaka: The Textile Machinery Society Japan, 1980.

6. Abbott NJ. The Measurement of Stiffness in Textile Fabrics. *Textile Research Journal* 1951; 21: 435-441. DOI: 10.1177/004051755102100610.

7. Schiefer HF. The Flexometer:An Instrument for Evaluating the Flexural Properties of Cloth and Similar Materials. *Bureau of Standards Journal of Research* 1933; 10: 647-657. DOI: 10.1177/004051753300300803.

8. Abbott NJ. Part II: A Study of the Peirce Cantilever Test for Stiffness of Textile Fabrics. *Textile Research Journal* 1951; 21: 441-444. DOI: 10.1177/004051755102100611.

9. Standards for Textile Matrials.

10. Cusick GE. *A study of fabric drape*. University of Manchester, Institute of Science and Technology, 1962.

11. Sanad RA and Cassidy T. Fabric objective measurement and drape. *Textile Progress* 2016; 47: 317-406. DOI: 10.1080/00405167.2015.1117243.

12. Eeg-Olofsson T. 7—Some Mechanical Properties of Viscose Rayon Fabrics. *Journal of the Textile Institute Transactions* 1959; 50: T112-T132.

13. Livesey RG and Owen JD. 47—CLOTH STIFFNESS AND HYSTERESIS IN BENDING. *Journal of the Textile Institute Transactions* 1964; 55: T516-T530. DOI: 10.1080/19447026408662430.

14. Owen JD. An Automatic Cloth-bending-hysteresis Tester and Some of its Applications. *Journal of the Textile Institute Transactions* 1966; 57: T435-T438. DOI: 10.1080/19447026608662388.

15. Abbott GM and Grosberg P. Measurement of Fabric Stiffness and Hysteresis in Bending. *Textile Research Journal* 1966; 36: 928-930. DOI: 10.1177/004051756603601012.

16. Owen JD. An Improved Manually Operated Cloth-bending-hysteresis Tester. *The Journal of The Textile Institute* 1967; 58: 589-592. DOI: 10.1080/00405006708659955.

17. Isshi T. Bending Tester for Fibers, Yarns and Fabrics. *Journal of the Textile Machinery Society of Japan* 1957; 3: 48-52. DOI: 10.4188/jte1955.3.2_48.

18. Popper P and Backer S. Letters to the Editor are brief communications intended to provide prompt publication of significant research results and to permit an exchange of views on papers previously published in the Journal. Letters are not submitted to formal review, and the authors assume full responsibility for information given or opinion expressed. Instrument for Measuring Bending-Moment Curvature Relationships in Textile Materials. *Textile Research Journal* 1968; 38: 870-873. DOI: 10.1177/004051756803800811.

19. Love A. A Treatise on the Mathematical Theory. *Elasticity, 4th Ed, Cambridge* 1927.

20. Jaeger J. Elasticity, Fracture and Flow, 152. *Methuen, New York* 1956.

21. Hearle JW, Grosberg P and Backer S. *Structural mechanics of fibers, yarns, and fabrics Volume 1*. New York: Wiley-Interscience, 1969.

22. Mack C and Taylor H. 39—the fitting of woven cloth to surfaces. *Journal of the Textile institute Transactions* 1956; 47: T477-T488.

23. Lindberg J, Behre B and Dahlberg B. Part III: Shearing and Buckling of Various Commercial Fabrics. *Textile Research Journal* 1961; 31: 99-122. DOI: 10.1177/004051756103100203.

24. Skelton J. Fundamentals of Fabric Shear. *Textile Research Journal* 1976; 46: 862-869. DOI: 10.1177/004051757604601202.

25. Kawabata S, Niwa M and Kawai H. 5—THE FINITE-DEFORMATION THEORY OF PLAIN-WEAVE FABRICS. PART III: THE SHEAR-DEFORMATION THEORY. *The Journal of The Textile Institute* 1973; 64: 62-85. DOI: 10.1080/00405007308630418.

26. Asvadi S and Postle R. An Analysis of Fabric Large Strain Shear Behavior Using Linear Viscoelasticity Theory. *Textile Research Journal* 1994; 64: 208-214. DOI: 10.1177/004051759406400404.

27. Mohammed U, Lekakou, C., Dong, L., & Bader, M. G. Shear deformation and micromechanics of woven fabrics. *Composites Part A: Applied Science and Manufacturing* 2000; 31: 299-308.

28. Sun H and Pan N. Shear deformation analysis for woven fabrics. *Composite Structures* 2005; 67: 317-322. DOI: 10.1016/j.compstruct.2004.01.013.

29. Amirbayat J and Hearle JWS. The Anatomy of Buckling of Textile Fabrics: Drape and Conformability. *The Journal of The Textile Institute* 1989; 80: 51-70. DOI: 10.1080/00405008908659185.

30. Buckenham P. Bias-extension Measurements on Woven Fabrics. *Journal of the Textile Institute* 1997; 88: 33-40. DOI: 10.1080/00405009708658527.

31. Potter K. Bias extension measurements on cross-plied unidirectional prepreg. *Composites Part A: Applied Science and Manufacturing* 2002; 33: 63-73. DOI: https://doi.org/10.1016/S1359-835X(01)00057-4.

32. Sang-Song L. Using the FAST system to establish translation equations for the drape coefficient. *Indian Journal of Fibre&Textile Research* 2003; 28: 270-274.

33. Zhao X, Liu G, Gong M, et al. Effect of tackification on in-plane shear behaviours of biaxial woven fabrics in bias extension test: Experiments and finite element modeling. *Composites Science and Technology* 2018; 159: 33-41. DOI: 10.1016/j.compscitech.2018.02.016.

34. Büyükbayraktar RB. An investigation on shear properties of woven fabrics by bias-extension test. *The Journal of The Textile Institute* 2020: 1-9. DOI: 10.1080/00405000.2020.1770011.

35. Peng XQ and Cao J. A continuum mechanics-based non-orthogonal constitutive model for woven composite fabrics. *Composites Part A: Applied Science and Manufacturing* 2005; 36: 859-874. DOI: https://doi.org/10.1016/j.compositesa.2004.08.008.

36. El Abed B, Msahli S, Bel Hadj Salah H, et al. Study of woven fabric shear behaviour. *Journal of the Textile Institute* 2011; 102: 322-331. DOI: 10.1080/00405001003771226.

37. Mörner B and Eeg-Olofsson T. Measurement of the Shearing Properties of Fabrics. *Textile Research Journal* 1957; 27: 611-615. DOI: 10.1177/004051755702700803.

38. Behre B. Mechanical Properties of Textile Fabrics Part I: Shearing. *Textile Research Journal* 1961; 31: 87-93. DOI: 10.1177/004051756103100201.

39. Treloar LRG. 42—THE EFFECT OF TEST-PIECE DIMENSIONS ON THE BEHAVIOUR OF FABRICS IN SHEAR. *Journal of the Textile Institute Transactions* 1965; 56: T533-T550. DOI: 10.1080/19447026508662313.

40. Lebrun G, Bureau MN and Denault J. Evaluation of bias-extension and picture-frame test methods for the measurement of intraply shear properties of PP/glass commingled fabrics. *Composite Structures* 2003; 61: 341-352. DOI: https://doi.org/10.1016/S0263-8223(03)00057-6.

41. Taha I, Abdin Y and Ebeid S. Comparison of picture frame and Bias-Extension tests for the characterization of shear behaviour in natural fibre woven fabrics. *Fibers and Polymers* 2013; 14: 338-344. DOI: 10.1007/s12221-013-0338-6.

42. Chu CC, Cummings CL and Teixeira NA. Mechanics of elastic performance of textile materials: Part V: A study of the factors affecting the drape of fabrics—the development of a drape meter. *Textile Research Journal* 1950; 20: 539-548.

43. Cusick GE. 46—the Dependence of Fabric Drape on Bending and Shear Stiffness. *Journal of the Textile Institute Transactions* 1965; 56: T596-T606. DOI: 10.1080/19447026508662319.

44. Cusick GE. 21—the Measurement of Fabric Drape. *Journal of the Textile Institute* 1968; 59: 253-260. DOI: 10.1080/00405006808659985.

45. BS 5058: 1973: Method for the assessment of drape of fabrics.

46. Collier BJ. Measurement of Fabric Drape and its relation to fabric mechanical properties and subjective evaluation. *Clothing and Textiles Research Journal* 1991; 10: 46-52.

47. JIS L 1096: 2010 Testing methods for woven and knitted fabrics.

48. Chu CC, Platt MM and Hamburger WJ. Investigation of the factors affecting the drapeability of fabrics. *Textile Research Journal* 1960; 30: 66-67.

49. Bhatia R and Phadke S. Influence of drape properties on clothing styles. 2005; 65: 283-286.

50. Behera BK and Mishra R. Fabric drape and mechanical properties. 2006; 37: 43-49.

51. Kenkare N and May-Plumlee T. Fabric drape measurement: A modified method using digital image processing. *Journal of Textile and Apparel, Technology and Management* 2005; 4: 1-8.

52. Behera BK and Mishra R. Objective measurement of fabric appearance using digital image processing. *Journal of the Textile Institute* 2006; 97: 147-153. DOI: 10.1533/joti.2005.0150.

53. Behera B and Pattanayak AK. Measurement and modeling of drape using digital image processing. *Indian Journal of Fibre & Textile Research* 2008; 33: 230-238.

54. Yang M and Matsudaira M. Measurement of Drape Coefficients of Fabrics and Description of Hanging Shapes of Fabrics. *Sen'i Kikai Gakkaishi* 1998; 51: T182-T191.

55. Matsudaira M and Yang M. Measurement of Drape Coefficients of Fabrics and Description of Hanged Shapes of Fabrics. *Sen'i Kikai Gakkaishi* 1997; 50: T242-T250.

56. Matsudaira M and Yang M. Some Features of the Static and Dynamic Drape Behaviour of Polyester-fibre Shingosen Fabrics. *Journal of the Textile Institute* 2000; 91: 600-615. DOI: 10.1080/00405000008659131.

57. Mizutani C, Amano T and Sakaguchi Y. A new apparatus for the study of fabric drape. *Textile Research Journal* 2005; 75: 81-87. DOI: 10.1177/004051750507500115.

58. Yu Z, Zhong Y, Gong RH, et al. New indicators on fabric drape evaluation based on three-dimensional model. *Textile Research Journal* 2019; 90: 1291-1300. DOI: 10.1177/0040517519888669.

59. Morooka H and Niwa M. Relation between drape coefficients and mechanical

properties of fabrics. *Journal of the Textile Machinery Society of Japan* 1976; 22: 67-73.

60. Niwa M and Seto F. Relationship between Drapability and Mechanical Properties of Fabrics. *Sen'i Kikai Gakkaishi* 1986; 39: T161-T168.

61. Jeong YJ. A Study of Fabric-drape Behaviour with Image Analysis Part I: Measurement, Characterisation, and Instability. *Journal of the Textile Institute* 1998; 89: 59-69. DOI: 10.1080/00405009808658597.

62. Jeong YJ and Phillips DG. A Study of Fabric-drape Behaviour with Image Analysis. Part II: The Effects of Fabric Structure and Mechanical Properties on Fabric Drape. *Journal of the Textile Institute* 1998; 89: 70-79. DOI: 10.1080/00405009808658598.

63. Nagai S, Suda N and Inagaki K. A Study on the Similarity Rule of F.R.L. Draped Figures for Fabrics. *Journal of the Japan Reseach Association for textile end-uses* 1998; 39: 181-187.

64. Nagai S, Suda N and Inagaki K. An Analysis of F.R.L. Draped Figures for Sheets by Using the Similarity Rule. *J Jpn Res Assoc Text End-Uses* 1999; 40: 738-743.

65. Nagai S, Suda N and Inagaki K. Similarity Rule of F.R.L. Draped Figures for Sheets with the Torsional Deformation. *J Jpn Res Assoc Text End-Uses* 2001; 42: 520-526.

66. Nagai S, Suda N and Inagaki K. An Estimation of the F.R.L. Draped Figures for Sheets by Using the π-number of the Similarity Rule. *J Jpn Res Assoc Text End-Uses* 2005; 46: 175-183.

67. Nagai S, Suda N and Inagaki K. Evaluation Method of the FRL Draped Figures-In the case of isotropic sheets. *J Jpn Res Assoc Text End-Uses* 2006; 47: 163-170.

68. Nagai S, Suda N and Inagaki K. Applicability of the Evaluation Method of Isotropic Sheets Drapability to That of Textile Fabrics. *J Jpn Res Assoc Text End-Uses* 2008; 49: 413-420.

69. Bickley WG. L.The heavy elastica. *The London, Edinburgh, and Dublin Philosophical Magazine and Journal of Science* 1934; 17: 603-622. DOI: 10.1080/14786443409462419.

70. Weissenberg K. 5—the Use of a Trellis Model in the Mechanics of Homogeneous Materials. *Journal of the Textile Institute Transactions* 1949; 40: T89-T110. DOI: 10.1080/19447024908659443.

71. Chadwick GE, Shorter SA and Weissenberg K. 6—a Trellis Model for the Application and Study of Simple Pulls in Textile Materials. *Journal of the Textile Institute Transactions* 1949; 40: T111-T160. DOI: 10.1080/19447024908659444.

72. Fish J and Belytschko T. *A First Course in Finite Elements*. Great Britain: Wiley, 2007.

73. Okabe H, Imaoka H and Akami H. Ifuku no tame no sanjigen CAD shisutemu

(Three-dimensional CAD system for apparel). *Journal of the Japan Society of Precision Engineering* 1985; 51: 512-515. DOI: 10.2493/jjspe1933.51.512.

74. Okabe H, Imaoka H and Akami H. PAPER PATTERNS OF DRESS FOR 3-DIMENSIONAL CAD/CAM AND THEIR AUTOMATICAL DIVISION INTO FINITE ELEMENTS. *Sen'i Gakkaishi* 1986; 42: T231-T239. DOI: 10.2115/fiber.42.4_T231.

75. Imaoka H, Okabe H, Tomiha T, et al. Prediction of three-dimensional shapes of garments from two-dimensional paper patterns. *Sen'i Gakkaishi* 1989; 45: 420-426.

76. Collier JR, Collier BJ, O'Toole G, et al. Drape Prediction by Means of Finite-element Analysis. *Journal of the Textile Institute* 1991; 82: 96-107. DOI: 10.1080/00405009108658741.

77. Gan L, Ly NG and Steven GP. A Study of Fabric Deformation Using Nonlinear Finite Elements. *Textile Research Journal* 1995; 65: 660-668. DOI: 10.1177/004051759506501106.

78. Chen B and Govindaraj M. A Physically Based Model of Fabric Drape Using Flexible Shell Theory. *Textile Research Journal* 1995; 65: 324-330. DOI: 10.1177/004051759506500603.

79. Kang TJ and Yu WR. Drape Simulation of Woven Fabric by Using the Finite-element Method. *Journal of the Textile Institute* 1995; 86: 635-648. DOI: 10.1080/00405009508659040.

80. Teng J, Chen S and Hu J. A finite-volume method for deformation analysis of woven fabrics. *International Journal for Numerical Methods in Engineering* 1999; 46: 2061-2098.

81. Hu J, Chen S-F and Teng JG. Numerical Drape Behavior of Circular Fabric Sheets Over Circular Pedestals. *Textile Research Journal* 2000; 70: 593-603. DOI: 10.1177/004051750007000706.

82. Eischen JW and Bigliani R. Continuum versus Particle Representations. In: House DH and Breen DE (eds) *Cloth Modeling an Animation*. Natick, MA: A K Peters, 2000, pp.92.

83. Breen DE, House DH and Getto PH. A physically-based particle model of woven cloth. *The Visual Computer* 1992; 8: 264-277.

84. Weil J. The synthesis of cloth objects. *ACM Siggraph Computer Graphics* 1986; 20: 49-54.

85. Terzopoulos D and Fleischer K. Modeling inelastic deformation: viscolelasticity, plasticity, fracture. In: *ACM Siggraph Computer Graphics* 1988, pp.269-278. ACM.

86. Aono M. A wrinkle propagation model for cloth. In: *Proceedings of the eighth international conference of the Computer Graphics Society on CG International* 1990, pp.95-115.

87. Lafleur B, Magnenat-Thalmann N and Thalmann D. Cloth animation with self-

collision detection. *Modeling in computer graphics*. Springer, 1991, pp.179-187.

88. Breen DE, House DH and Wozny MJ. A particle-based model for simulating the draping behavior of woven cloth. *Textile Research Journal* 1994; 64: 663-685.

89. Breen DE, House DH and Wozny MJ. Predicting the drape of woven cloth using interacting particles. In: *Proceedings of the 21st annual conference on Computer graphics and interactive techniques* 1994, pp.365-372.

90. Eberhardt B, Weber A and Strasser W. A fast, flexible, particle-system model for cloth draping. *IEEE Computer Graphics and Applications* 1996; 16: 52-59.

91. Volino P, Courchesne M and Magnenat Thalmann N. Versatile and efficient techniques for simulating cloth and other deformable objects. In: *Proceedings of the 22nd annual conference on Computer graphics and interactive techniques* 1995, pp.137-144. ACM.

92. Mitsui S, Komai D, Dai X, et al. Particle Model Reflecting Non-linearity and Anisotropy of the Mechanical Properties of Cloth and Its Collision and Repulsion Mechanism. *The Journal of the Institute of Image Information and Television Engineers* 2000; 54: 1762-1770. DOI: 10.3169/itej.54.1762.

93. Dai X, Furukawa T, Mitsui S, et al. Drape formation based on geometric constraints and its application to skirt modelling. *International Journal of Clothing Science and Technology* 2001; 13: 23-37. DOI: 10.1108/09556220110384842.

94. Dai X, Li Y and Zhang X. Simulating anisotropic woven fabric deformation with a new particle model. *Textile research journal* 2003; 73: 1091-1099.

95. Fan J, Newton E, Au R, et al. Predicting Garment Drape with a Fuzzy-Neural Network. *Textile Research Journal* 2001; 71: 605-608. DOI: 10.1177/004051750107100706.

96. Volino P, Cordier F and Magnenat-Thalmann N. From early virtual garment simulation to interactive fashion design. *Computer-Aided Design* 2005; 37: 593-608. DOI: 10.1016/j.cad.2004.09.003.

Chapter 3

Effect of fabric dimension on limits of the drape coefficient

Chapter 3 Effect of fabric dimension on limits of the drape coefficient

3.1 Introduction

Fabric drape is an important factor to consider when selecting fabrics for clothing design. Drape is a complex deformation resulting from gravity and the mechanical properties of the fabric. The drape coefficient (DC) was proposed by Chu et. al.[1] is standardized by a drape meter in Fabric Research Laboratories (FRL) drape tests, and is widely used in evaluating fabric drapability[2-4]. The DC is defined as the ratio of the projected area of a circular fabric before and after draping:

$$\text{DC}\ (\%)= \frac{A_d - S_2}{S_1 - S_2} \times 100\%, \tag{3.1}$$

where S_1 and A_d are respectively the areas of the projected shadow of the fabric sample before and after draping and S_2 is the area of the support disk in the drape test. In the FRL drape test, the sample radius (R) is 5 inches (12.7 cm) and the radius of the support disc (r) is either 2 inches (5.08 cm) or 2.5 inches (6.35 cm). Cusick[5] proposed using r of 9 cm and R of 12 and 18 cm instead of R of 15 cm when measuring the DCs of very stiff and very limp fabrics with the FRL drape meter. Today, the British Standard (BS5058)[3] and International Organization for Standardization (ISO 9073-9:2008)[4] use Cusick's method. Meanwhile, R is 12.7 cm and r is half of R in the Japanese Industrial Standard (JIS) L 1096 drape test[2].

To obtain the DC efficiently, digital image analysis of the DC has been developed[6-9]. Many other indicators for drapability have been introduced for the evaluation of drape[10]. In addition, garments have been simulated for the quantitative assessment of fabric

drapability[11-13] and garment drape[12, 14-17]. However, the principle of measuring drapability has not changed and the DC is still the most widely used indicator.

Fabric structural properties affect the drapability of fabric. The relationship between structural properties and fabric mechanical properties has been studied by many researchers, such as Hearle et al[18], Hearle and Shanahan[19], and Zheng et al.[20]. Fabric structural properties affect the mechanical properties of fabric, such as bending, shearing, and anisotropy. Those mechanical properties affect the fabric drape. Thus, investigating drape deformation using the mechanical properties instead of using yarn and structural properties is more practical[21].

Many studies[5, 22-25] have investigated the effects of mechanical properties of the fabric on the DC. In experimental analysis, Collier[22] found that the bending rigidity is the main property affecting the DC for a 5-inch-diameter (12.7-cm-diameter) support disk, while the thickness and bending rigidity together affect the DC for a 3-inch-diameter (7.62-cm-diameter) support disk. Morooka and Niwa[23] and Niwa and Seto[24] investigated relationships of mechanical properties of the fabric and the DC by measuring the DC following JIS procedures[26] while Hu and Chan[25] investigated the relationships by measuring the DC following BS 5058 procedures[27]. They showed that the bending and shear properties are major factors determining the DC and obtained experimental relationships between the mechanical properties and DC. However, they did not present a theoretical analysis or consider the effects of dimensions. In theoretical analysis, Cusick[5, 28, 29] studied the mechanism of fabric drape taking into account the shear effect in addition to bending. Cusick[28] investigated the DC for zero and infinite shear stiffness with specified dimensions of r = 9 cm and R = 15 cm. The limits of the DC are derived with these values of stiffness. Moreover, Cusick[28] presented the relationship among the bending length, c, and the DC limits for different node numbers of drape under specified dimensions. However, Cusick did not discuss the effects of dimensions on the limits of the DC.

Dimensions affect the DC because the DC is a ratio of areas. Table 3.1 summarizes the various dimensions used in previous research. Although many studies investigated the relationships between mechanical properties and the DC, they did not mention the effects

of dimensions on the DC. It is thus necessary to discuss the effects of dimensions on DC. If the DC using single or a few of parameters that includes the dimensional effect can be predicted, it will help unify the results of drape test with various dimensions. It will also benefit the simulation of fabric drape for different dimensions. To express the DC with as few independent variables as possible, a theoretical relationship between the DC and fabric mechanical properties and dimension is analyzed.

Peirce[30] defined the bending length (c) in a fabric cantilever test as $(B/w')^{1/3}$, where B is the bending rigidity for the unit width and w' is the weight per unit area of the fabric strip. In a cantilever test, the dimension effect has been incorporated into a nondimensional parameter k [31, 32] as

$$k = \frac{l}{c} = l \cdot \sqrt[3]{\frac{w'}{B}}, \tag{3.2}$$

where l is the fabric length. For the same value of k, cantilevers of different fabrics have similar bending shapes. However, because fabric drape has a circular shape in contrast to the cantilever, it is necessary to introduce a new parameter for fabric drape theoretically. If a similarity rule using this parameter for the fabric drape is found, the DCs for different dimensions can be predicted. A similarity rule for the FRL drape test using k was investigated by Nagai et al.[33-35]. They conducted a drape test while changing the dimensions but keeping the ratio of R and r at 2. They experimentally showed that fabrics with the same k values had similar drape forms and that the shear modulus affects the drape form in the case of the same k. However, they did not present a theoretical analysis and did not show the relationship between k and the limits of the DC. The relationship of k and the limits of the DC will help clarify how drape changes in response to a dimensional change and the mechanism of drape. It is therefore necessary to investigate the limits of the DC for different dimensions of fabrics taking into account the effects of shear.

The present paper, as a detailed investigation on fabric drape, aims to clarify the effects of dimension in drape test and the limits of the fabric DC under various combinations of the fabric and support disk radii. A theory of the DC limit taking into account bending, weight, and fabric dimensions for infinite and zero shear stiffness, which can be

analytically obtained, is proposed.

The theoretical limits are verified with experimental results obtained for eight fabric drapes and one sheet having different dimensions. The present study is a basic theoretical investigation of the mechanism of drape and its findings will benefit the further investigation of drape deformation.

Table 3.1 Dimensions of FRL drape tests and those pros and cons

Developer/ Researcher	Radii in the FRL drape test		Achievement	Pros	Cons
	R (cm)	*r* (cm)			
BS5058 ISO 9073-9:2008	12, 15, and 18	9	Standardized Cusick (1968)'s proposal	Widely used	Compatibility for other dimensions is unknown
JIS L 1096	12.7	6.35	Standardized Chu et al.'s proposal	Widely used	Compatibility for other dimensions is unknown
Chu et al. 1950	12.7	5.8 and 6.35	Invented the first drape meter, proposed the DC	Was the first attempt to evaluate fabric drapability quantitatively	A few of fabric samples were used
Cusick 1962	15	9	Proposed a mechanism of fabric drape	Investigated the relationship of DC and bending length; Considered the shear effects on DC	Used strip cantilever to calculate the theoretical DC and did not discuss the effects of dimensions on the limits of the DC
Cusick 1968	12, 15, and 18	9	Developed the cut and weigh method of the drape meter using different sample sizes for precise measurement	Increased the accuracy of measured DC; Proposed that DC should be measured according to fabric stiffness	Did not change the measuring principle of DC
Morooka and Niwa 1976	12.7	6.35	Found that the DC is related with $(B/w)^{1/3}$	Investigated the relationship between DC and mechanical properties of bending measured by KES system experimentally	Did not discussed other properties such as shear

Table 3.1 Continued

Developer/ Researcher	Radii in the FRL drape test		Achievement	Pros	Cons
	R (cm)	r (cm)			
Niwa and Seto 1986	12.7	6.35	Obtained an experimental regression equation using $(B/w)^{1/3}$, $(2HB/w)^{1/3}$, $(G/w)^{1/3}$, and $(2\overline{HG}/w)^{1/3}$ as parameters	Investigated the relationship between DC and mechanical properties of bending, shear, and hysteresis measured by KES system experimentally	Did not discussed them theoretically
Collier 1991	Not clear	3.81 and 6.35	Found that mechanical properties have different functions using support disks of different size	Discussed the effects of dimensions on DC experimentally	Only two kinds of sizes were considered
Hu and Chan 1998	15	9	Obtained regression equations different from Niwa and Seto's results even when using the same parameters	Was the first attempt to find the relationship of full KES properties and DC	Used different dimensions but the same parameters with Niwa and Seto's research but obtained different results
Mizutani et al. 2005 [36]	12.7	6.35	Developed a drape elevator	High accuracy of measurements	Compatibility for other dimensions is unknown
Nagai et al. 2008	2r	r for k = 3, 3.5, 4, and 4.5	Investigated the effects of shear and bending on fabric drape, defined drape forms using the term $(w/E)^{2/3}$	Experimentally showed the relationship of k values and drape forms	Not theoretically discussed the effects of dimension on drape

3.2 Theoretical details

Cusick[28] proposed a model of fabric drape for different node numbers (n) to investigate the limit of the DC in the case that r is 9 cm and R is 15 cm. He discussed the relationship between c and the DC in the case of infinite and zero values of shear stiffness, G. For infinite shear stiffness, the drape deforms only because of bending. Cusick used the approximate deflection of Bickley[31] for a strip cantilever instead of using the deflection of a circular segment cantilever in calculating an approximate DC. The calculated DC values are smaller than the actual DC values obtained with circular segment cantilevers owing to the different weights and shapes. For precise calculation, it is necessary to consider the DC using a circular segment cantilever that is considered to have infinite

shear stiffness in the case of only considering bending rigidity. Moreover, Cusick did not discuss the effect of dimensions on DC.

Therefore, the DC for infinite shear stiffness (upper limit) is recalculated using a circular segment cantilever. For zero shear stiffness, the deformation can be represented by a circular array of independent strip cantilevers[28]. To obtain the limit of the DC for zero shear stiffness (lower limit), the DC is calculated by taking the sum over narrow strip cantilevers following Cusick's method[18, 28] of using cantilevers of equal length in all radial directions but applying numerical integration to the differential equation. Using these results, the drape limits considering the effect of dimensions on the drape tester are discussed.

3.2.1 Theoretical deformation of the drape shape for the upper limit of the DC

According to Cusick's model in which drape deforms only because of bending, the circular fabric deformation is divided into flat areas and segment cantilevers. In the case of the upper limit of the DC, Figure 3.1(a) shows the coordinate system of the fabric drape for infinite shear stiffness in the initial state. A circular segment of a circular sector from h_0 to R bends as a circular segment cantilever as shown in Figure 3.1 (b). I assume drape can be divided into n congruent circular segment cantilevers. Figure 3.1 shows one segment of drape for $n = 3$.

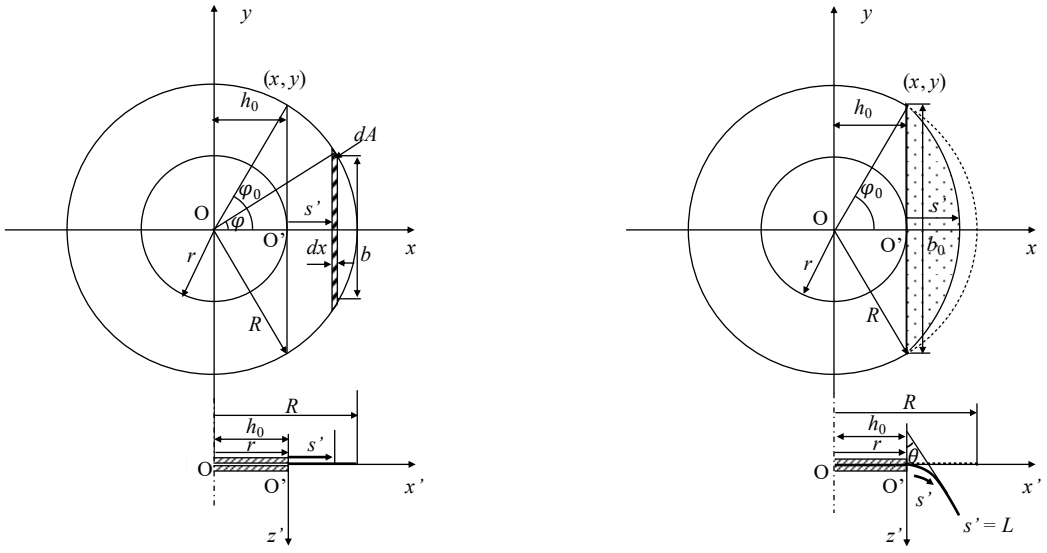

Figure 3.1 Coordinate system for the fabric drape: (a) initial state and (b) deformed state.

The following notations are used.

O: origin of coordinates (i.e., center of the circular fabric)

x, y: orthogonal coordinates on the initial plane of the circular fabric

R: radius of the fabric sample

r: radius of the support disk

O': *x* coordinate of the fixed end of the circular segment cantilever

x′, z′: orthogonal coordinates with origin at O′

h_0: distance from O to O′

B: bending rigidity of the fabric per unit width

s′: arc length of the cantilever at an arbitrary position relative to O′

θ: angle between the tangent of the cantilever and the vertical at *s′*

φ: half the central angle of a sector at *s′*

φ_0: half the central angle of a sector at $s' = 0$; $\varphi_0 = \cos^{-1}\frac{h_0}{R}$

b: width of a circular segment at s'

w': weight per unit area of the fabric

w: weight per unit length of the fabric at s'; $w = bw'$

A: area of the circular segment cantilever

m: ratio of the radii of the fabric and support disk; $m = R/r$

m': ratio of radii of the circumscribed and inscribed circles of an n-gon

L: difference between the radii of the fabric and support disk; $L = R - r$

L': length of the segment cantilever; $L' = R - h_0$

k: non-dimensional parameter for a strip cantilever

K: non-dimensional parameter for a segment cantilever in Cases I and II

K': non-dimensional parameter for a segment cantilever in Cases III

For any point on the arc of the circular segment at φ,

$$\begin{cases} x = R\cos\varphi \\ y = R\sin\varphi = \dfrac{b}{2} \end{cases}. \tag{3.3}$$

A small area dA of the flat circular segment cantilever at x is then expressed as

$$dA = bdx = -2R^2\sin^2\varphi\, d\varphi. \tag{3.4}$$

The area of the circular segment $A_{x\text{-}R}$ from x to R can thus be described as

$$A_{x\text{-}R} = \int_x^R dA = -2R^2\int_{\varphi=\cos^{-1}\frac{x}{R}}^{0}\sin^2\varphi d\varphi, \tag{3.5}$$

$$= -2R^2\frac{\varphi - \frac{1}{2}\sin 2\varphi}{2}\Bigg|_{\cos^{-1}\frac{x}{R}}^{0}, \tag{3.6}$$

$$= R^2 \left[\cos^{-1}\frac{x}{R} - \frac{1}{2}\sin\left(2\cos^{-1}\frac{x}{R}\right)\right]. \quad \textbf{(3.7)}$$

For large deformation of a cantilever, analysis usually begins with the Bernoulli–Euler law:

$$\frac{1}{\rho} = -\frac{M}{bB} = \frac{d\theta}{ds'} \quad \textbf{(3.8)}$$

where M is the bending moment at any point of the cantilever and ρ is the radius of curvature at s'. b is the width of a circular segment at s'.

Differentiating Equation (3.8) yields

$$\frac{d^2\theta}{ds'^2} = -\frac{1}{bB}\cdot\frac{dM}{ds'}. \quad \textbf{(3.9)}$$

The equilibrium of the local moment of the segment cantilever[32, 37] yields

$$\frac{dM}{ds'} = w' A_{x\text{-}R} \sin\theta. \quad \textbf{(3.10)}$$

From Equations (3.9) and (3.10), I obtain the differential equation

$$-bB\frac{d^2\theta}{ds'^2} = w' A_{x\text{-}R} \sin\theta. \quad \textbf{(3.11)}$$

For a strip cantilever, b is constant and $A_{x\text{-}R} = (L - s')\cdot b$, where L is the length of the cantilever. In this case, Equation (3.11) can be rewritten as

$$-B\frac{d^2\theta}{ds'^2} = w'(L - s')\sin\theta. \quad \textbf{(3.12)}$$

For a segment cantilever, b is given by

$$b = 2R\sin\varphi = 2R\sqrt{1 - \frac{x^2}{R^2}}. \quad \textbf{(3.13)}$$

I use $x = s' + h_0$ to obtain x from s'. Here, h_0 is the radius of the inscribed circle in a regular n-gon given by

$$h_0 = R' \cos\frac{\pi}{n}, \tag{3.14}$$

where R' is the radius of the circumscribed circle of the regular n-gon.

Substituting Equations (3.7) and (3.13) and $x = s' + h_0$ into Equation (3.11), I obtain a differential equation for the deflection of a circular segment:

$$-2B\frac{d^2\theta}{ds'^2} = w' \frac{R}{\sqrt{1-\left(\frac{s'+h_0}{R}\right)^2}}\left[\cos^{-1}\frac{s'+h_0}{R} - \frac{1}{2}\sin\left(2\cos^{-1}\frac{s'+h_0}{R}\right)\right]\sin\theta. \tag{3.15}$$

3.2.1.1 The model in three cases according to the relationship of m and m'

The segment cantilever area in the drape test depends on the relation of R and r, or the relation of R' and h_0 as follows.

When the ratio of the radii of the fabric and support disk, m, is defined as

$$m = \frac{R}{r} \tag{3.16}$$

and the ratio of radii of the circumscribed and inscribed circles of the n-gon, m', is defined as

$$m' = \frac{R'}{h_0} = \sec\frac{\pi}{n}, \tag{3.17}$$

the segment cantilever area can be described with the relation of m and m' in the following three cases.

Case I: When $R = R'$, $h_0 = r = \frac{1}{m}R = \frac{1}{m'}R$; i.e., $m' = m$, as shown in Figure 3.2 (a). In this case, the dimensions of the circumscribed and inscribed circles are the same with the dimensions of the fabric and support disk.

Case II: When $R < R'$, $h_0 = r = \frac{1}{m}R > \frac{1}{m'}R$; i.e., $m' > m$, as shown in Figure 3.2 (b). In this case, the fabric is smaller than the circumscribed circle, while the dimensions of the inscribed circle and the support disk are the same.

Case III: When $R = R'$, $h_0 = \frac{1}{m'}R > r = \frac{1}{m}R$; i.e., $m' < m$, as shown in Figure 3.2 (c) and Figure 3.3. In this case, the support disk is smaller than the inscribed circle, while the dimensions of the circumscribed circle and the fabric are the same.

Case I is a typical case of Cases II and III. In this study, I first analyze Case I and then generalize to Cases II and III.

Cusick presented a model[28] of infinite shear stiffness and discussed the drape shape and the relation of c and DC when R is 15 cm and r is 9 cm. His model belongs to Case II when n is 3 and Case III when n is 4 or 5.

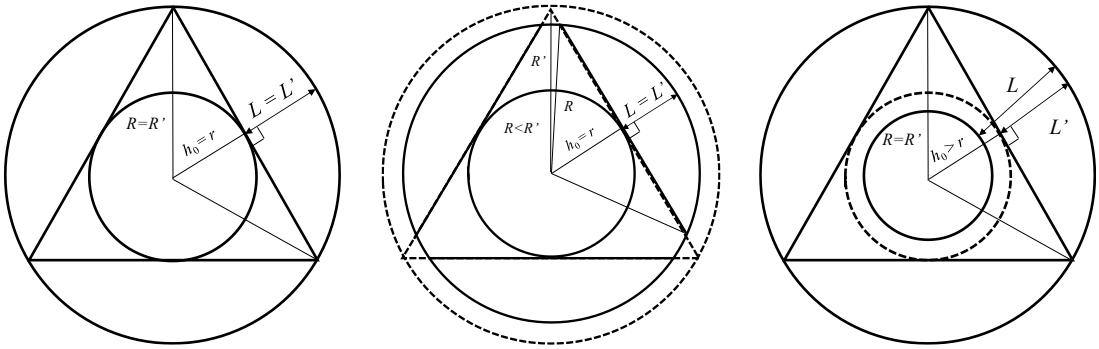

(a) Case I: $R = R'$, $h_0 = r = \frac{1}{2}R$

(b) Case II: $R < R'$, $h_0 = r > \frac{1}{2}R$

(c) Case III: $R = R'$, $h_0 = \frac{1}{2}R > r$

Figure 3.2 Drape forming lines depending on the ratio of the radii for various m with $n = 3$ and $m' = 2$.

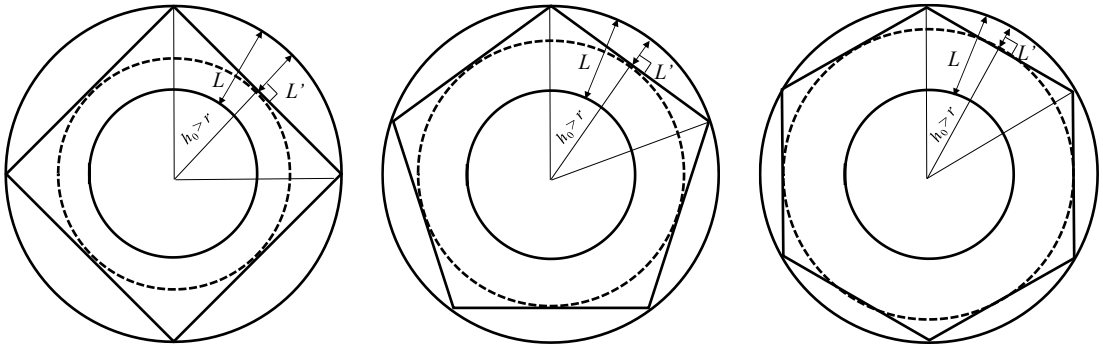

(a) $n = 4$ (b) $n = 5$ (c) $n = 6$

Figure 3.3 Drape forming lines of various n and m', with $m = 2$ for Case III ($R = R'$ (and $h_0 = R'\cos\frac{\pi}{n} > r$).

3.2.1.2 Deflection calculation for the segment cantilever in Cases I and II

In Case I, the chord of the circular segment is a tangent of the support disk. By substituting $h_0 = r = \frac{1}{m}R$, Equation (3.15) is rewritten as

$$-2B\frac{d^2\theta}{ds'^2} = w' \frac{R}{\sqrt{1-\left(\frac{s'}{R}+\frac{1}{m}\right)^2}} \left\{ \cos^{-1}\left(\frac{s'}{R}+\frac{1}{m}\right) - \frac{1}{2}\sin\left[2\cos^{-1}\left(\frac{s'}{R}+\frac{1}{m}\right)\right]\right\} \sin\theta. \tag{3.18}$$

The interval of integration for s' is $[0, R - h_0] = [0, \frac{m-1}{m}R]$, which represents the arc length from the fixed end to the free end of the circular segment cantilever.

I introduce the normalized arc length q to normalize s' by the arc length:

$$q = \frac{s'}{\frac{m-1}{m}R} = \frac{m}{m-1}\cdot\frac{s'}{R}. \tag{3.19}$$

The second derivative of θ in Equation (3.18) can then be expressed as

$$\frac{d^2\theta}{ds'^2} = \frac{d}{ds'}\left(\frac{d\theta}{ds'}\right) = \left(\frac{m}{m-1}\right)^2 \cdot \frac{1}{R^2}\cdot\frac{d^2\theta}{dq^2}. \tag{3.20}$$

Substituting Equation (3.20) into Equation (3.18) gives

$$\frac{d^2\theta}{dq^2}=\frac{w'R^3}{B}\left(\frac{m\text{-}1}{m}\right)^3\frac{1}{-2\left(\frac{m\text{-}1}{m}\right)\sqrt{1-\left(\frac{s'}{R}+\frac{1}{m}\right)^2}}\left\{\cos^{-1}\left(\frac{s'}{R}+\frac{1}{m}\right)-\frac{1}{2}\sin\left[2\cos^{-1}\left(\frac{s'}{R}+\frac{1}{m}\right)\right]\right\}\sin\theta. \tag{3.21}$$

In this case, the length of the segment cantilever L' is

$$L' = L = R - r = \frac{m-1}{m}R. \tag{3.22}$$

Substituting Equation (3.22) into Equation (3.2) gives

$$K = R\frac{m-1}{m}\cdot\sqrt[3]{\frac{w'}{B}}. \tag{3.23}$$

Substituting Equation (3.23) into Equation (3.21) gives

$$\frac{d^2\theta}{dq^2}=-K^3\frac{1}{2\left(\frac{m-1}{m}\right)\sqrt{1-\left(\frac{m-1}{m}q+\frac{1}{m}\right)^2}}\left\{\cos^{-1}\left(\frac{m-1}{m}q+\frac{1}{m}\right)-\frac{1}{2}\sin\left[2\cos^{-1}\left(\frac{m-1}{m}q+\frac{1}{m}\right)\right]\right\}\sin\theta. \tag{3.24}$$

The interval of integration for q is [0, 1]. The deflection of the segment cantilever is therefore determined by m and K.

The boundary conditions are $\theta = 0$ at $q = 0$ and $\frac{d\theta}{dq} = 0$ at $q = 1$. Integrating Equation (3.24) using the fourth-order Runge–Kutta method with respect to q, I obtain a relationship between q and θ. The orthogonal coordinates of the deflection curve can be obtained according to

$$x' = \int_0^{s'}\sin\theta\,ds', \quad z' = \int_0^{s'}\cos\theta\,ds'. \tag{3.25}$$

The orthogonal coordinates of the edges of the segment cantilever y' at s' are

determined by b, which is given by Equation (3.13).

Using the normalized arc length q given by Equations (3.19) and (3.25), I obtain the normalized coordinates

$$x' = \frac{m-1}{m} R \int_0^q \sin\theta \, dq, \quad z' = \frac{m-1}{m} R \int_0^q \cos\theta \, dq. \tag{3.26}$$

Normalized coordinates x'/R and z'/R are therefore given by

$$\frac{x'}{R} = \frac{m-1}{m} \int_0^q \sin\theta \, dq, \quad \frac{z'}{R} = \frac{m-1}{m} \int_0^q \cos\theta \, dq. \tag{3.27}$$

The normalized coordinates of the deflection curve are obtained through the numerical integration of Equation (3.27) with respect to q.

The projected area of the circular segment cantilever on the xy plane, A_{seg}, is given by

$$A_{\text{seg}} = \int_{s'=0}^{L'} b \, dx'. \tag{3.28}$$

Here, coordinates of the deflection curve x' and the width of a circular segment b are functions of s'.

Combining the normalized coordinate x'/R with the normalized width b/R, the normalized projected area of the circular segment cantilever on the xy plane can be written as

$$\frac{A_{\text{seg}}}{R^2} = \int_{s'=0}^{s'=L'=L} \frac{b}{R} d\frac{x'}{R}. \tag{3.29}$$

The normalized projected area can therefore be numerically calculated using Equation (3.29) and $\frac{x'}{R}$ calculated using Equation (3.27). The calculated normalized projected area will be used for the DC calculation.

In Case II, as in Case I, L' is equal to $\frac{m-1}{m} R$. The deformation of the segment cantilever can thus be calculated using Equations (3.27) and (3.29).

3.2.1.3 Calculation of the deflection of the segment cantilever in Case III

In Case III, $R = R'$; hence, h_0 is given by R/m'. L' is smaller than L because h_0 is larger than r. Thus, K shown in Equation (3.23) is reconsidered as K', which is determined by $L' = R - h_0$. Under this condition, K' is defined as

$$K' = R\frac{m'-1}{m'}\cdot\sqrt[3]{\frac{w'}{B}}. \tag{3.30}$$

The deflection of the segment cantilever is determined by m' and K' in this case.

Using K' and m' instead of K and m in Equation (3.24), I obtain normalized coordinates in cooperating K' and m' as shown in Equation (3.31). The normalized projected area can be numerically calculated according to

$$\frac{x'}{R} = \frac{m'-1}{m'}\int_0^q \sin\theta\, dq, \quad \frac{z'}{R} = \frac{m'-1}{m'}\int_0^q \cos\theta\, dq, \tag{3.31}$$

$$\frac{A_{\text{seg}}}{R^2} = \int_{s'=0}^{s'=L'=R-h_0} \frac{b}{R} d\frac{x'}{R}. \tag{3.32}$$

3.2.2 Theoretical deformation of the drape shape for the lower limits of the DC

In the calculation of the lower limit using a strip cantilever, I use Equation (3.12) following Cusick's method as shown in Figure 3.4. To normalize $L - s'$ by fabric length, I introduce the normalized fabric length t, expressed as

$$t = \frac{L-s'}{L}. \tag{3.33}$$

The normalized differential equation for the deflection of the strip cantilever in Equation (3.12) is then given by

$$\frac{d^2\theta}{dt^2} = -\frac{w'L^3}{B} t\sin\theta = -K^3 t\sin\theta. \tag{3.34}$$

To compare upper and lower limits in Case III, it is necessary to obtain the relation of

K and K'. Equations (3.23) and (3.30) give the relation as

$$\frac{K}{K'} = \frac{m'}{m'-1} \cdot \frac{m-1}{m}. \tag{3.35}$$

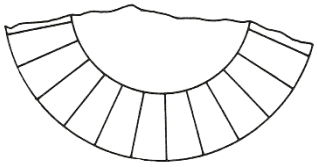

(a) Wedge-shaped cantilevers

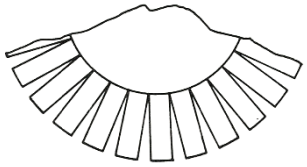

(b) Approximation treatment of wedge-shaped cantilevers as strip cantilevers

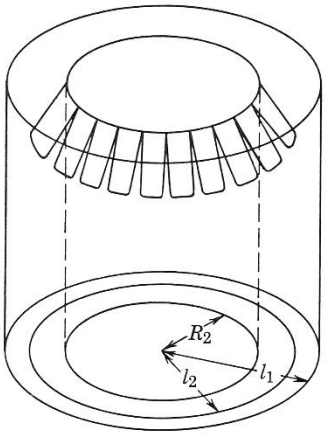

(c) Strip cantilevers bending over to define drape diagram

Figure 3.4 Lower limit for drape of zero shear stiffness

(Source: Hearle et al., 1969[18])

3.2.3 Calculation of the DC

In Cases I and II, because the DC is a ratio of the projected area of the fabric before and after draping, the expression for the DC in Equation (3.1) can be rewritten as

$$\mathrm{DC}(\%) = \frac{nA_{\mathrm{seg}} + A_{n\text{-gon}} - S_2}{S_1 - S_2} \times 100\%, \tag{3.36}$$

$$= \frac{nA_{\text{seg}} + nR^2 \cos\frac{\pi}{n}\sin\frac{\pi}{n} - \pi\frac{R^2}{m^2}}{\pi R^2(1-\frac{1}{m^2})} \times 100\%, \tag{3.37}$$

$$= \frac{\frac{nA_{\text{seg}}}{R^2} + \frac{n}{2}\sin\frac{2\pi}{n} - \pi\frac{1}{m^2}}{\pi(1-\frac{1}{m^2})} \times 100\%, \tag{3.38}$$

where $A_{n\text{-gon}}$ is the area of the polygon. Thus, for given n and m, the DC can be determined using Equation (3.38) and the normalized projection area in Equation (3.29). The minimum DC for infinite shear stiffness can be obtained by substituting zero into A_{seg}.

In Cases I and II, A_{seg} is calculated using Equations (3.27) and (3.29), and the DC is therefore related to m. In Case III, A_{seg} is calculated using Equations (3.31) and (3.32) and the DC is therefore related to m', but m is also needed to calculate the DC. The DC is thus related to both m and m' in Case III.

The DC for zero shear stiffness is obtained using Equation (3.12).

3.3 Experimental details

To verify the proposed theoretical model for fabric drape deformation, 1392 drape tests (for nine types of sample, four nodes, 14 types of dimension, and three measurements) were performed on eight different fabrics and a sheet while changing the radii of the support disk and sample. The radius r of the support disk was set from 1.5 to 8 cm at intervals of 0.5 cm. For each disk radius, the sample radius R was set as twice the disk radius r; i.e., $R = 2r$. The disk radius r is thus equal to the sample length L in this case. The node number n of the drapes was manually set at 3, 4, 5, and 6. To calculate the DC, photographs (6016 × 4016 pixels, NIKON D750) were taken from a position 200 cm above the drape tester. DCs of the samples were calculated by counting the pixels of the fabric drape in each photograph using Photoshop CC (Adobe Systems Co., Ltd., CA, USA). To count the pixels of the drape, the Pen Tool in Photoshop was used to select the area of the drape including the disk area in the photograph. Then, the pixel value of the

selected area could be read in the Histogram panel. Using Equation (2.9), the DC can then be obtained. The DC of each sample was measured three times for each n and the average value taken.

Specifications of the fabric and sheet samples are listed in Table 3.2. The bending rigidity and shear stiffness of the samples were respectively measured employing a KES-FB2 pure bending tester and KES-FB1 tensile and shear tester (Kato Tech Co. Ltd., Kyoto, Japan).

The theoretical and experimental drapes were compared in terms of the K–DC and K'–DC relationships and projected drape shape. In the theoretical analysis, the K and K' values were obtained using Equation (3.23) for Cases I and II and using Equation (3.30) for Case III.

In the experimental analysis, K values of the samples were calculated using Equation (3.23) while K' values of the samples were calculated using Equations (3.23) and (3.35). The average of the measured bending rigidity in warp, weft, and 45º bias directions was used for B.

Table 3.2 Specifications of samples

Sample	Material*1	Weave*2	Thickness (mm)	Area density w' ($g \cdot m^{-2}$)	Linear density	Density	Bending rigidity (KES *B*) (10^{-4} $cN \cdot m^2 \cdot m^{-1}$)			Shear stiffness (KES *G*) ($cN \cdot m^{-1} \cdot degree^{-1}$)		
					Warp × Weft (tex)	Warp × Weft (number·cm^{-1})	Warpwise	Weftwise	Bias(45°)	Mean	Sliding in warp direction	Sliding in weft direction	Mean
Broadcloth 1	CO 100%	P	0.431	111.5	11.6 × 11.4	61.4 × 30.7	5.23	4.01	3.47	4.24	68.6	91.1	79.9
Gabardine 1	WO 100%	T 2/1	0.509	187.6	32.4 × 24.8	36.2 × 23.6	8.91	5.33	6.74	6.99	54.9	75.5	65.2
Saxony	WO 100%	T 2/2	0.697	188.3	39.2 × 38.8	25.2 × 20.5	8.99	6.15	7.58	7.57	57.8	48.0	52.9
Herringbone 2	WO 80% AF 20%	Broken T	1.944	307.0	237.2 × 252.0	6.7 × 6.7	23.18	18.01	13.21	18.13	57.8	69.6	63.7
Chiffon georgette 1	PL 100%	P	0.179	37.2	4.5 × 4.0	42.9 × 39.4	0.65	0.53	0.72	0.64	41.2	37.2	39.2
Denim 2	CO 100%	T 2/1	0.941	285.3	58.0 × 55.4	25.6 × 16.5	25.92	17.32	24.94	22.73	319	299	309
Denim 3	CO 100%	T 2/1	1.066	226.1	53.2 × 34.4	24.8 × 16.5	13.16	2.83	4.74	6.91	109	124	116
Triacetate fabric	TA 70% PL 30%	P	0.297	77.3	9.8 × 15.8	36.2 × 24.4	1.02	7.90	1.30	3.40	22.21	32.67	27.44
Silicon rubber	SI 100%	–	0.100	119.7	–	–	0.38	0.36	0.38	0.37	155.49	149.29	152.39

*[1]CO: cotton; WO: wool; AF: other; PL: polyester; TA: triacetate; SI: silicon rubber

*[2]P: plain; T: twill

3.4 Results and discussion

3.4.1 Theoretical fabric deformation

3.4.1.1 Relationship between the DC and *K* or *K*' for different *n*

Figure 3.5 shows the theoretical deformation of drape upper limits for different values of *K* in Case I with $n = 3$ and K' in Case III with $n = 4$, 5, and 6 obtained using the obtained orthogonal coordinates in Equations (3.27) and (3.31). *n* segments of the drape shape are arranged around the center. When *m* and *K* differ from *m*' and K', the deflections are different as shown in Figure 3.5. As *K* and K' increase, the projected segment area reduces irrespectively of *n*. With greater *n*, the projected segment areas also reduce with increasing *K* and K'.

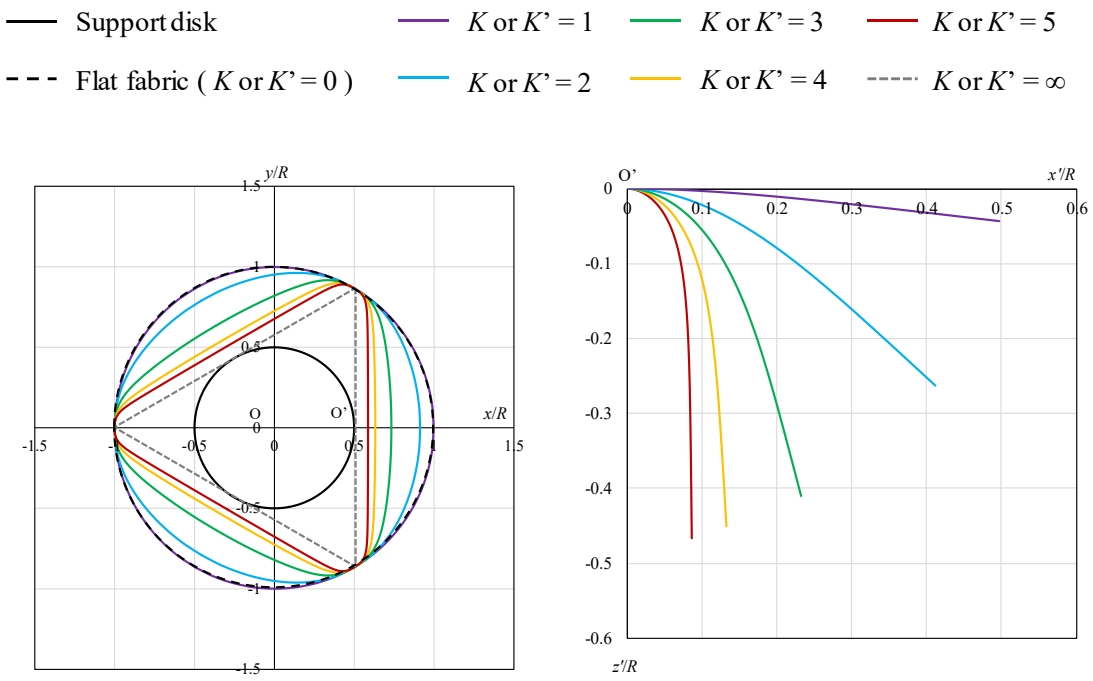

(a) Top view of the theoretical drape when $n = 3$ ($m' = 2$) for different values of K

(b) Side view of the theoretical drape when $n = 3$ ($m' = 2$) for different values of K

(c) Top view of the theoretical drape when $n = 4$ ($m' = 1.414$) for different values of K'

(d) Side view of the theoretical drape when $n = 4$ ($m' = 1.414$) for different values of K'

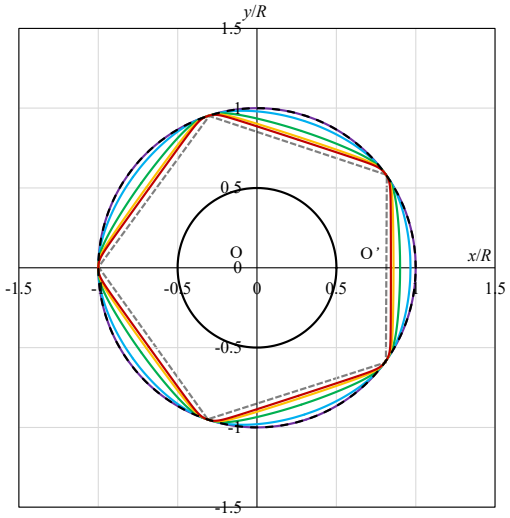

(e) Top view of the theoretical drape when $n = 5$ ($m' = 1.236$) for different values of K'

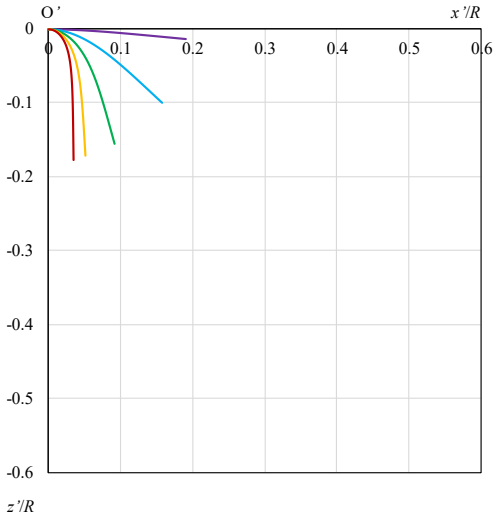

(f) Side view of the theoretical drape when $n = 5$ ($m' = 1.236$) for different values of K'

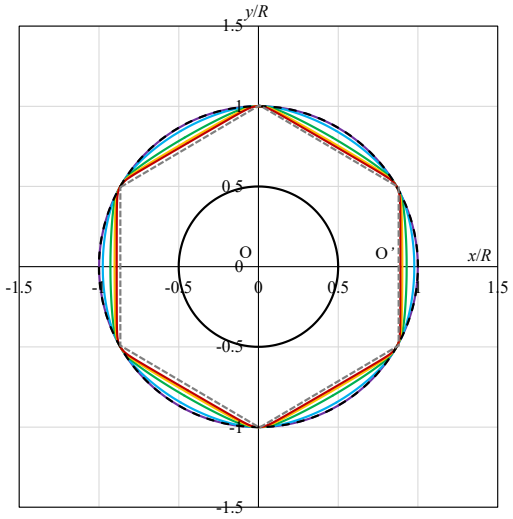

(g) Top view of the theoretical drape when $n = 6$ ($m' = 1.155$) for different values of K'

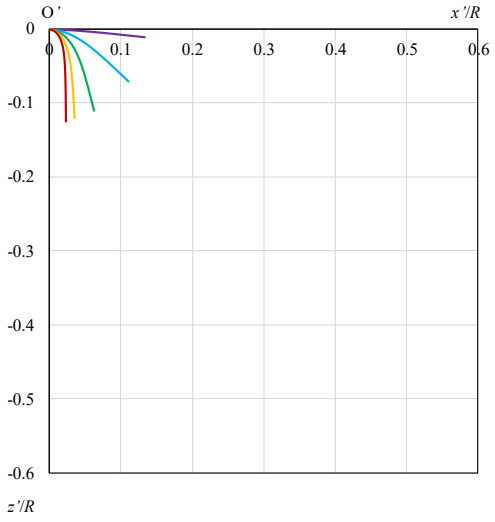

(h) Side view of the theoretical drape when $n = 6$ ($m' = 1.155$) for different values of K'

Figure 3.5 Top and side views of calculated drape shapes for different *K* or *K'*.

3.4.1.2 Relationship between the DC and K or K' for $n = 3$

Figure 3.6 shows the relationship between the DC and K for $n = 3$ with different values of m for upper ($G = \infty$) and lower ($G = 0$) limits. This situation refers to Cases I and II. The curves of the upper limit of the DC versus K fall notably as m increases while the curves of the lower limit of the DC versus K are similar for all m. Both DC limits decrease as m increases while the difference between the two limits decreases with increasing m for the same K. Table 3.3 gives the minimum DC values for infinite K and different values of m. The minimum DC for the upper limit decreases as m increases while that for the lower limit is zero irrespective of m.

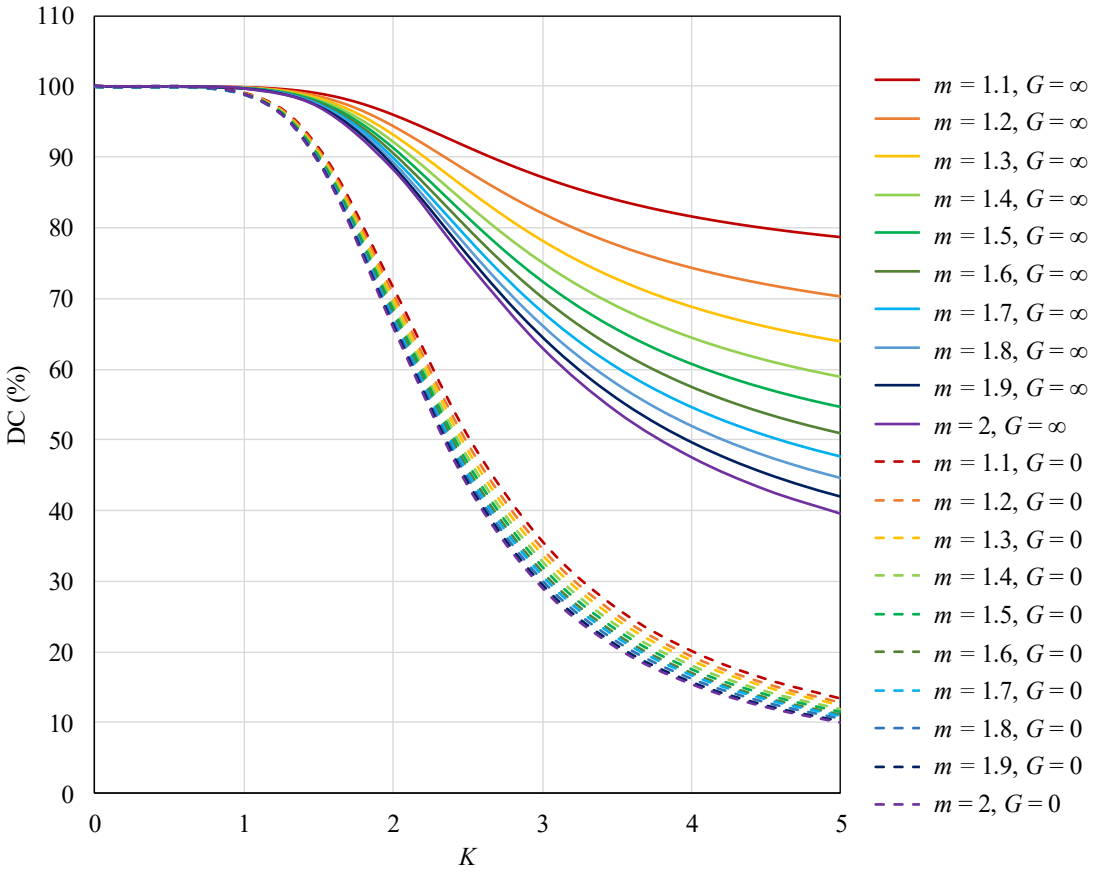

Figure 3.6 Upper and lower limits of the calculated DC versus K for $m \leq 2$ when $n = 3$ (Cases I ($m = 2$) and II ($m = 1.1$–1.9)).

Table 3.3 Minimum DCs for different $m \leq 2$ when $n = 3$

n	m	G	Minimum DC (%)
3	1.1	∞	71.95
3	1.2	∞	60.92
3	1.3	∞	52.84
3	1.4	∞	46.33
3	1.5	∞	40.84
3	1.6	∞	36.10
3	1.7	∞	31.92
3	1.8	∞	29.20
3	1.9	∞	24.84
3	2	∞	21.80
3	–	0	0

Figure 3.7 shows the upper and lower limits of the DC according to K' for different values of m when $n = 3$ and $m' = 2$. This situation refers to Case III. Irrespective of the value of m, both the upper and lower limits of the DC decrease with increasing K'. As m increases, the curves of the upper limit rise while the curves of the lower limit fall. Table 3.4 gives the minimum DC values for infinite K' and different m. The minimum DC for the upper limit increases as m increases while that for the lower limit is zero irrespective of m.

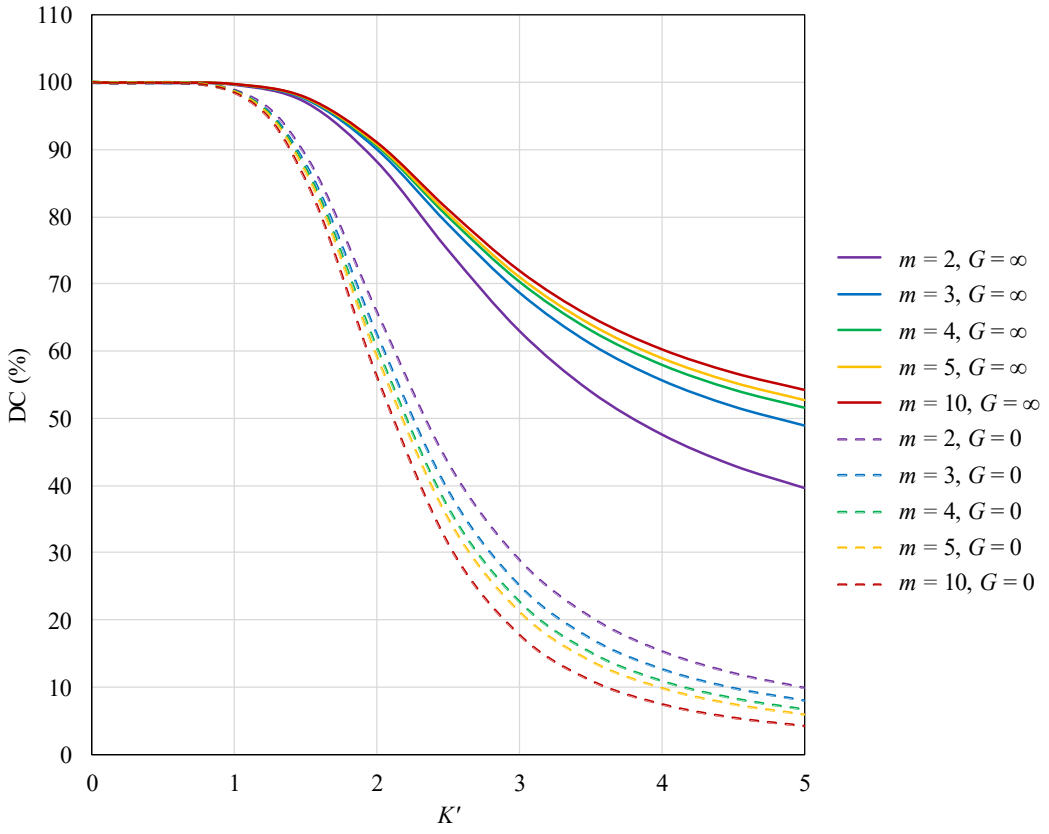

Figure 3.7 Upper and lower limits of the calculated DC versus *K′* for different *m* when *n* = 3 and *m′* = 2 (Case III).

Table 3.4 Minimum DCs for different *m* when *n* = 3

n	*m*	*m′*	*G*	Minimum DC (%)
3	2	2	∞	21.80
3	3	2	∞	34.02
3	4	2	∞	37.44
3	5	2	∞	38.91
3	10	2	∞	40.76
3	–	2	0	0

In terms of the upper limits for all cases in Figure 3.6 and Figure 3.7, the DC decreases with increasing K or K'. In Case I, the area of the circular fabric is the same as that of the circumscribed circle and the DC has the smallest value among all cases. In Case II, the circumscribed circle is larger than the circular fabric. In this case, the deflection area of the fabric decreases with decreasing m. This means that the projected area of the fabric is larger than all the areas for DC determination. This explains why the DC in Case II is larger than the DC in Case I. In Case III, the inscribed circle is larger than the support disk. In this case, the difference between the area of the support disk and the circular fabric is large. This explains why the DC in Case III is larger than the DC in Case I.

In terms of the lower limits for all cases in Figure 3.6 and Figure 3.7, the DC increases with decreasing m. The DC approaches 0% with increasing K or K' irrespective of m for all cases.

Comparing upper and lower limits in Cases I and II, the DC–K curves in Figure 3.6 show a similar tendency for increasing m when the node number is the same. Meanwhile, comparing upper and lower limits in Case III, the DC-K' curves in Figure 3.7 show different tendencies for increasing m when the node number is the same. The DC increases with increasing m for the upper limits in Case III while the DC decreases with increasing m for the lower limits in Case III. In the case of the upper limits, with greater m, the flat area of the n-gon becomes larger. This leads to a larger DC according to Equation (3.38). In the case of the lower limits, the calculated DC is only affected by the deflection of strip cantilever. With greater m, the projected area of deflection decreases, leading to a smaller DC.

3.4.1.3 Relationship between the DC and K or K' for different n and m'

Figure 3.8 shows the upper and lower limits of the DC according to K or K' for different n and m' when $m = 2$. The curves of the upper limit increase with increasing n. The curves of the lower limit decrease with increasing n owing to the smaller K'. Table 3.5 gives the minimum DC values for infinite K and different n. The minimum DC for the upper limit decreases as m' increases while that for the lower limit is the same as zero irrespective of m'.

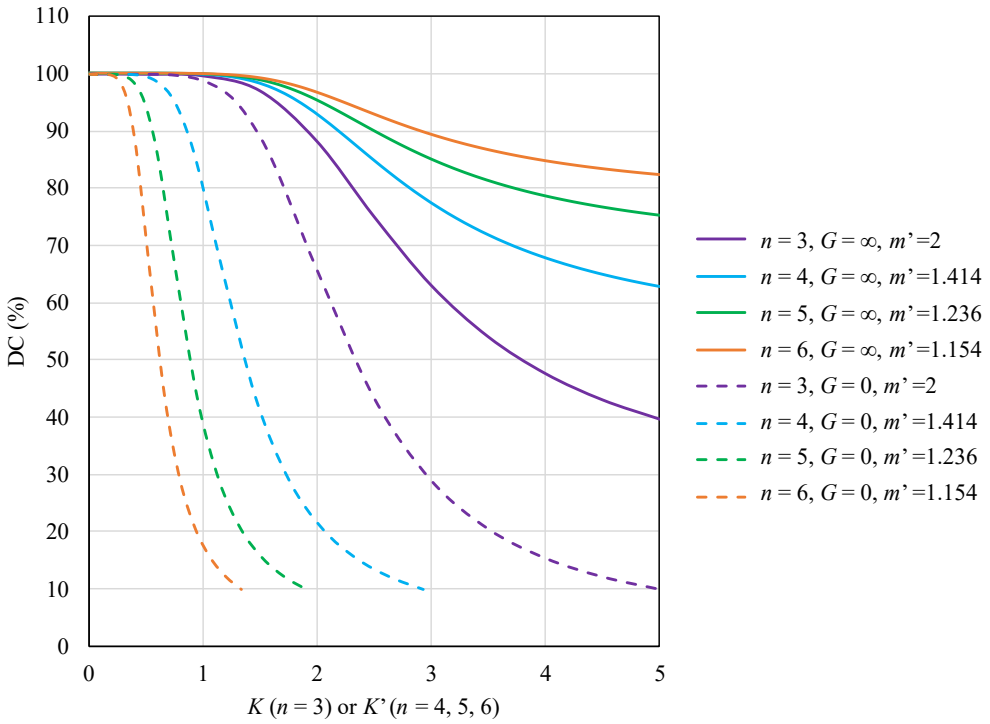

Figure 3.8 Upper and lower limits of the calculated DC versus *K* or *K′* for different *n* when *m* = 2 (Case III).

Table 3.5 Minimum DCs for different *n* when *m* = 2

m	*n*	*m′*	*G*	Minimum DC (%)
2	3	2	∞	21.80
2	4	1.414	∞	51.54
2	5	1.236	∞	67.58
2	6	1.154	∞	76.93
–	–	–	0	0

3.4.2 Comparison of calculated and experimental projected drape shapes

Figure 3.9 shows the superposed drape shapes of the calculated and experimental drapes. K or K' values of the samples having different bending rigidities and weights are normalized with the dimension respectively calculated using Equation (3.23) for K, or Equation (3.23) with Equation (3.35) for K'. To compare the experimental and calculated shapes with K or K' values, experimental K or K' values close to the calculated values are used with about 5% difference. In the cases of $K \approx 1$, 2, and 3 and $n = 3$, the experimental shapes are similar to the shapes of the calculated upper limit as shown in Figure 3.9 (a), (b), and (c). In the case of $K' \approx 1$ and $n = 4$, the experimental shapes are similar to the shapes of the calculated upper limit as shown in Figure 3.9 (d). However, in the cases of $K' \approx 2$ and 3 and $n = 4$, the experimental shapes are closer to the shapes of the calculated lower limits as shown in Figure 3.9 (e) and (f). In the cases of $n = 5$ and 6 for K', the experimental shapes are closer to the shapes of the lower limits calculated with larger K' values.

Drape depressions between adjacent nodes or double-curvature bending have been observed[38]. However, the fabrics deform in an area that is assumed to be not deformable in theory. Therefore, the experimental shapes of some samples do not agree with the calculated shapes owing to the presence of depressions. These results could be due to different values of shear stiffness.

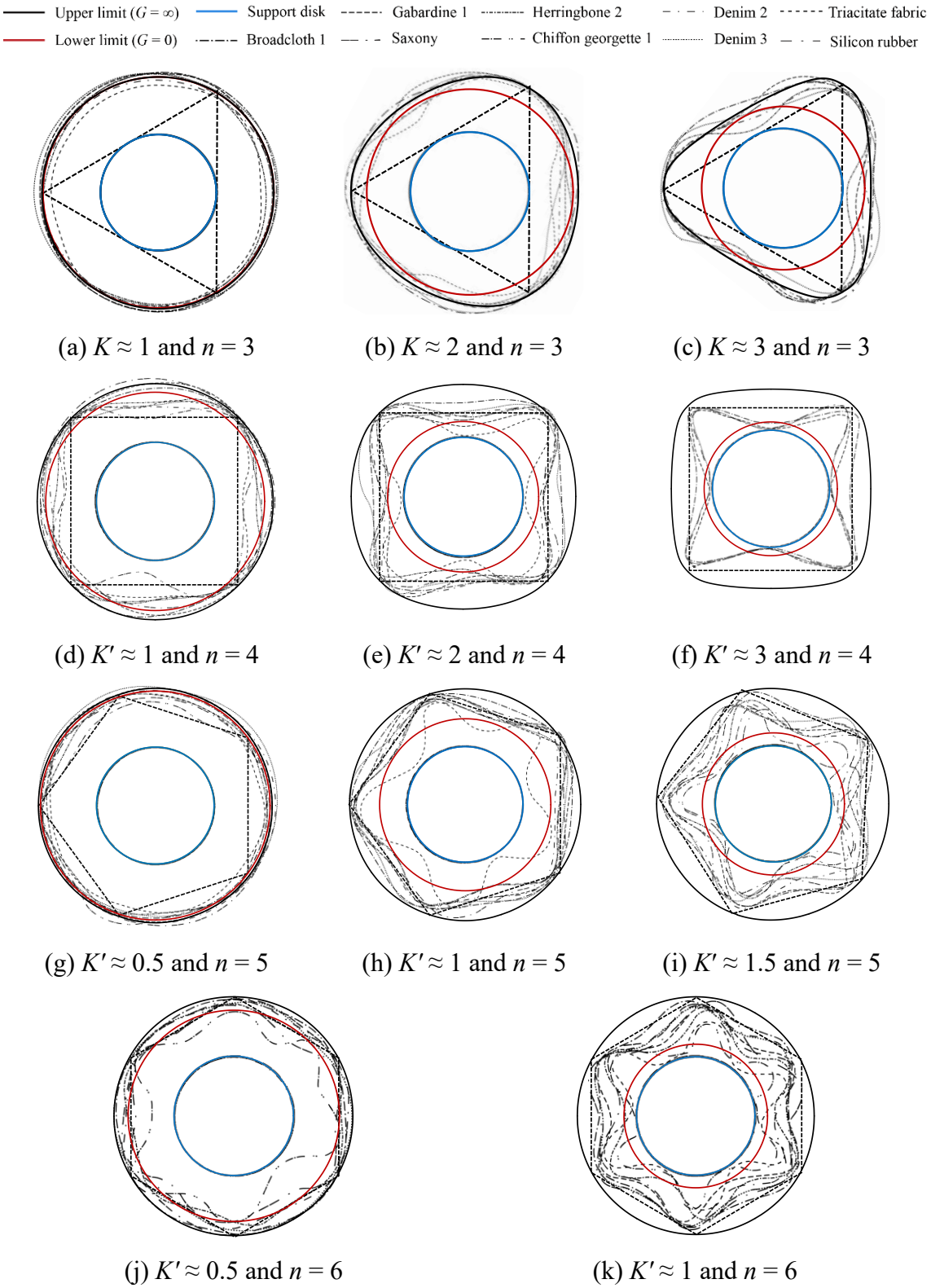

(a) $K \approx 1$ and $n = 3$ (b) $K \approx 2$ and $n = 3$ (c) $K \approx 3$ and $n = 3$

(d) $K' \approx 1$ and $n = 4$ (e) $K' \approx 2$ and $n = 4$ (f) $K' \approx 3$ and $n = 4$

(g) $K' \approx 0.5$ and $n = 5$ (h) $K' \approx 1$ and $n = 5$ (i) $K' \approx 1.5$ and $n = 5$

(j) $K' \approx 0.5$ and $n = 6$ (k) $K' \approx 1$ and $n = 6$

Figure 3.9 Comparison of theoretical and experimental drape shapes according to *K*.

3.4.3 Comparison of experimental and calculated DCs for *K* or *K′*

Figure 3.10 compares the calculated limits and experimental DC–*K* or DC–*K′* curves for different *n*. Irrespective of *n*, the DC–*K* or DC–*K′* curves of most of the samples are between the two limits.

When $n = 3$ as shown in Figure 3.10 (a), the experimental curves of chiffon georgette 1 and triacetate fabric are lower than the lower limit. These samples have lower shear stiffness than the other samples as shown in Table 3.2. For samples with lower shear stiffness, the fabrics depress between adjacent nodes and there is bending deformation in the circumferential direction with buckling, and the curves are thus close to the lower limit. On the other hand, the experimental curves of broadcloth 1 and denim 3 exceed the upper limits. Broadcloth 1 and denim 3 have lower bending rigidity and higher shear stiffness than the other samples as shown in Table 3.2. For these samples, the depression in the middle of two adjacent nodes and bending deformation to the opposite side near the nodes occurs at the same time. Besides, the actual fabric would not compose a regular triangle every time due to the anisotropy. Those reasons lead to the actual projection area are larger than the theoretical projection area. Hence, the experimental lines of them are above the upper limits.

When $n \geq 4$ as shown in Figure 3.10 (b), (c), and (d), irrespective of *n*, the DC–*K′* curves of the samples are between the two limits except chiffon georgette 1 and triacetate fabric. The experimental curves are close to the lower limit rather than the upper limit. As the same as the results when $n = 3$, the curves of chiffon georgette 1 and triacetate fabric are lower than the lower limit. The reason of the exceeding results is due to the double curvature occurred in the area where are assumed to be not deformable in the theory as I mentioned in 3.4.2 *Comparison of calculated and experimental projected drape shapes*.

The DC decreases with increasing *n* for all samples. With increasing *n*, fabrics undergo more depression, which leads to a lower DC as shown in Figure 3.9 (h) and (k).

Although there were some differences between the theoretical and experimental results, most results were between the lower and upper limits, which validate the model.

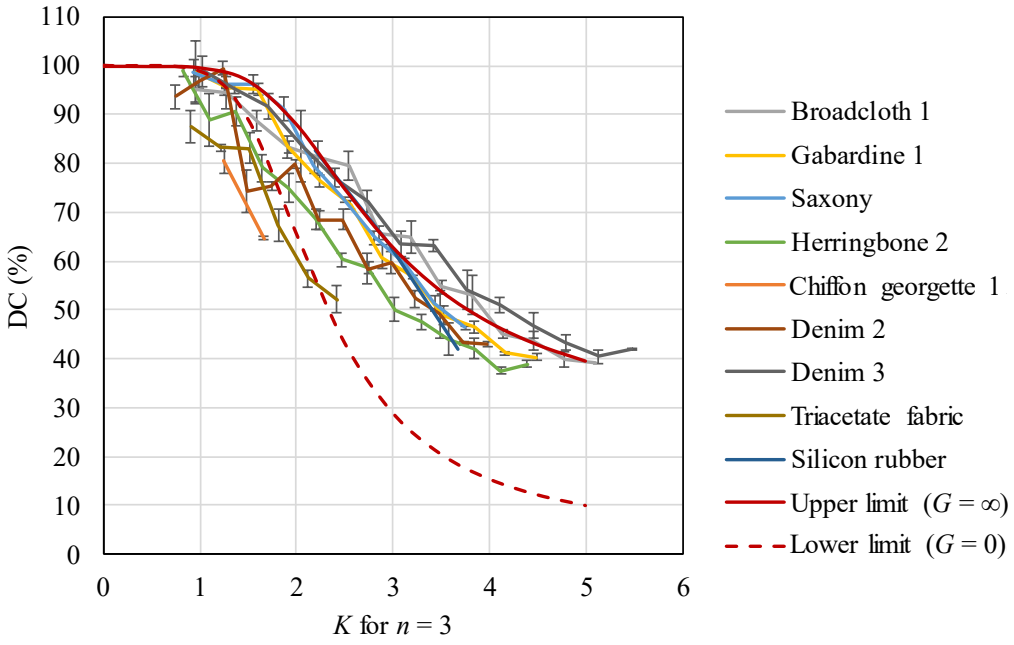
110
100
90
80
70
60
50
40
30
20
10
0
DC (%)
0
1
2
3
4
5
6
K for n = 3
Broadcloth 1
Gabardine 1
Saxony
Herringbone 2
Chiffon georgette 1
Denim 2
Denim 3
Triacetate fabric
Silicon rubber
Upper limit (G = ∞)
Lower limit (G = 0)

(a) $n = 3$

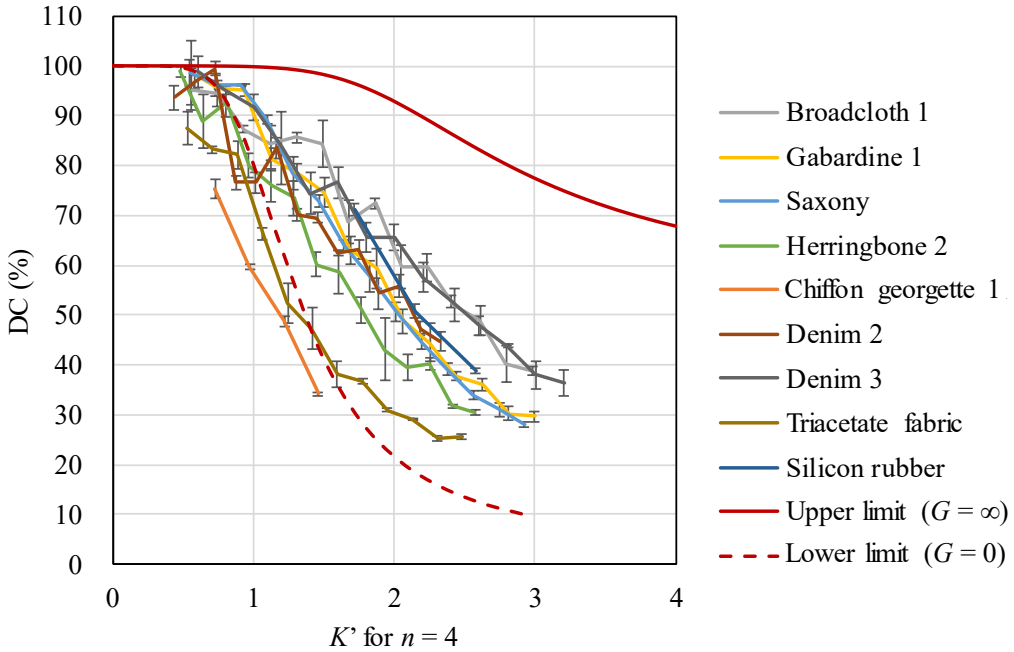
110
100
90
80
70
60
50
40
30
20
10
0
DC (%)
0
1
2
3
4
K' for n = 4
Broadcloth 1
Gabardine 1
Saxony
Herringbone 2
Chiffon georgette 1
Denim 2
Denim 3
Triacetate fabric
Silicon rubber
Upper limit (G = ∞)
Lower limit (G = 0)

(b) $n = 4$

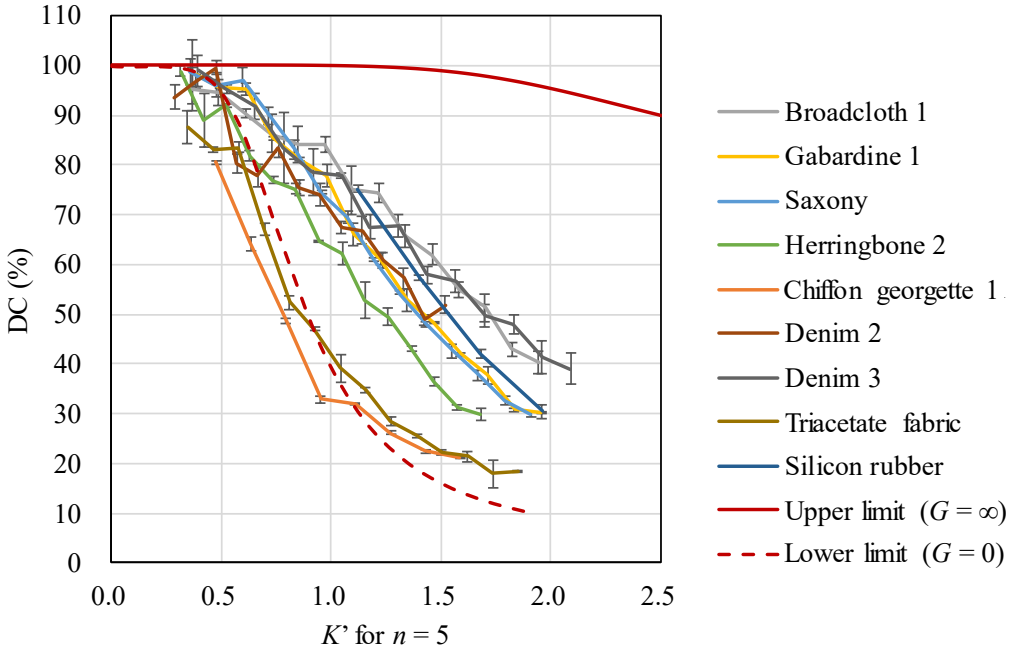

(c) $n = 5$

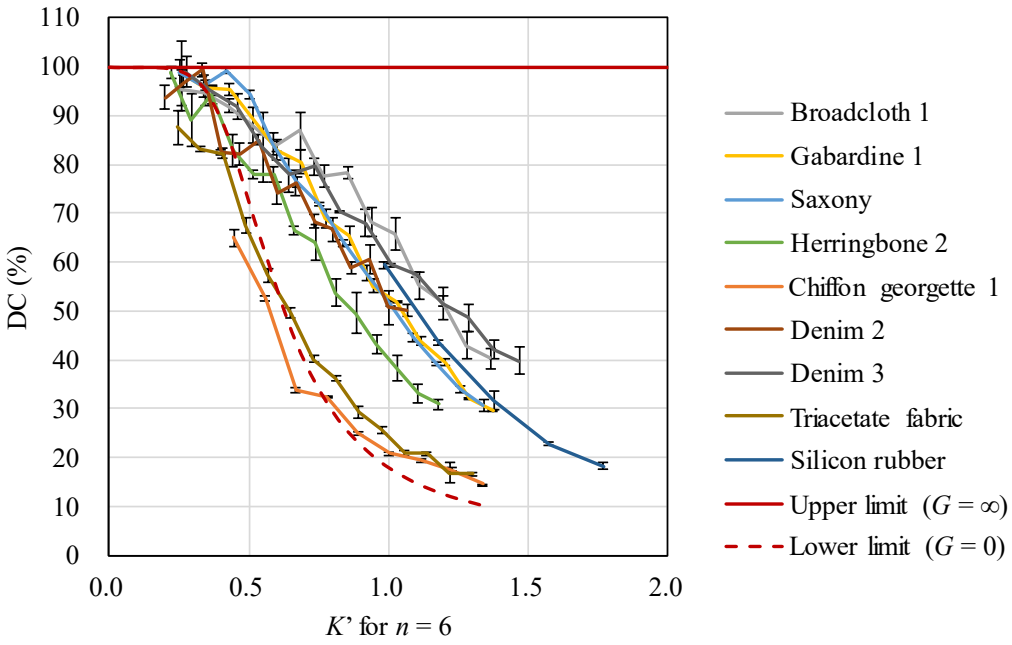

(d) $n = 6$

Figure 3.10 Comparison of DC–*K* or DC–*K′* curves from theory and experiment for *m* = 2.

Figure 3.11 shows the relationship of the root-mean-square error (RMSE) of the theoretical drape (i.e., DC) relative to the experimental drape versus shear stiffness of the samples. It is seen that the RMSEs for the upper limit and lower limit decrease with decreasing n.

The RMSE for the upper limit decreases with increasing G while the RMSE for the lower limit increases with increasing G except in the case of silicon rubber. Chiffon georgette 1 and triacetate fabric have a larger RMSE of the upper limit and a smaller RMSE of the lower limit than other fabrics. This is due to their lower shear stiffness.

Silicon rubber has a large RMSE. Compared with other fabrics, silicon rubber has lower bending rigidity and higher shear stiffness, which makes it easier to bend in a circular direction. There is thus buckling and bending deformation in the circular direction, resulting in the larger RMSE. This is a topic of future study.

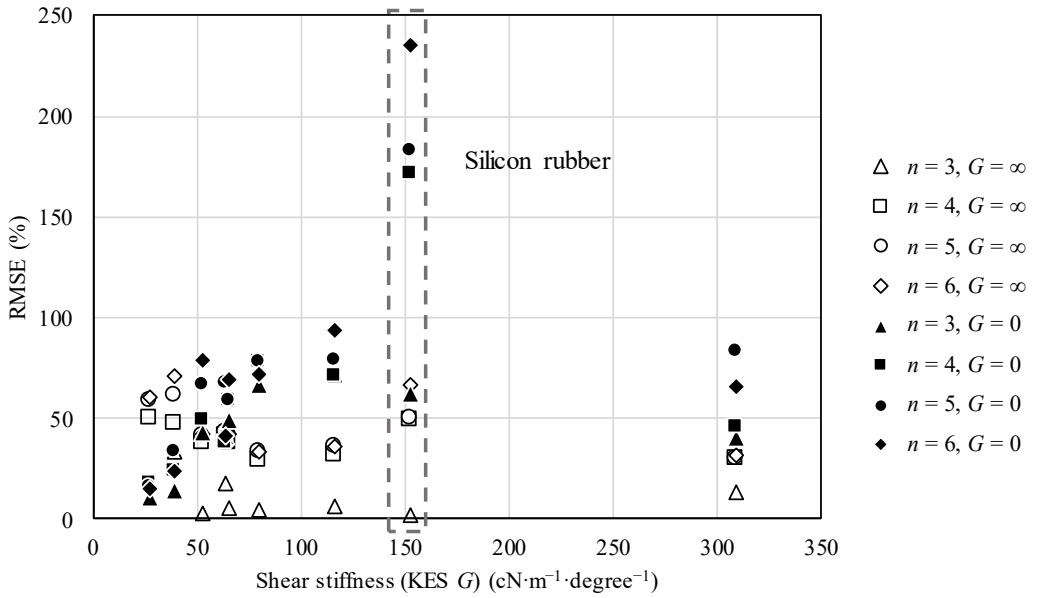

Figure 3.11 Relationship between the RMSE of the DC and shear stiffness

3.4.4 Comparison with Cusick's results

To compare my results with Cusick's results, I calculated the theoretical limits using Cusick's dimensions. Cusick[28] used R = 15 cm and r = 9 cm, which means L' is 6 cm for n = 3 and 6. Cusick gave the relationship between the theoretical DC limit and $c = (B/w')^{1/3}$. The c value in my model corresponds to $c = L'/K$ according to Equations (3.22) and (3.23) for Case II or $c = L'/K'$ according to $L' = R - h_0$ and Equation (3.30) for Case III.

Figure 3.12 compares c–DC curves between the results of Cusick and the present study for lower limit and upper limits when n = 3, 4, 5, and 6. For the lower limit (G = 0), the present model provides results similar to those of Cusick's model when $c > 2$. There are differences between the two models when $c < 2$ owing to the error introduced by Cusick's approximation of using a strip cantilever.

Cusick presented the relationship between the upper limit of the DC and c for n = 3 and 6. There are differences between Cusick's results and my results. For n = 6, Cusick's results are smaller than mine. For n = 3, Cusick's results are again smaller than mine but with larger differences than for n = 6. This is because my model is based on the deflection of a segment cantilever while Cusick's is based on the deflection of a strip cantilever as mentioned in 3.1 *Introduction*. For n = 4 and 5, curves are between those for n = 3 and 6.

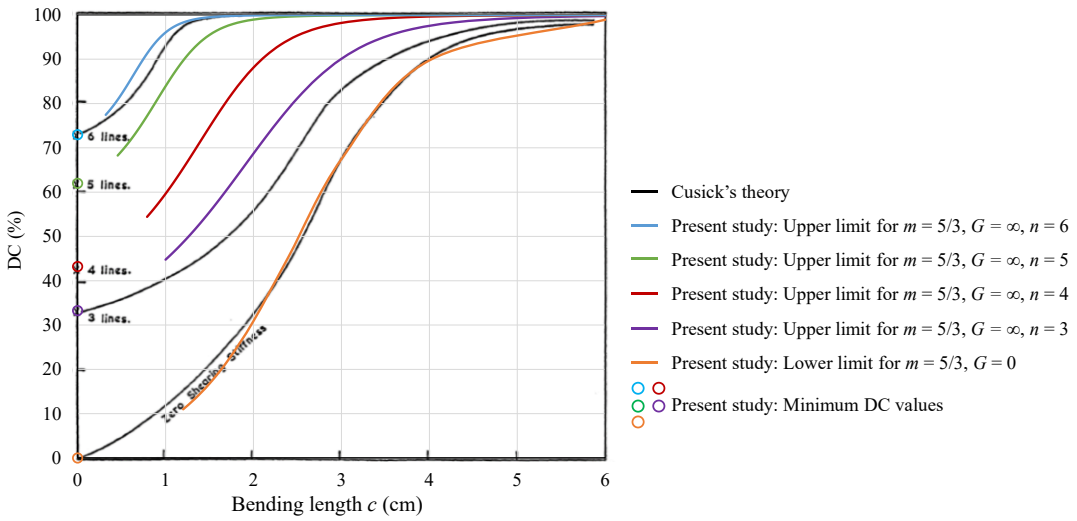

Figure 3.12 Comparison of DC–c curves obtained using Cusick's theory[28] and the presented model when m = 5/3 and L' = 6 cm.

3.5 Conclusion

To investigate the effect of fabric dimension on drape deformation, fabric drapes under various conditions of fabric and support disk radii were numerically analyzed considering the bending rigidity for infinite and zero shear stiffness. A segment cantilever was employed in the theoretical upper-limit calculation of infinite shear stiffness. In the theoretical lower-limit calculation of zero shear stiffness, strip cantilevers of equal length in all radial directions were used in the numerical integration of a differential equation.

For the upper-limit calculation of drape deflection, the drape deformation was categorized into three cases according to the parameters m and m', which are obtained using the relationship between the fabric radius and segment cantilever length. The effects of the segment cantilever length, weight, and bending rigidity are expressed as nondimensional parameters K for Cases I and II and K' for Case III. The normalized deflections are determined by m and K in Cases I and II, and by m' and K' in Case III. For the lower-limit calculation of drape deflection, the deflection is determined by K. The upper and lower limits were compared for the same K or K' in different cases. For Cases I and II, the K values of lower limits can be used directly; for Case III, the K values of lower limits are converted into K'. Even for different fabrics, a similar drape shape is obtained when m and K, or m' and K', are equal in each case. The effects of dimensions on the fabric drape were therefore clarified theoretically. Comparing with Cusick's drape calculation using a strip cantilever, the proposed calculation method using a segment cantilever is more appropriate.

The proposed calculation method was verified with drapes experimentally obtained for eight woven fabrics and one sheet with 14 conditions of radii of the fabric and support disk. The DCs of fabrics, except fabrics having shear stiffness lower than 40 $cN \cdot m^{-1} \cdot degree^{-1}$ among the samples, were between the theoretical upper and lower limit curves for infinite and zero shear stiffness. The DCs of fabric with lower shear stiffness were below but close to the lower limit. When $n = 3$, experimental DCs were close to the upper limit except for fabrics with shear stiffness lower than 40 $cN \cdot m^{-1} \cdot degree^{-1}$ among the samples, the values of which were close to the lower limit. For $n \geq 4$, all experimental DCs approached the lower limit. This is due to double-curvature deformation resulting

from shear stiffness.

Consequently, the effects of dimensions in the drape test considering bending rigidity for infinite and zero shear stiffness were clarified theoretically and experimentally. From the theoretical and experimental results, for both upper and lower limits, with the increase in the dimensionless parameters m and K, or m' and K', the fabric DCs decrease. This is because of the increased own weight of fabric along to the increases in dimensions. In the experimental results, although the fabric DCs are varied due to the differences in bending and shear properties, they are between the upper and lower limits. Hence, the DCs of different fabric with different dimensions can be predict using m and K, or m' and K'. The results in this study will help unify the results of drape test with various dimensions and benefit the simulation of fabric drape for different dimensions. Those results will also help clarify the mechanism of drape and further investigate drape deformation.

A limitation of the present research was that the calculation did not consider the effects of shear stiffness (except for infinite and zero shear stiffness), anisotropy, and structural properties, which are important to drape, but difficult to be obtained with an analytical form. For such calculations, it is necessary to adopt methods such as the finite element method using the results of this study.

References

1. Chu CC, Cummings CL and Teixeira NA. Mechanics of elastic performance of textile materials: Part V: A study of the factors affecting the drape of fabrics—the development of a drape meter. *Textile Research Journal* 1950; 20: 539-548.

2. JIS L 1096: 2010 Testing methods for woven and knitted fabrics.

3. BS 5058: 1973: Method for the assessment of drape of fabrics.

4. ISO 9073-9:2008-Textiles — Test methods for nonwovens — Part 9: Determination of drapability including drape coefficient.

5. Cusick GE. 21—the Measurement of Fabric Drape. *Journal of the Textile Institute* 1968; 59: 253-260. DOI: 10.1080/00405006808659985.

6. Vangheluwe L and Kiekens P. Time Dependence of the Drape Coefficient of Fabrics. *International Journal of Clothing Science and Technology* 1993; 5: 5-8. DOI: 10.1108/eb003022.

7. Kenkare N and May-Plumlee T. Fabric drape measurement: A modified method using digital image processing. *Journal of Textile and Apparel, Technology and Management* 2005; 4: 1-8.

8. Behera BK and Mishra R. Objective measurement of fabric appearance using digital image processing. *Journal of the Textile Institute* 2006; 97: 147-153. DOI: 10.1533/joti.2005.0150.

9. Behera B and Pattanayak AK. Measurement and modeling of drape using digital image processing. *Indian Journal of Fibre & Textile Research* 2008; 33: 230-238.

10. Carrera-Gallissà E, Capdevila X and Valldeperas J. Evaluating drape shape in woven fabrics. *The Journal of The Textile Institute* 2017; 108: 325-336. DOI: 10.1080/00405000.2016.1166804.

11. May-Plumlee T, Eischen J, Kenkare N, et al. Evaluating 3D Drape Simulations: Methods and Metrics. In: *International Textile Design and Engineering Conference (INT-EDEC)* 2003.

12. Pandurangan P, Eischen J, Kenkare N, et al. Enhancing accuracy of drape simulation. Part II: Optimized drape simulation using industry-specific software. *Journal of the Textile Institute* 2008; 99: 219-226. DOI: 10.1080/00405000701489198.

13. Kuijpers A. *Evaluation of Physical and Virtual Fabric Drape Created from Objective Fabric Properties*. The University of Manchester, 2017.

14. Wu YY, Mok PY, Kwok YL, et al. An investigation on the validity of 3D simulation for garment fit evaluation. In: *International conference on Innovative Methods in Product Design* Venice, 2011, pp.463-468.

15. Power J. Fabric objective measurements for commercial 3D virtual garment

simulation. *International Journal of Clothing Science and Technology* 2013; 25: 423-439. DOI: 10.1108/ijcst-12-2012-0080.

16. Kim SH, Kim S and Park CK. Development of similarity evaluation method between virtual and actual clothing. *International Journal of Clothing Science and Technology* 2017; 29: 743-750. DOI: 10.1108/ijcst-01-2017-0001.

17. Sayem ASM. Objective analysis of the drape behaviour of virtual shirt, part 2: technical parameters and findings. *International Journal of Fashion Design, Technology and Education* 2017; 10: 180-189. DOI: 10.1080/17543266.2016.1223810.

18. Hearle JW, Grosberg P and Backer S. *Structural mechanics of fibers, yarns, and fabrics Volume 1*. New York: Wiley-Interscience, 1969.

19. Hearle JWS and Shanahan WJ. 11—an Energy Method for Calculations in Fabric Mechanics Part I: Principles of the Method. *The Journal of The Textile Institute* 1978; 69: 81-91. DOI: 10.1080/00405007808631425.

20. Zheng J, Takatera M, Inui S, et al. Measuring technology of the anisotropic tensile properties of woven fabrics. *Textile Research Journal* 2008; 78: 1116-1123. DOI: 10.1177/0040517507083437.

21. Peiffer J, Kim K and Takatera M. Verification of the effect of yarn torsional rigidity on fabric bending rigidity in any direction. *Textile Research Journal* 2017; 87: 424-432. DOI: 10.1177/0040517516631321.

22. Collier BJ. Measurement of Fabric Drape and its relation to fabric mechanical properties and subjective evaluation. *Clothing and Textiles Research Journal* 1991; 10: 46-52.

23. Morooka H and Niwa M. Relation between drape coefficients and mechanical properties of fabrics. *Journal of the Textile Machinery Society of Japan* 1976; 22: 67-73.

24. Niwa M and Seto F. Relationship between Drapability and Mechanical Properties of Fabrics. *Sen'i Kikai Gakkaishi* 1986; 39: T161-T168.

25. Hu J and Chan Y-F. Effect of Fabric Mechanical Properties on Drape. *Textile Research Journal* 1998; 68: 57-64. DOI: 10.1177/004051759806800107.

26. Testing methods for woven and knitted fabrics.

27. Method for the assessment of drape of fabrics.

28. Cusick GE. *A study of fabric drape*. University of Manchester, Institute of Science and Technology, 1962.

29. Cusick GE. 46—the Dependence of Fabric Drape on Bending and Shear Stiffness. *Journal of the Textile Institute Transactions* 1965; 56: T596-T606. DOI: 10.1080/19447026508662319.

30. Peirce FT. 26—the “Handle” of Cloth as a Measurable Quantity. *Journal of the Textile Institute Transactions* 1930; 21: T377-T416. DOI: 10.1080/19447023008661529.

31. Bickley WG. L.The heavy elastica. *The London, Edinburgh, and Dublin Philosophical Magazine and Journal of Science* 1934; 17: 603-622. DOI: 10.1080/14786443409462419.

32. Takatera M and Shinohara A. An Analysis to Compare Conventional Methods for Estimating Bending Rigidity of Fabrics. *Journal of the Textile Machinery Society of Japan* 1996; 42: 86-92. DOI: 10.4188/jte1955.42.86.

33. Nagai S, Suda N and Inagaki K. An Analysis of F.R.L. Draped Figures for Sheets by Using the Similarity Rule. *J Jpn Res Assoc Text End-Uses* 1999; 40: 738-743.

34. Nagai S, Suda N and Inagaki K. An Estimation of the F.R.L. Draped Figures for Sheets by Using the π-number of the Similarity Rule. *J Jpn Res Assoc Text End-Uses* 2005; 46: 175-183.

35. Nagai S, Suda N and Inagaki K. Applicability of the Evaluation Method of Isotropic Sheets Drapability to That of Textile Fabrics. *J Jpn Res Assoc Text End-Uses* 2008; 49: 413-420.

36. Mizutani C, Amano T and Sakaguchi Y. A new apparatus for the study of fabric drape. *Textile Research Journal* 2005; 75: 81-87. DOI: 10.1177/004051750507500115.

37. Frisch-Fay R. *Flexible bars*. Butterworths, 1962.

38. Hearle JWS, Grosberg P and Backer S. *Structural mechanics of fibers, yarns, and fabrics Volume 1*. Wiley-Interscience, 1969.

Chapter 4

Measurement of local shear deformation in fabric drape using three-dimensional scanning

Chapter 4 Measurement of local shear deformation in fabric drape using three-dimensional scanning

4.1 Introduction

Drape is the large three-dimensional (3D) deformation of fabric that results from gravity and the mechanical properties of fabric. The drapability of fabric is important to a garment's appearance and thus the selection of fabric. The relationship between the drapability and mechanical properties of fabric has been studied since the 1950s. In 1950, Chu et al.[1] proposed the Fabric Research Laboratories (FRL) drape test and defined the drape coefficient (DC), which is an index widely used to evaluate drapability quantitatively. In 1960, they reported that the drapability of fabric was affected by fabric weight, and Young's modulus and the moment of inertia of area, the product of which is the bending rigidity.[2] Cusick[3] investigated the dependence of drape on the bending rigidity and shear stiffness by statistically analyzing the relationship between the DC and those mechanical properties. He showed that both bending and shear properties affect drape where the drape has curvature in more than one direction. Morooka and Niwa[4] investigated the effect of the bending rigidity of fabric on drape in the warp, weft, and 45° bias directions. They conducted multiple regressions to express the DC using the bending rigidity and weight. Niwa and Seto[5] examined the DC using both shear and bending properties, and indicated the effect of shear and bending hysteresis on the DC. Nagai et al.[6] investigated the effects of shear and bending on fabric drape and showed the effect of weight and Young's modulus in the 45° bias direction, which represents the shear stiffness. These studies revealed that drape deformation is affected by the bending rigidity, shear stiffness, and weight. Drape should thus be composed of bending and shear deformation. Whenever bending occurs in more than one direction, because of the double curvature in drape, shear deformation definitely occurs and the deformation

could be unequal[7]. Thus, it is necessary to discuss the effects of bending and shear on fabric drape simultaneously.

These effects on fabric drape have been theoretically analyzed using numerical calculation under appropriate assumptions and restrictions. Cusick[8] calculated the DC using the bending deformation model of a strip cantilever under the conditions of infinite and zero shear stiffness. In Chapter 3, the effect of the fabric dimension on drape deformation has been analyzed using the model of a circular segment cantilever for infinite shear stiffness and the deflection of strip cantilevers in radial directions for zero shear stiffness. Although they showed the effect of shear deformation on drape, it was only discussed for two cases: infinite shear stiffness and zero shear stiffness because of the limitation of theoretical analysis.

To overcome this limitation, many researchers have analyzed fabric drape using the finite element method (FEM) with the measured and/or assumed mechanical properties of fabric. Imaoka et al.[9] and Kang et al.[10] calculated drape deformation using the FEM with the measured or estimated tensile and shear modulus, bending rigidity, and Poisson's ratio. They compared the shapes and contour lines of experimental and calculated drapes. Teng et al.[11] and Hu et al.[12] simulated fabric drape behavior over circular pedestals and compared the simulated drape shape with the experimental shape. Although these researchers were able to calculate drape shape, neither study discussed the local deformation on drape.

By contrast, a particle method using a mass-spring model has also been used to simulate fabric drape for modeling and animation. Lafleur et al.[13] were pioneers of clothing animation using a particle model. Breen et al.[14] conducted drape simulation with approximated bending and shear curves derived from bending and shear properties. Based on their method, many researchers have developed fabric drape models by considering the mechanical properties of fabric. Mitsui et al.[15] calculated fabric drape considering the nonlinearity and anisotropy of fabric. They compared their results with Breen's method from the perspective of bending and shear recovering forces. Dai et al.[16] simulated fabric drape from a drape model by reflecting the mechanical properties of fabric. In addition to bending and shear properties, Dai et al.[17] accounted for fabric twist,

and force and displacement relationships of various types of deformation. They simulated fabric in heart-loop tests and compared it with actual fabric. However, they showed the agreement of only the shape and essential features, and local deformation in drape was not verified because of the lack of a measurement method for local shear deformation.

The drape simulations were conducted based on the measured or estimated mechanical properties. By contrast, some researchers have estimated fabric deformation theoretically or geometrically. Mack and Taylor[18], Shinohara and Uchida[19], and Moriguchi and Sato[20] presented fitting equations based on the shearing behavior of woven fabric on spherical surfaces. For other 3D deformation of fabric, some researchers have proposed algorithms for covering or fitting 3D objects, such as spherical and tubular surfaces, considering the shear deformation of fabric. Heisey et al.[21, 22] proposed a projection method by projecting a known 3D fabric surface onto a two-dimensional surface. Van Der Weeën[23] introduced algorithms for drape fabrics on doubly curved surfaces. Potluri et al.[24] developed a comprehensive drape model for 3D tubular surfaces using existing drape algorithms, but not the fabric drape. Vanclooster et al.[25] conducted forming simulations of woven textile composites using an explicit FEM. Cho et al.[26] proposed a 3D covering algorithm for individual pattern making. Mohammed et al.[27] and Kim et al.[28] investigated the shear deformation of fabric on a spherical surface. Despite many researchers[21-28] proposing calculating algorithms for shear deformation to form composites or for pattern making for garments, the applicability of these algorithms to fabric drape has not been verified.

By applying these algorithms to drape shapes, it will be possible to measure the local deformation of draped fabric. However, researchers have focused on the outline of the drape shape and, to the best of my knowledge, there have been no studies on the measurement of local deformation on draped fabric. To compare the shape of simulated and actual drape, May-Plumlee et al.[29], Kenkare et al.[30], and Pandurangan et al.[31] measured 3D drape shape using 3D scanning technologies. Although they compared the shapes, they focused on the outline of the drape shape and did not discuss the local deformation on drape.

To clarify the effects of shear deformation on drape, in the present paper, I investigate local shear deformation in drape by measuring shear deformation in drape quantitatively, adopting 3D scanning and geometrical covering. My fabric model covers the scanned 3D drape geometrically to allow shear and bending (out-of-plane pin joint rotation) deformation. I calculate the shear angles in the fabric model.[26, 32] By adopting this method, I managed to measure local shear angles in FRL drape, which had not been measured yet. I clarified the locations where the angle of shear deformation occurs in drapes. I also investigated the effects of the relative positions of the node to grainlines that cross at the fabric center (center grainlines), and the bending and shear properties of fabric on local shear deformation. Through this study, the local shear deformation and effect of shear deformation on FRL drape can be clarifed.

4.2 Calculating method for shear deformation

The method for calculating shear deformation is based on the 3D fitting of a woven fabric model to a surface proposed by Cho et al.[26] A 3D scanned surface composed of triangle patches is covered with a fabric model, which is composed of square cells at an interval of r_1. To construct the fabric model that covers the surface, two crossing grainlines are assigned on the surface. From the crossing point of the two grainlines, the cells start to be constructed by allowing trellis (pin-joint) shear deformation, without elongation in the yarn direction. Because compared with shear deformation, the deformation of a woven fabric in the yarn direction under low tension is negligible, thus I assumed no elongation in the yarn direction in my method.[7] Then, the construction of cells repeats at a regular interval of r_1 along the grainlines. It can be used as the covering fabric model. Consequently, the fabric model that covers the surface can be obtained by setting the two grainlines. The fitting algorithm is as follows: Consider a triangle patch $\triangle ABC$ of a 3D scanned surface that has the vertices A, B, and C in 3D space, as shown in Figure 4.1. The assigned grainlines provide three points, P_0, P_1, and P_2, on the surface, where P_0 is the intersection of the two grainlines, and P_1 and P_2 are given by points along each grainline

with a distance r_1 from P_0. To create a cell on $\triangle ABC$, it is necessary to determine a point P_3 that meets the following conditions: (a) it is at an equal distance r_1 from P_1 and P_2; and (b) it is located in $\triangle ABC$.

To determine P_3, I assume two spheres of center points P_1 and P_2, with radius r_1. These two spheres intersect with a plane including P_0. The intersection plane is called Plane Π. This plane includes a circle with the center point Q and radius r_2. Then, P_3 is determined to be a point located on the circle except P_0. The position vector $\boldsymbol{Q}$ of Q can then be expressed using the position vectors $\boldsymbol{P}_1$ and $\boldsymbol{P}_2$ of points P_1 and P_2:

$$\boldsymbol{Q} = \frac{\boldsymbol{P}_1 + \boldsymbol{P}_2}{2} = \frac{2\boldsymbol{P}_1 + \boldsymbol{P}_{12}}{2},\ \boldsymbol{P}_{12} = \boldsymbol{P}_2 - \boldsymbol{P}_{1,} \tag{4.1}$$

where $\boldsymbol{P}_{12}$ is a normal vector to Plane Π.

To investigate which edge of $\triangle ABC$ intersects Plane Π, the scalar products of the vectors $\overrightarrow{QA}$, $\overrightarrow{QB}$, and $\overrightarrow{QC}$,with $\boldsymbol{P}_{12}$, are introduced.

Three conditions need to be discussed:

I: $\overrightarrow{QA} \cdot \boldsymbol{P}_{12} \geq 0$

II: $\overrightarrow{QB} \cdot \boldsymbol{P}_{12} \geq 0$

III: $\overrightarrow{QC} \cdot \boldsymbol{P}_{12} \geq 0$

1. Either condition I is satisfied or condition II and condition III both are satisfied. $\triangle ABC$ is separated by Plane Π, with A on one side, and B, C on the other side; that is, edges AB and AC intersect Plane Π.

2. Either condition II is satisfied or condition I and condition III both are satisfied. $\triangle ABC$ is separated by Plane Π, with B on one side, and A, C on the other side; that is, edges AB and BC intersect Plane Π.

3. Either condition III is satisfied or condition I and condition II both are satisfied. $\triangle ABC$ is separated by Plane Π with C on one side, and A, B on the other side; that is,

edges AC and BC intersect Plane Π.

4. Otherwise, $\triangle ABC$ is parallel to Plane Π; that is, no edge intersects Plane Π.

Based on the above conditions, two intersections E, F of $\triangle ABC$ and Plane Π are defined[33]. Thus, if I want to confirm whether P_3 is located in $\triangle ABC$, it is necessary to investigate whether P_3 is located on line EF.

Because the point F is unknown, to find F, I introduce direction vector $\boldsymbol{L}$ and position vector $\boldsymbol{E}$ of E to express $\overrightarrow{EF}$ as

$$\overrightarrow{EF} = \boldsymbol{E} + \boldsymbol{L}t, \tag{4.2}$$

where t is located at a distance r_2 from Q.

Thus, if P_3 is on EF, it needs to meet the condition that the distance from Q to line EF is r_2. Therefore, the position of P_3 on the surface is determined if the point meets the condition. Then, the cell can be fitted to the curved surface. By repeating the process, a fabric model is obtained that covers the entire surface. The covering process stops when P_3 cannot be found on the surface.

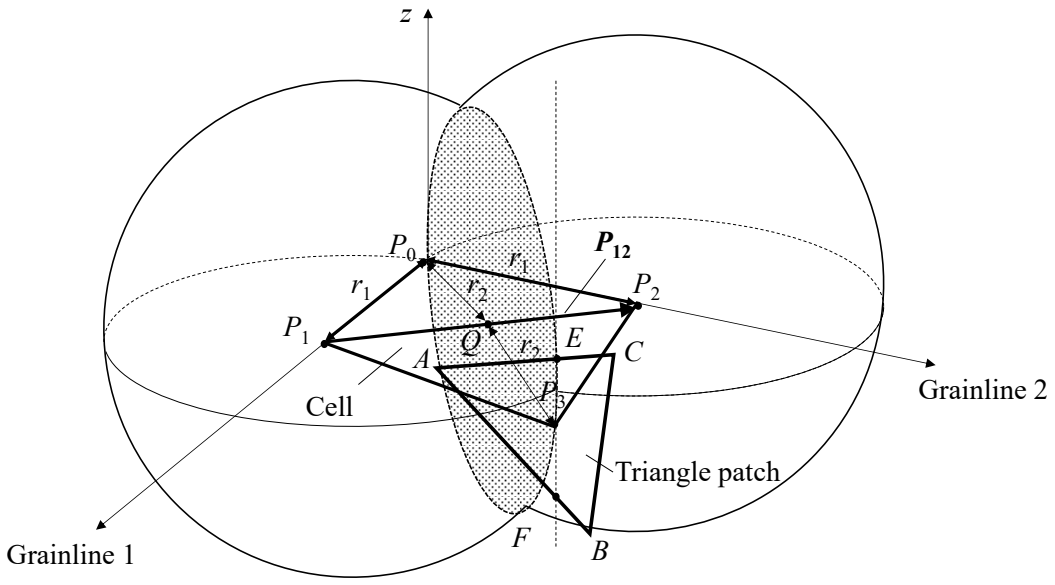

Figure 4.1 Fitting method

With the obtained fabric model, the shear angle of each cell can be calculated. Regarding the calculation of the shear deformation of one cell, because trellis shear is assumed, shear angle θ of each fabric model cell is defined, as shown in Figure 4.2. Among the four angles of each fabric model cell, shear angle θ close to the crossing position of the center grainline is obtained.

To calculate shear angle θ, let $\boldsymbol{P}_0$, $\boldsymbol{P}_2$, $\boldsymbol{P}_{3o}$, and $\boldsymbol{P}_{1o}$ be the position vectors of the vertices for the initial state of a fabric model cell. When $\boldsymbol{P}_{3o}$ and $\boldsymbol{P}_{1o}$ of the cell are deformed to $\boldsymbol{P}_3$ and $\boldsymbol{P}_1$, shear angle θ at $\boldsymbol{P}_0$ is obtained according to the scalar products of two vectors as

$$\cos\left(\frac{\pi}{2}-\theta\right)=\frac{(\boldsymbol{P}_1-\boldsymbol{P}_0)\cdot(\boldsymbol{P}_2-\boldsymbol{P}_0)}{|\boldsymbol{P}_1-\boldsymbol{P}_0||\boldsymbol{P}_2-\boldsymbol{P}_0|}. \tag{4.3}$$

When $\theta \geq 0$, the cell has shear deformation with elongation in the $\boldsymbol{P}_0 - \boldsymbol{P}_3$ direction, as shown in Figure 4.2; and when $\theta < 0$, the cell has shear deformation with elongation in the $\boldsymbol{P}_2 - \boldsymbol{P}_1$ direction.

The absolute value of shear angle θ is used to represent the shear deformation of each fabric cell. The elongated direction is indicated in each cell using its diagonal line.

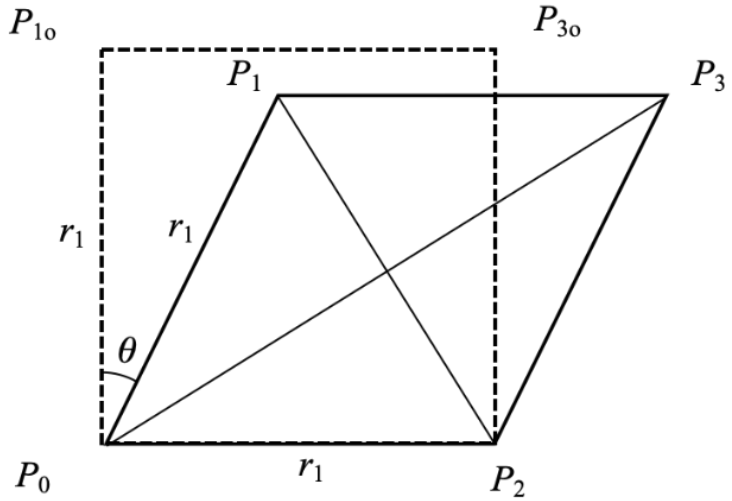

Figure 4.2 Calculation of shear angle θ

4.3 Experimental method and validation of the proposed method

4.3.1 Validation experiment 1: Comparison of the square cells' deformation and position for the calculation and fabric

To confirm the validity of the proposed method, the FRL drape test was performed when the node number (n) was 4 for a woven fabric of wool gabardine as shown in Table 4.1.. In the FRL drape test, the fabric radius (R) of 14 cm and disk radius (r) of 7 cm were used according to Yang et al.[34]

The warp and weft grainlines of the circular sample fabrics were traced as crossing at the center. These grainlines are defined as the center grainlines. Square cells with dimensions of 1 cm × 1 cm were drawn on the fabric parallelly along the center grainlines. The fabric was sandwiched between two disks with the radius of 7 cm. Then, draped fabric with drawn lattices was obtained.

Figure 4.3 shows the coordinate system and the measuring method of drape. The draped shape of the sample was scanned using a portable structured light 3D scanner (Artec Eva Lite, Artec 3D, Luxembourg, Luxembourg)[35]. The scanner had two geometry-capturing cameras, one texture-capturing camera, and one light generator. The structured light pattern generated by the light generator was projected onto an object. Then, the two geometry cameras captured the object image with the deformed light pattern, and the texture camera captured the object photo image without the light pattern, which is called the texture. The triangulation of the object was performed using a structured light tracking algorithm based on the captured images. The ability of a scanning system to resolve detail in the scanned object was up to 0.5 mm.

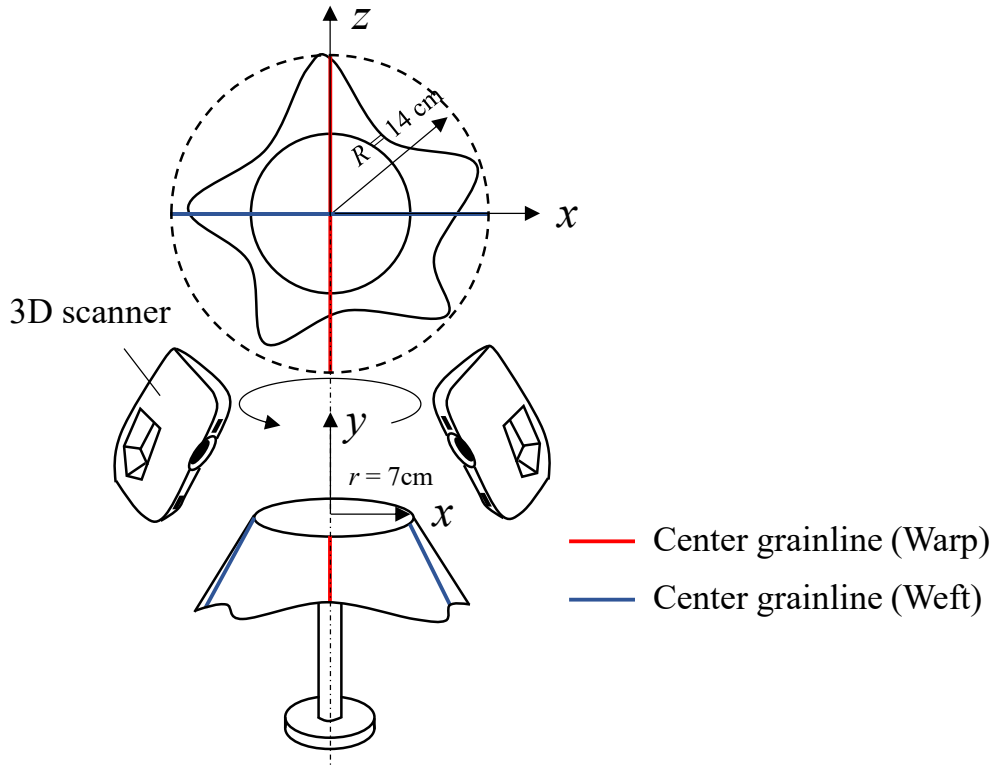

Figure 4.3 Drape test and 3D scanning

Scanning was conducted from multiple directions by moving the scanner around the drape shape manually, as shown in Figure 4.3 A 3D polygon mesh of drape (drape mesh) with texture (photographic image of the surface) was obtained using Artec Studio v9.2 software (Artec 3D, Luxembourg, Luxembourg). At this stage, the obtained drape mesh could not be used because of noise on the surface. To remove noise, a smoothing process was applied to the drape mesh, and a new smoothed drape mesh was obtained, but the texture disappeared. To set the grainlines on the smoothed 3D drape mesh, it was necessary to confirm the position of the grainlines using the texture on the smoothed drape mesh. Thus, screen images of the drape mesh with texture were captured from multiple angles in advance and the captured images were superposed on the surface of the smoothed drape mesh at the same scale. A smooth drape mesh with texture was thus obtained. The unnecessary thickness of the disk was removed. By tracing the center grainlines on the texture, the center grainlines on the smoothed drape mesh were set. Then, the obtained drape mesh was covered with the fabric model, which had a cell size of 1cm × 1cm. Simultaneously, the shear angle of each fabric model cell was calculated.

Then to evaluate the accuracy of fitting of the square fabric model cells on the 3D drape mesh, the lattices marked on the drape mesh and the fabric model cells were compared in terms of shape and position. I compared the coordinates of crossing points of the lattice on the scanned 3D drape mesh and crossing points of the square cells in the fabric model, in the areas of the four nodes where the texture can be clearly obtained. I calculated the root mean square deviation (RMSD) of the coordinates and the distances of the corresponded points to evaluate the error.

Results

Figure 4.4(a) shows the 3D drape mesh with lattices after the disk was cut. Figure 4.4(b) shows the superposed results of lattices marked on the 3D drape mesh and the fabric model cells. Figure 4.4(c) shows the proposed fabric model, with colors representing the shear angle in each cell. As shown in Figure 4.4(b), the fabric model cells coincide with the lattices drawn on the fabric in terms of both the deformed shape and position.

Using x, y, z coordinate system shown in Figure 4.3, I obtained 203 sets of coordinate values for the crossing points of the lattice on the scanned 3D drape mesh and compared them with corresponded coordinate values for the crossing points of square fabric cells. Figure 4.5 shows the comparison of the coordinate values. The results showed a good agreement between the points of scanned 3D drape mesh and the points of square fabric cells. In terms of x, y, and z coordinate values, all of them had high coefficients of determination of 0.99. Those average differences of x, y, and z components are 0.60 mm, 0.98 mm, and 0.59 mm. The RMSDs are 0.30, 0.70, and 0.30, respectively. The average distance between the corresponded points is 0.86 mm. The RSMD is 0.93. The deviation of them is considered due to the error of the 3D scanner (0.5mm). Thus, the validity of the method is demonstrated. Therefore, by determining two center grainlines on the drape surface, local shear deformation was obtained.

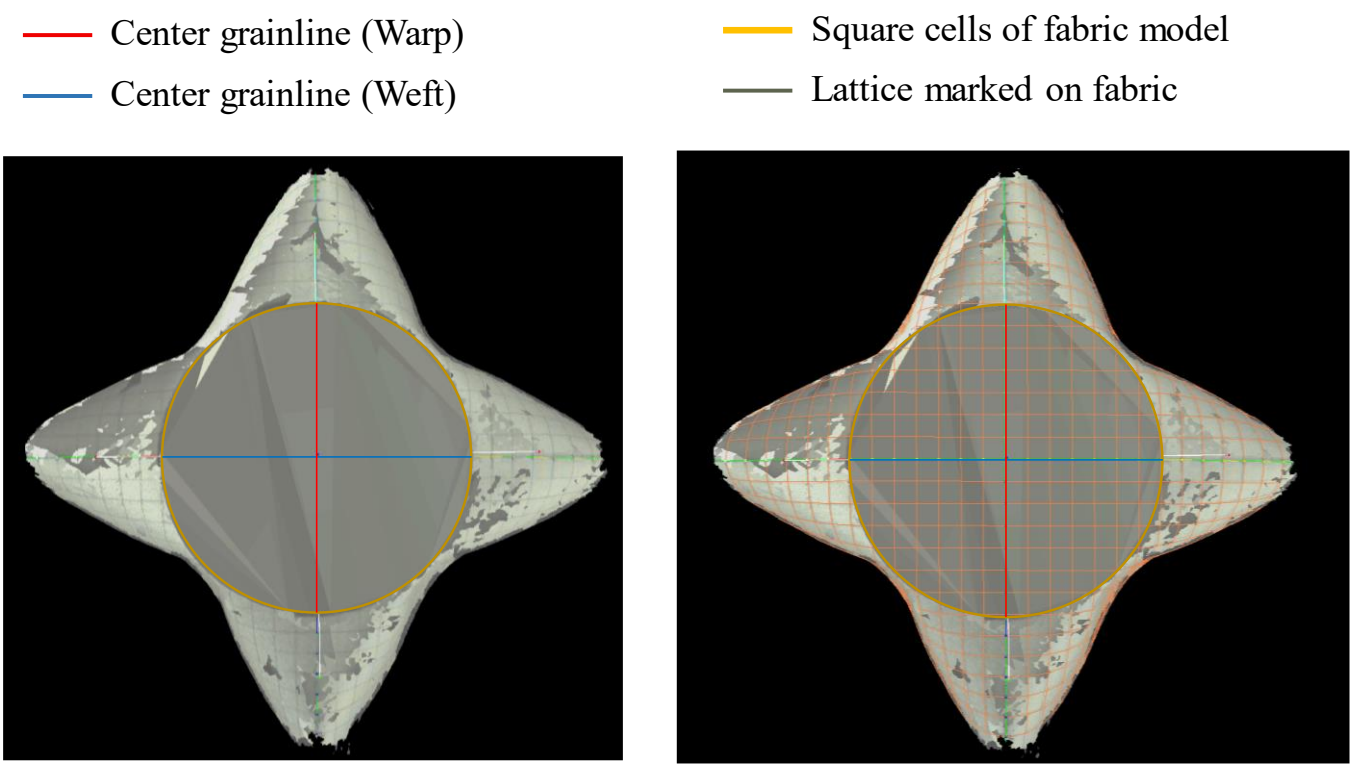

(a) 3D fabric drape mesh with lattices after the disk was cut

(b) Superposed results of marked lattices on the 3D fabric drape mesh and the fabric model cells

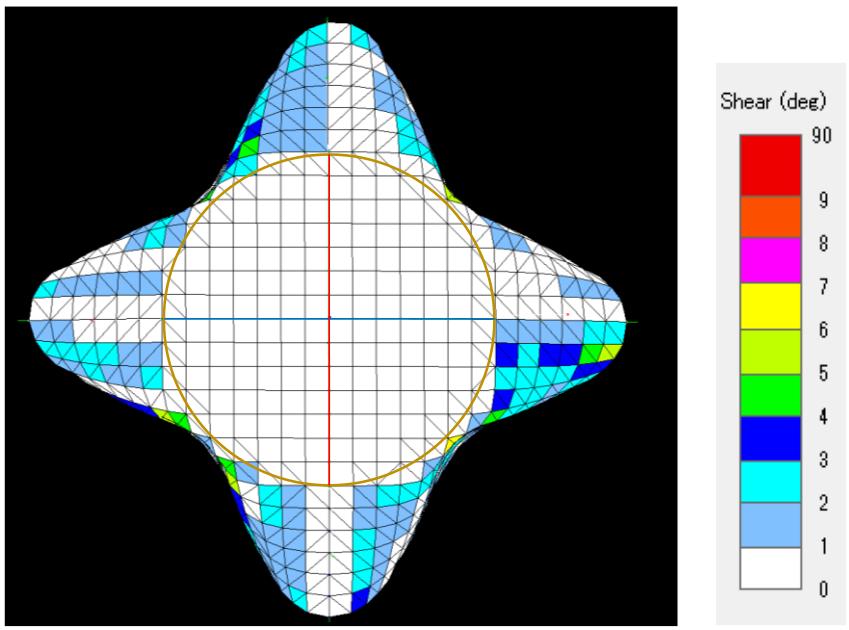

(c) Fabric model with square cells (Color indicates shear angle.)

Figure 4.4 Lattice marked on the fabric and square fabric model cells

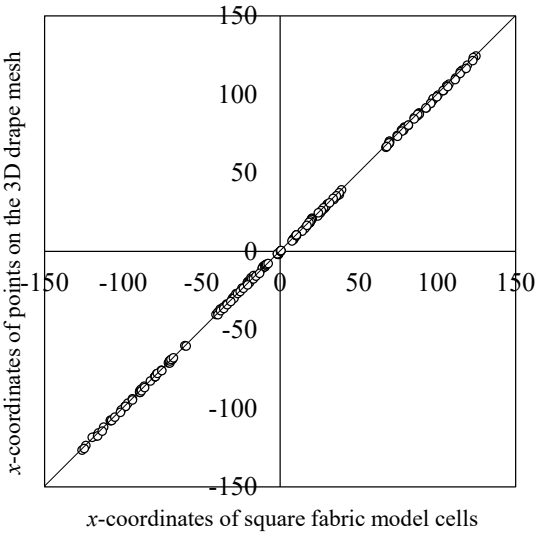

(a) *x*-coordinate

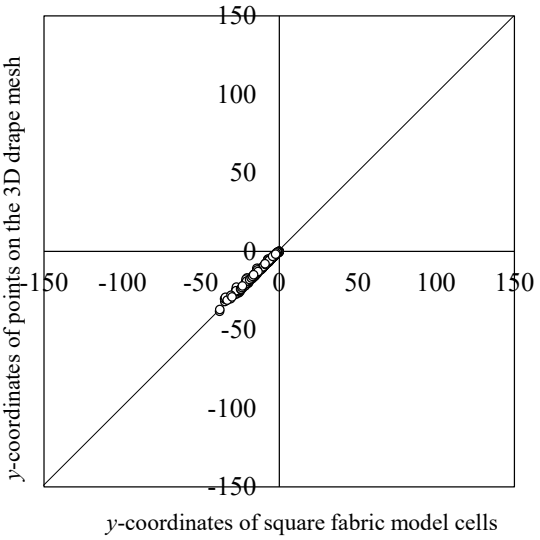

(b) *y*-coordinate

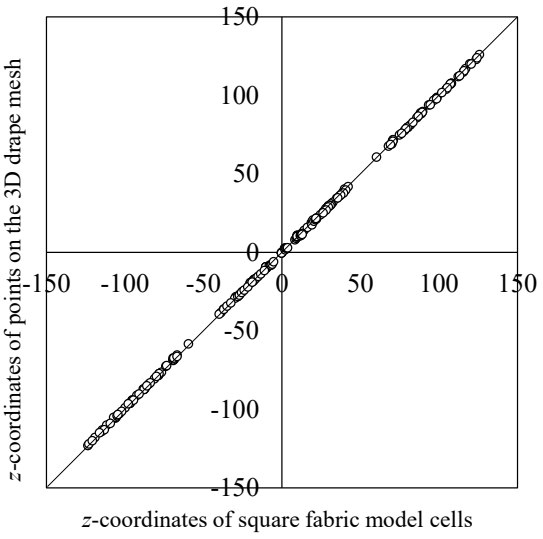

(c) *z*-coordinate

Figure 4.5 Comparison of the coordinate values for the crossing points of marked lattice on the scanned 3D drape mesh and the corresponding points on square fabric cells

4.3.2 Validation experiment 2: Effect of the cell size on the fabric model calculation

To evaluate the effect of the square cell size, the calculated shear angles of cotton broadcloth as shown in Table 4.1 were compared for $n = 3$, but with different cell sizes of 3 mm, 5 mm, and 10 mm. The difference between shear angles for different cell sizes was evaluated using the shear angle ratio of each angle range defined as follows:

$$\text{Shear angle ratio in a given angle range (\%)} = \frac{\text{Number of cells in the given angle range}}{\text{Total number of cells} - \text{Number of square cells in the disk area}} \times 100. \quad \textbf{(4.4)}$$

Because the shear angle of the fabric was considered to be below 10º, the shear angle range was divided into 10 groups.

Results

Figure 4.6 shows a comparison of the obtained shear angle ratio for the same sample but with different cell sizes. The average of three sizes and the standard deviation among the obtained shear angle ratio for the three cell sizes are also shown. The maximum standard deviation was 2.31% for shear angles in the range of 1º–2º, which means that the difference caused by the linear approximation of a cell was small.

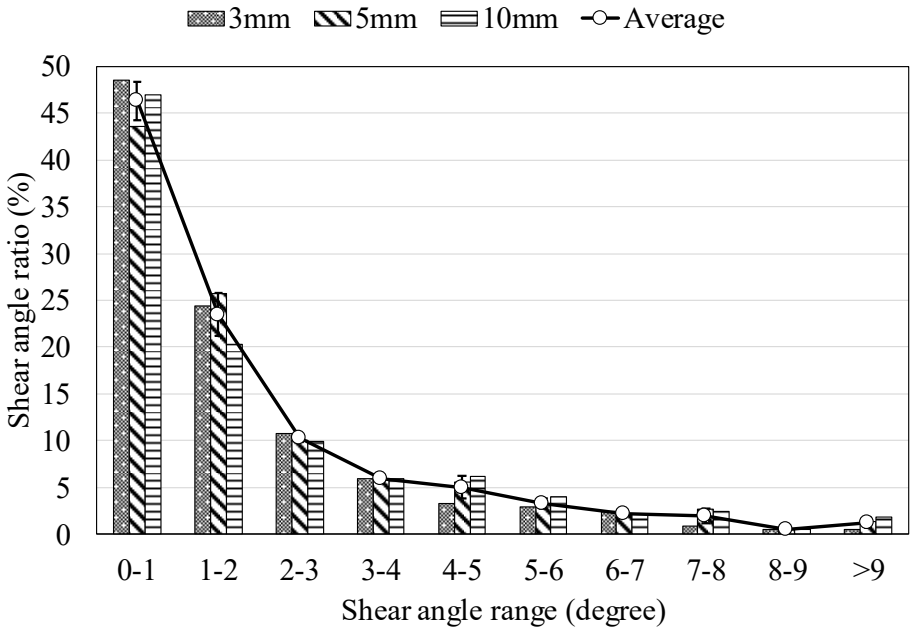

Figure 4.6 Comparison of the shear angle ratio for broadcloth (n =3) but with different square cell sizes in the fabric model

4.4 Measurement of local shear deformation on FRL drape for various node numbers

Because I demonstrated the validity of the proposed method, I investigated the local shear deformation on FRL drape using the proposed method.

FRL drape tests were performed using four types of woven fabric (broadcloth, taffeta, satin, and denim) to measure the shear angle of draped fabrics. The experimental conditions for the radii of the fabric sample and disks were the same as those in 4.3.1 *Validation experiment 1*. The node number (n) in the tests was manually set to 3, 4, 5, and 6.[34] To investigate the effect of the grainline direction on local shear deformation, the node locations of n=4 were controlled with respect to the grainlines; that is, along the center grainline directions and in the bias directions. Then, the scanning process was conducted to obtain the drape mesh.

The obtained drape mesh was covered with the fabric model, which had cell sizes of

0.5cm × 0.5cm. Simultaneously, the shear angle of each fabric model cell was calculated. To investigate local shear deformation, the shear angle ratios for each drape mesh were calculated for the same nine groups using Equation (4).

The sample properties are presented in Table 4.1. The bending rigidity and shear stiffness of the samples were measured using the Kawabata Evaluation System for Fabrics (KES-FB, Kato Tech., Kyoto).[36]

Table 4.1 Sample specifications

Sample	Material	Weave	Thickness(mm)	Area density w ($g \cdot m^{-2}$)	Bending rigidity B (10^{-4} $cN \cdot m^2 \cdot m^{-1}$)				Shear stiffness G ($cN \cdot m^{-1} \cdot degree^{-1}$)		
					Warpwise	Weftwise	Bias(45°)	Mean	Sliding in warp direction	Sliding in weft direction	Mean
Gabardine	Wool 100%	Twill	0.509	188	8.91	5.33	6.74	6.99	54.9	75.5	65.2
Broadcloth	Cotton 100%	Plain	0.431	112	5.23	4.01	3.47	4.24	68.6	91.1	79.9
Taffeta	Polyester 100%	Plain	0.199	82.6	11.1	10.0	6.05	6.50	227	175	201
Satin	Polyester 100%	Satin	0.435	187	10.6	67.0	19.4	32.3	139	110	125
Denim	Cotton 100%	Twill	1.07	226	13.2	2.83	4.74	6.91	109	124	116

4.5 Results and discussion

4.5.1 Local shear deformation in FRL drape

Figures 4.7- 4.10 show colored cells according to the calculated shear angles of the sample fabrics in drapes and those depicted on the initial flattened patterns for various node numbers (n). The shear angle range was divided into 10 groups with an interval of

1° using the same method used in 4.3.2 *Validation experiment 2*. Figure 4.11 shows the shear angle ratio of the samples binned with a shear interval of 1° for different node numbers.

Figure 4.11 shows that the shear angle ratio in the shear angle range 0°–1° was highest; over 40% for all fabrics, except denim, which was over 30%. Then, the shear angle ratio decreased as the shear angle ranges increased for all samples. Relatively large shear angles over 3º were below 16% for all samples. Among the same shear angle ranges for different node numbers for a shear angle ratio for shear angles >1°, no obvious increase nor decrease was observed. However, the shear angle ratio in the range 0°–1° increased from n = 3 to n = 4 and then decreased from n = 4 to n = 6. The percentage of node numbers along the center grainlines for all nodes when n = 4 in the center grainlines (4/4 = 100%) was higher than that when n = 3 (1/3 = 33%), 5 (1/5 = 20%), and 6 (2/6 = 33%). Therefore, the shear angle ratio is related to the node position relative to the center grainlines.

From Figures 4.7- 4.10, irrespective of the value of n and the fabric, most of the shear deformation with shear angles in the range 0º–3º was observed in the areas along the center grainlines, such as the two sides of a single node and the depressed area between adjacent nodes along those directions. Shear deformation with a shear angle >3º occurred for nodes and the depressed area in the bias directions, and along the tangents to the support disk. The results demonstrated that discontinuous deformation occurred in these areas of drape, such as buckling wrinkles. In Figure 4.7 (b-2) and Figure 4.10 (d-2), larger shear angles over 7º occurred on the edges of the fabric circle. This could be because of the large depression at the edge by double curvature.

From the observations obtained from Figures 4.7- 4.10, a drape surface is classified into four areas for shear deformation, as shown in Figure 4.12.

- Area a: area without deformation; that is, the area of the support disk plane such that there is no bending nor shear deformation.
- Polygon edge b: polygonal edges connected with tangents to the support disk with a relatively large shear deformation. There is a sudden change of fabric deformation, such as wrinkling, which could lead to discontinuous shear and bending

deformation.

- Area c1: areas along the center grainlines with relatively low shear angle deformation. These areas are not planar, so they could deform with single curvature bending, which is bending deformation with zero Gaussian curvature. These areas are divided into two areas, Area c1-c and Area c1-d, which are the convex area of the node and the depressed area between adjacent nodes, respectively.

- Area c2: areas not along the center grainlines with non-uniform and relatively large shear angle deformation. It could deform with double curvature bending and is not in a developable surface that requires elongation and/or contraction to form. Therefore, fabric could be elongated in the bias directions because it is easy to shear. These areas are also divided into two areas: Area c2-c and Area c2-d, which are the convex area of the node and the depressed area between two adjacent nodes, respectively.

From these local shear deformations, the results demonstrate that drape deformation is characterized by four areas according to shear deformation. Consequently, the results clarify that the relative node positions along the center grainlines affect local shear deformation.

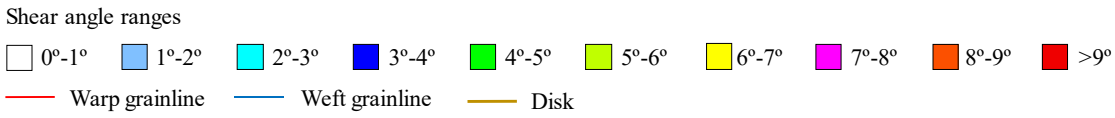

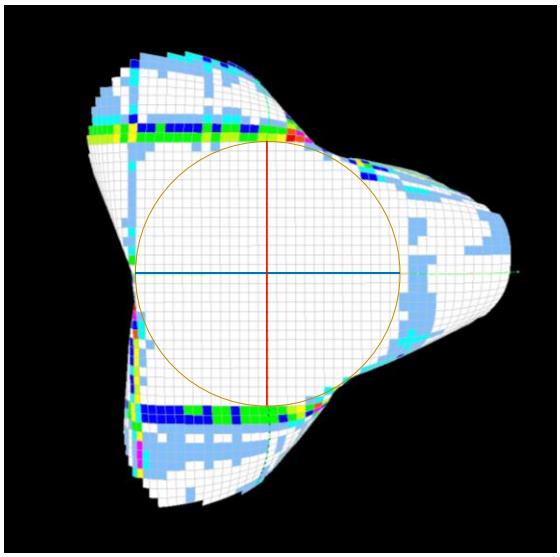

(a-1) Shear angles in drape for $n = 3$

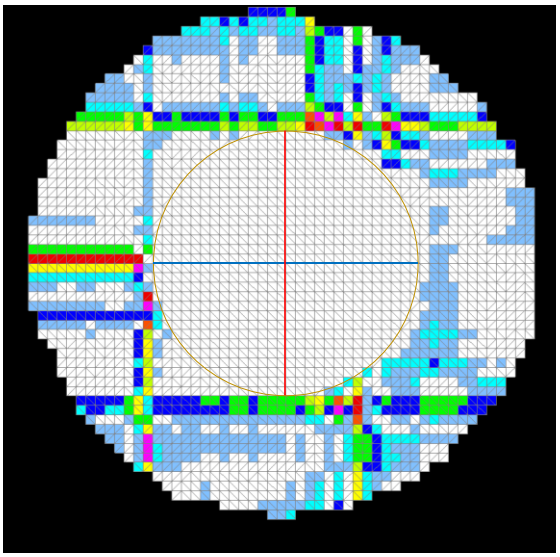

(a-2) Shear angles depicted to the plane for $n = 3$

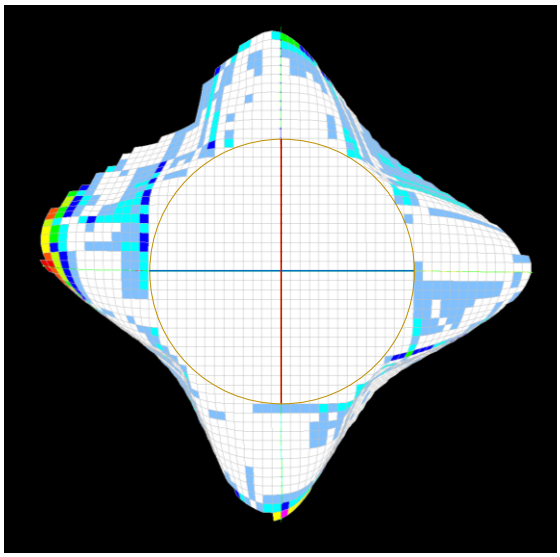

(b-1) Shear angles in drape for $n = 4$ (nodes along the center grainline directions)

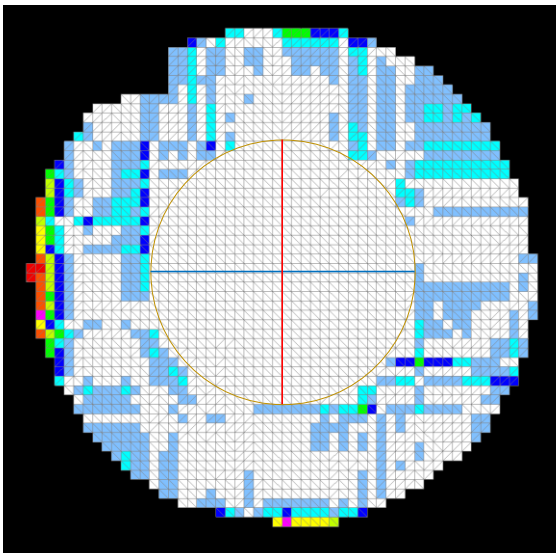

(b-2) Shear angles depicted to the plane for $n = 4$ (nodes along the center grainline directions)

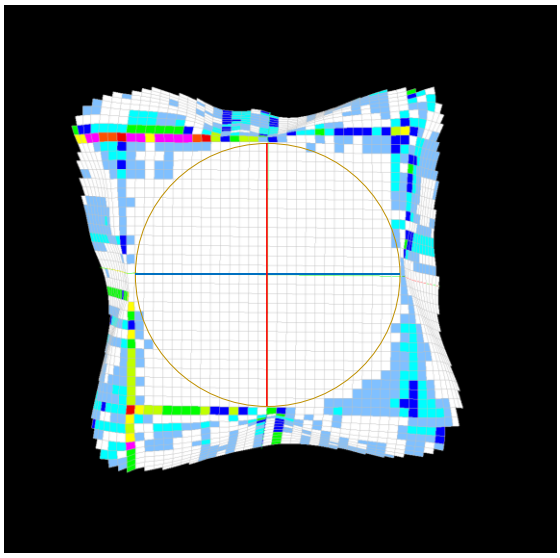

(c-1) Shear angles in drape for $n = 4$
(nodes in the bias directions)

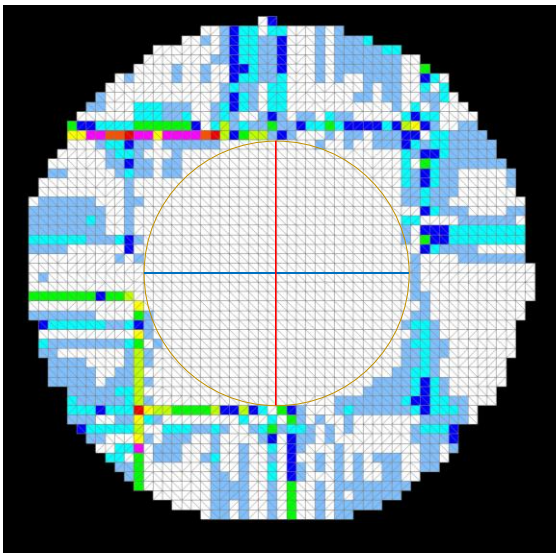

(c-2) Shear angles depicted to the plane for $n = 4$
(nodes in the bias directions)

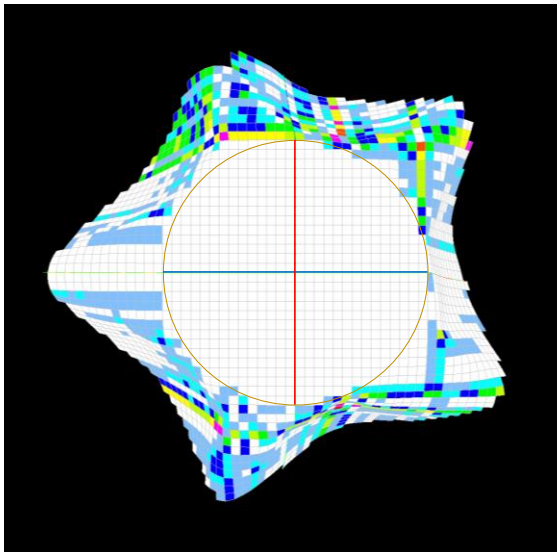

(d-1) Shear angles in drape for $n = 5$

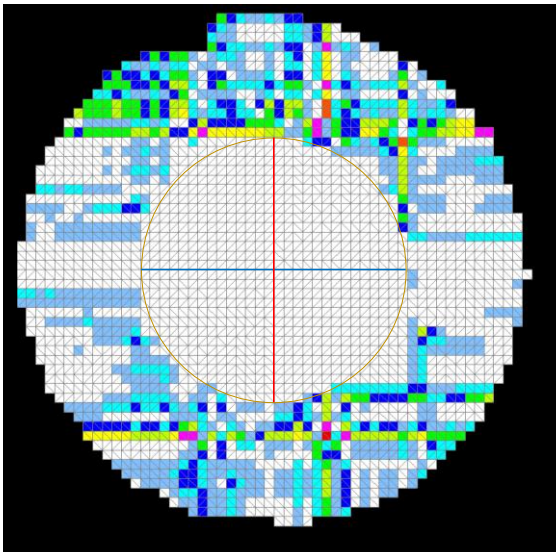

(d-2) Shear angles depicted to the plane for $n = 5$

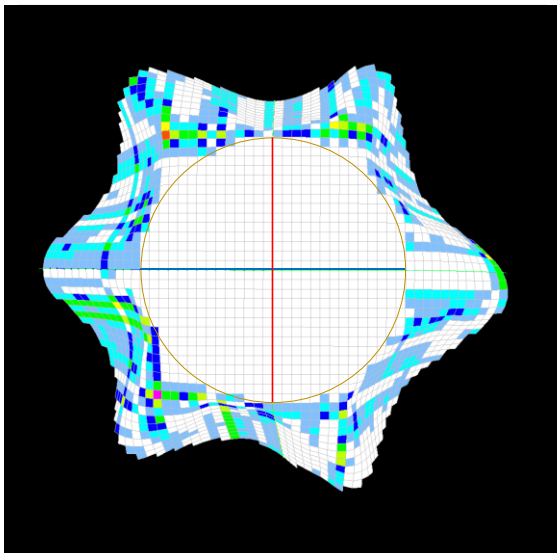

(e-1) Shear angles in drape for $n = 6$

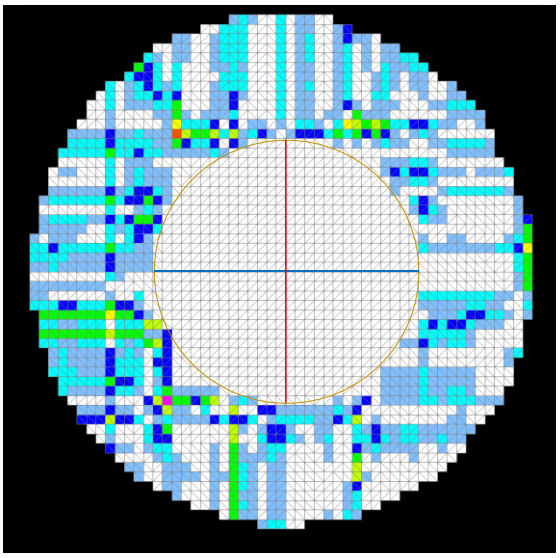

(e-2) Shear angles depicted to the plane for $n = 6$

Figure 4.7 Calculated shear angles for draped broadcloth and those depicted on the initial flattened patterns for various node numbers (*n*)

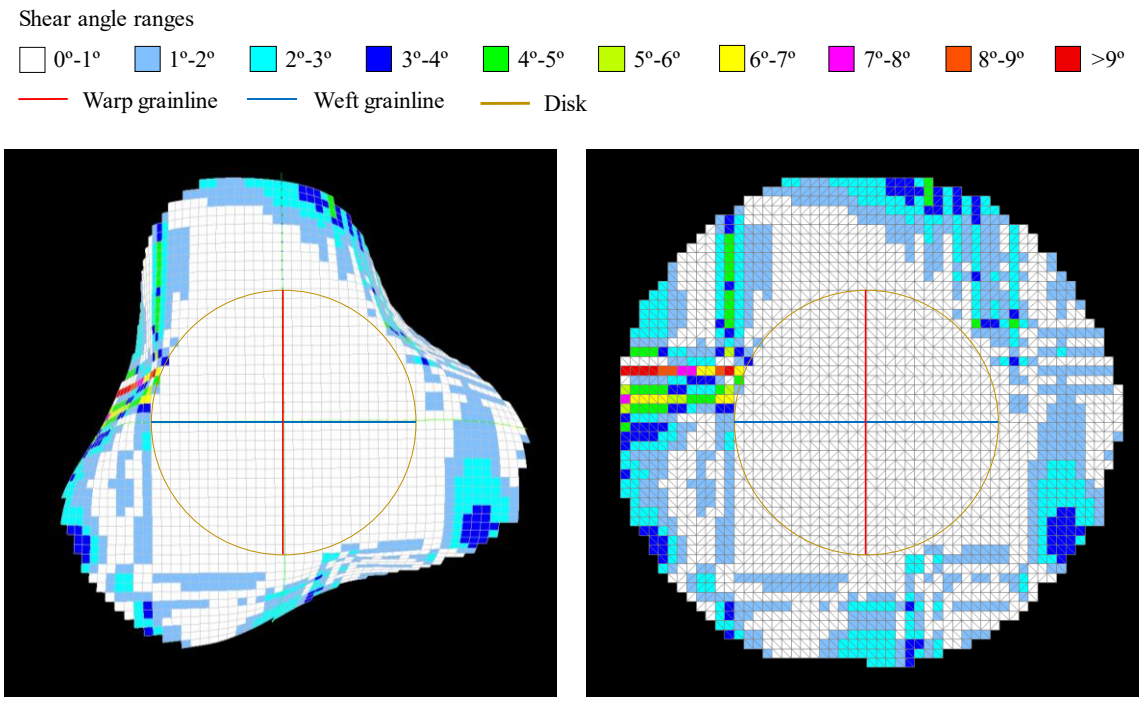

(a-1) Shear angles in drape for $n = 3$

(a-2) Shear angles depicted to the plane for $n = 3$

(b-1) Shear angles in drape for $n = 4$ (nodes along the center grainline directions)

(b-2) Shear angles depicted to the plane for $n = 4$ (nodes along the center grainline directions)

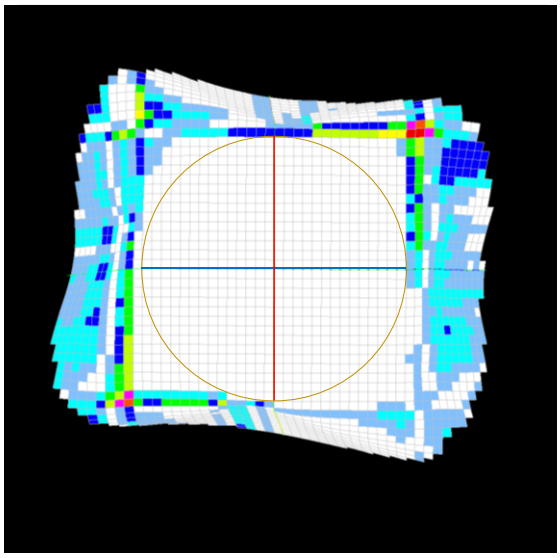

(c-1) Shear angles in drape for $n = 4$
(nodes in the bias directions)

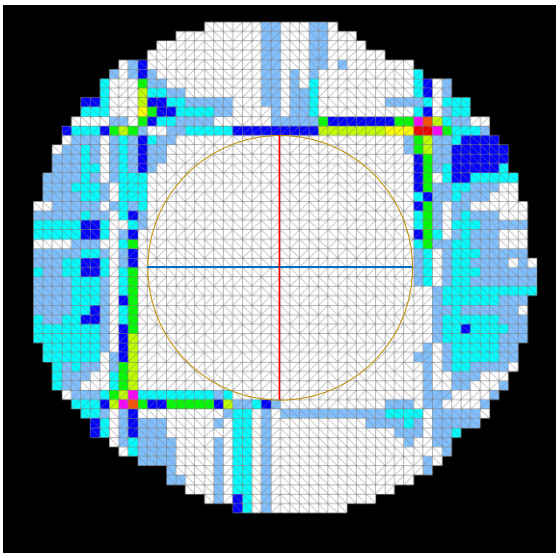

(c-2) Shear angles depicted to the plane for $n = 4$
(nodes in the bias directions)

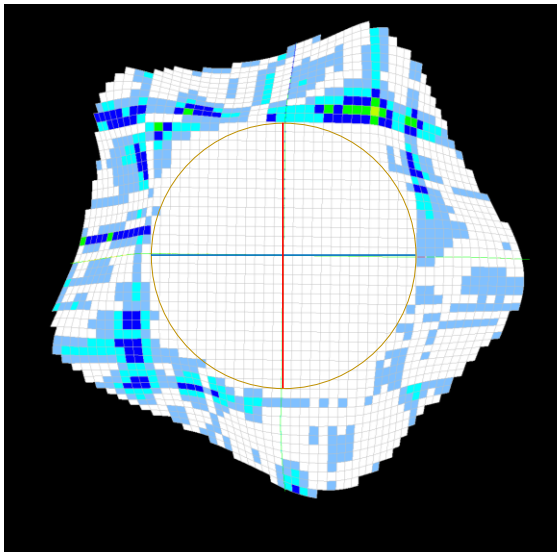

(d-1) Shear angles in drape for $n = 5$

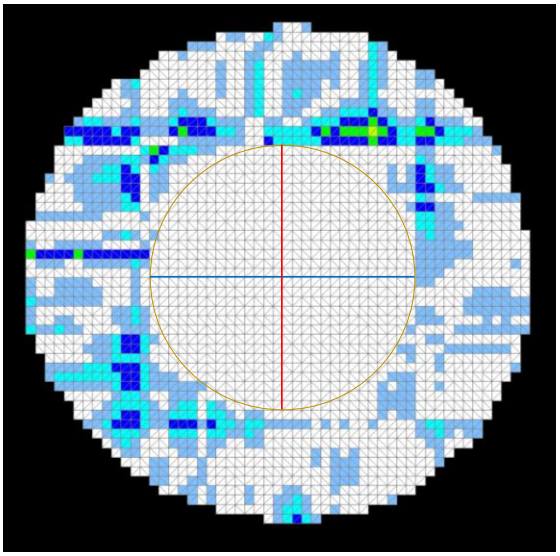

(d-2) Shear angles depicted to the plane for $n = 5$

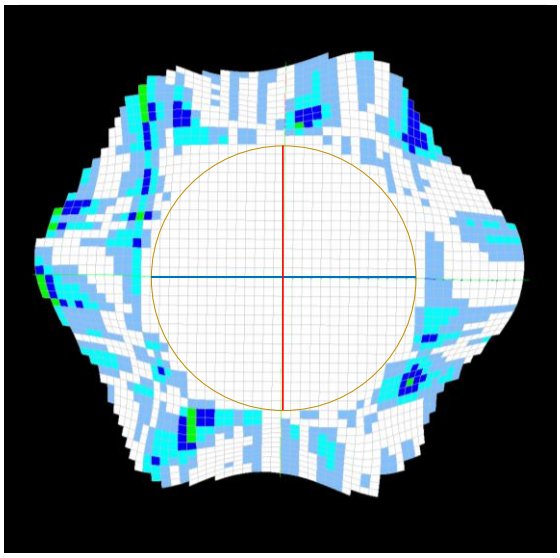

(e-1) Shear angles in drape for n = 6

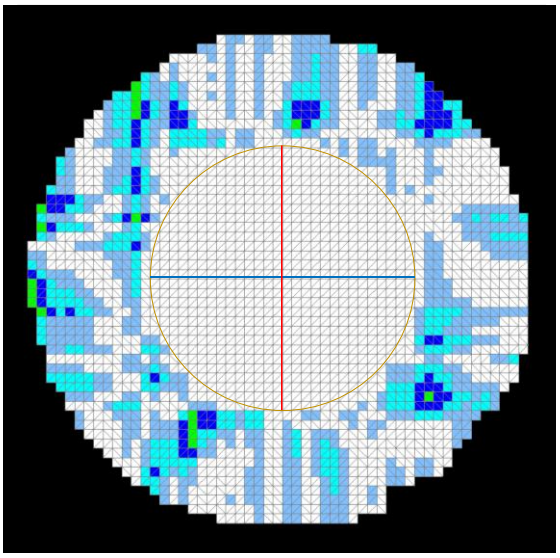

(e-2) Shear angles depicted to the plane for n = 6

Figure 4.8 Calculated shear angles for draped taffeta and those depicted on the initial flattened patterns for various node numbers (n)

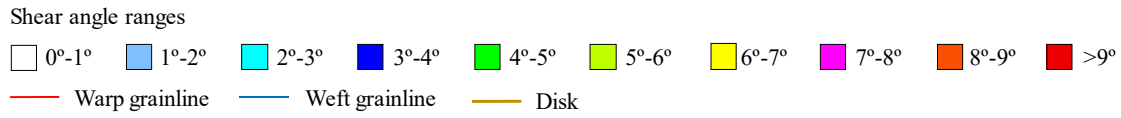

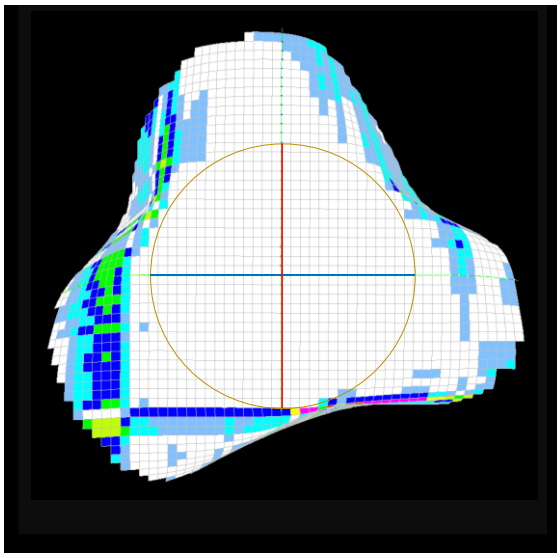

(a-1) Shear angles in drape for $n = 3$

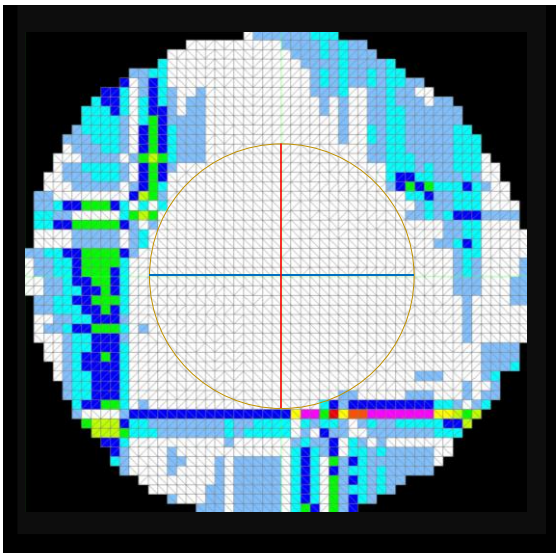

(a-2) Shear angles depicted to the plane for $n = 3$

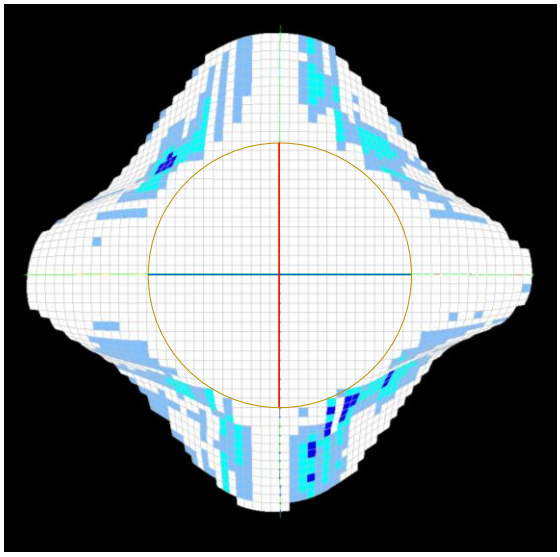

(b-1) Shear angles in drape for $n = 4$ (nodes along the center grainline directions)

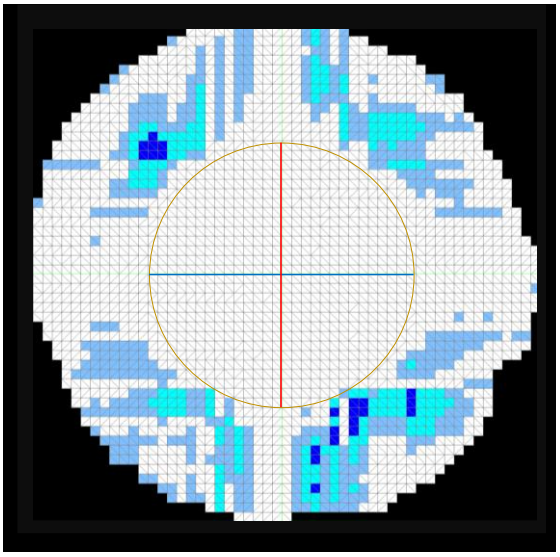

(b-2) Shear angles depicted to the plane for $n = 4$ (nodes along the center grainline directions)

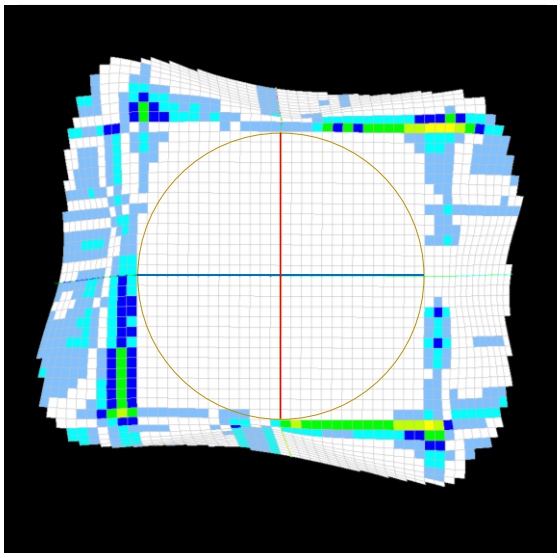

(c-1) Shear angles in drape for $n = 4$
(nodes in the bias directions)

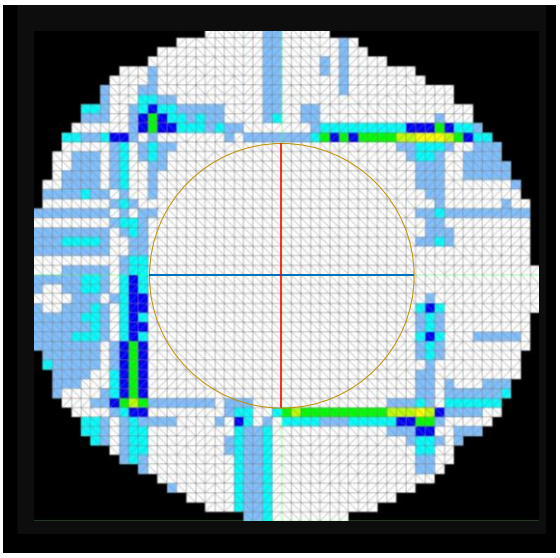

(c-2) Shear angles depicted to the plane for $n = 4$
(nodes in the bias directions)

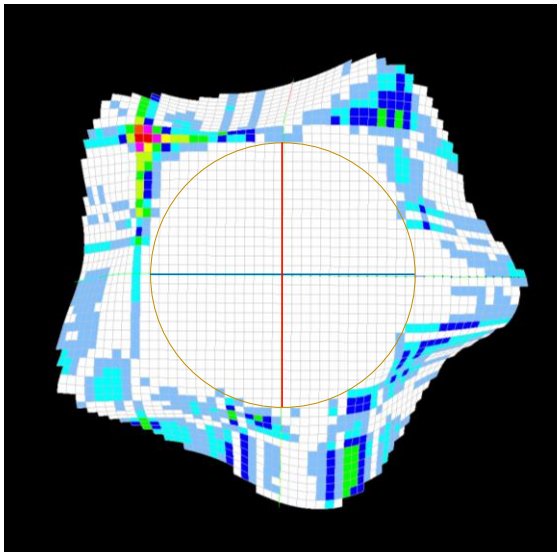

(d-1) Shear angles in drape for $n = 5$

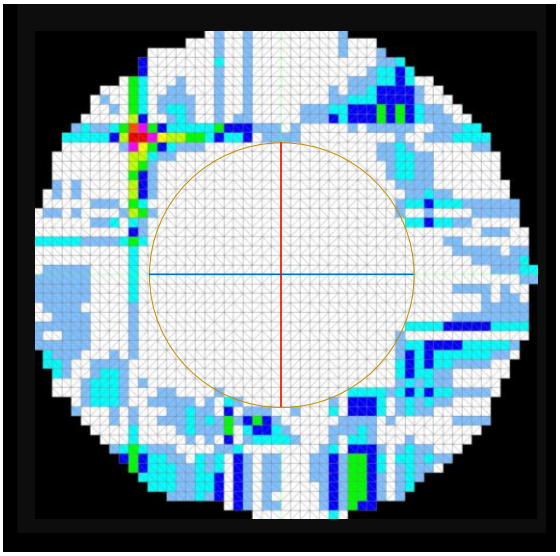

(d-2) Shear angles depicted to the plane for $n = 5$

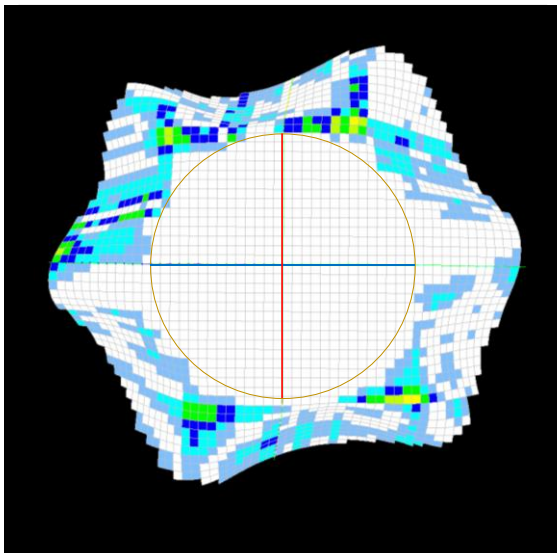

(e-1) Shear angles in drape for n = 6

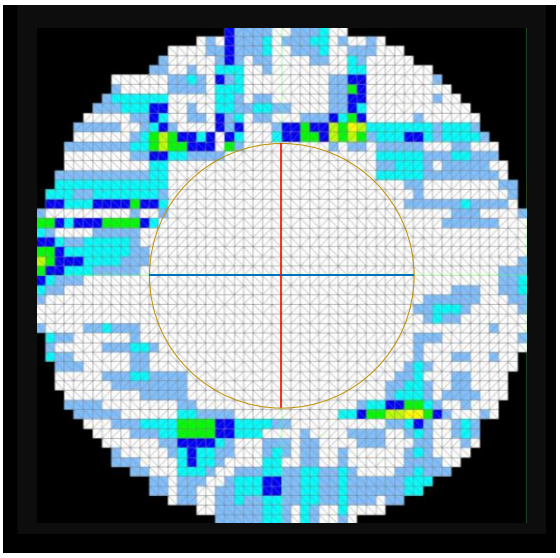

(e-2) Shear angles depicted to the plane for n = 6

Figure 4.9 Calculated shear angles for draped satin and those depicted on the initial flattened patterns for various node numbers (n)

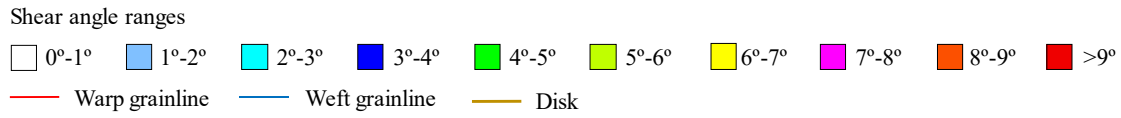

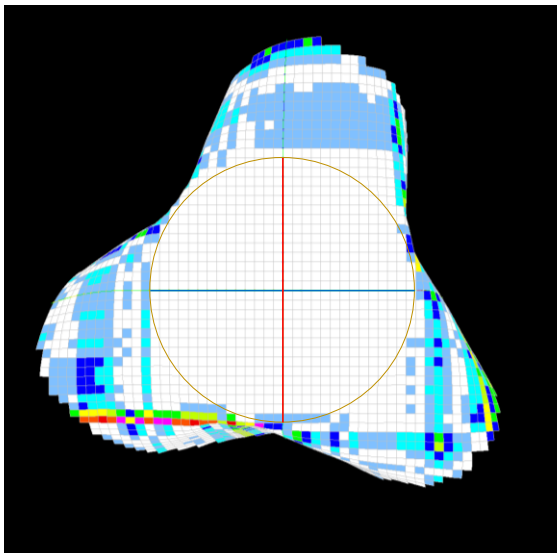

(a-1) Shear angles in drape for $n = 3$

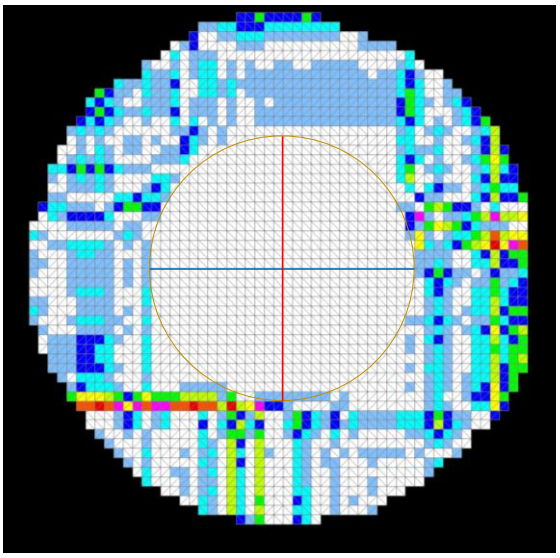

(a-2) Shear angles depicted to the plane for $n = 3$

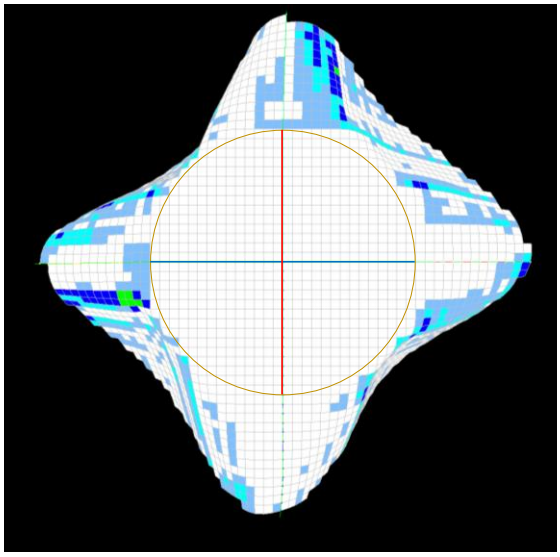

(b-1) Shear angles in drape for $n = 4$ (nodes along the center grainline directions)

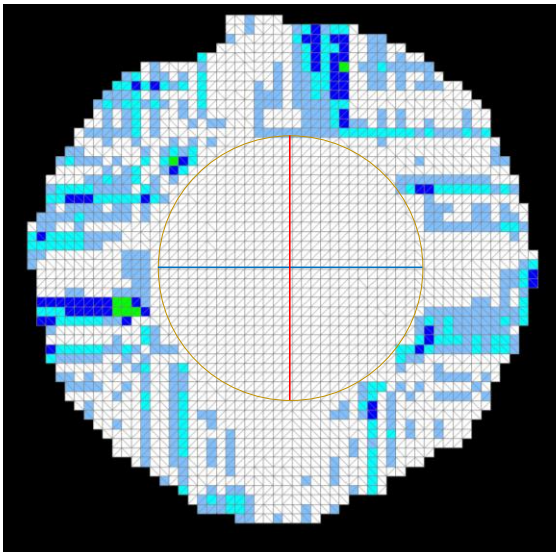

(b-2) Shear angles depicted to the plane for $n = 4$ (nodes along the center grainline directions)

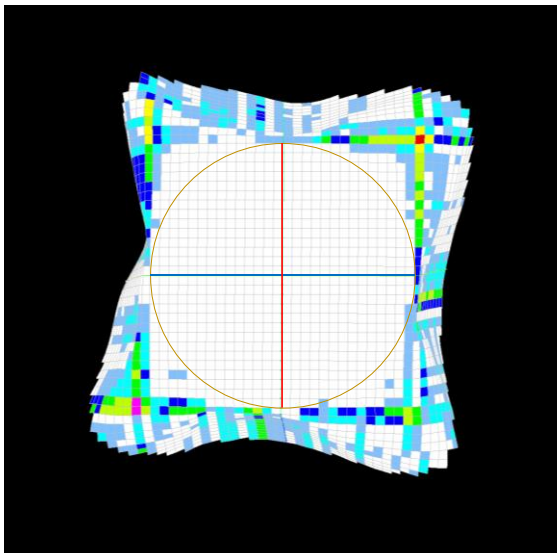

(c-1) Shear angles in drape for $n = 4$
(nodes in the bias directions)

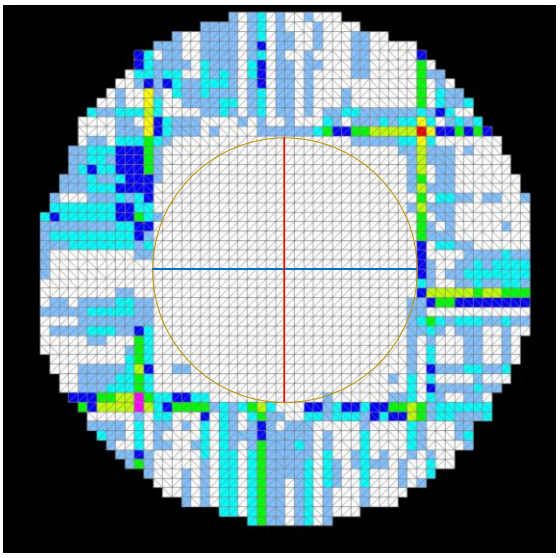

(c-2) Shear angles depicted to the plane for $n = 4$
(nodes in the bias directions)

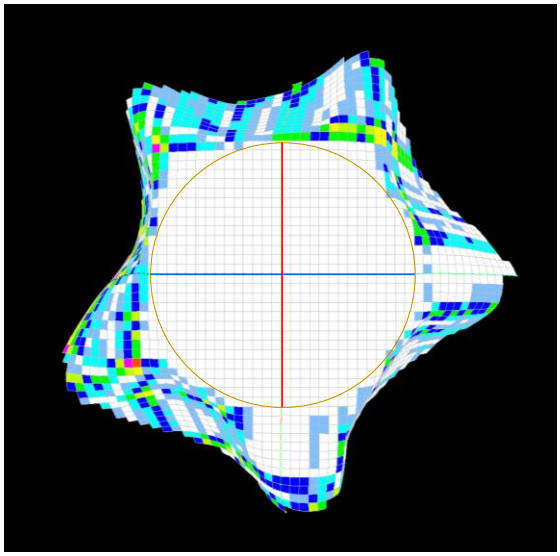

(d-1) Shear angles in drape for $n = 5$

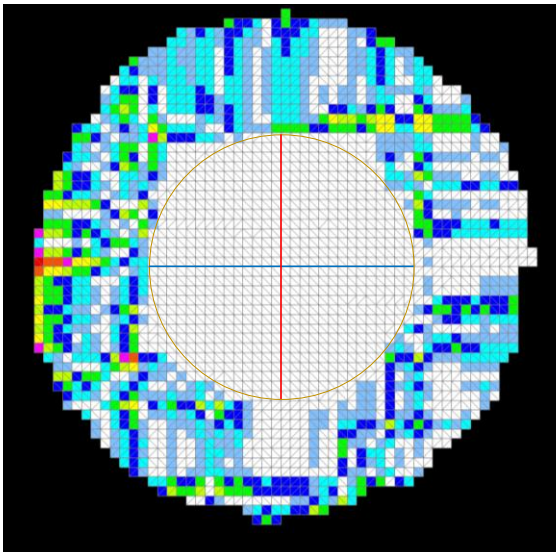

(d-2) Shear angles depicted to the plane for $n = 5$

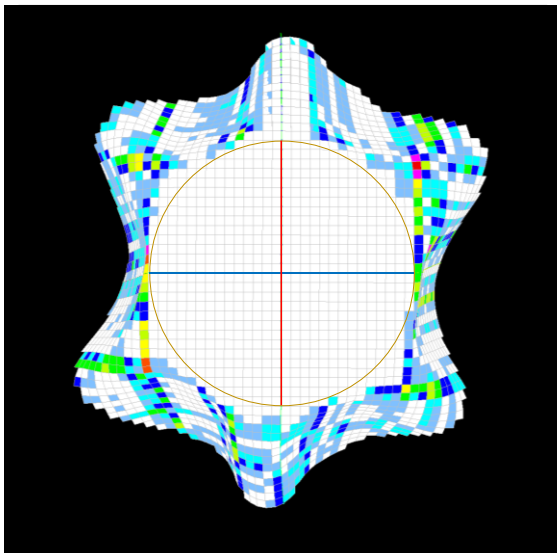

(e-1) Shear angles in drape for $n = 6$

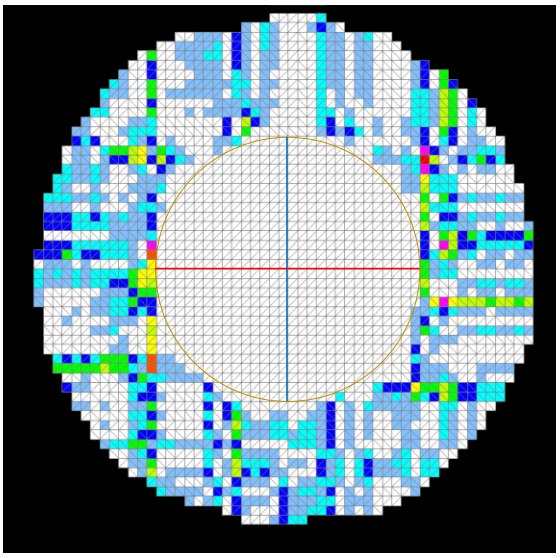

(e-2) Shear angles depicted to the plane for $n = 6$

Figure 4.10 Calculated shear angles for draped denim and those depicted on the initial flattened patterns for various node numbers (n)

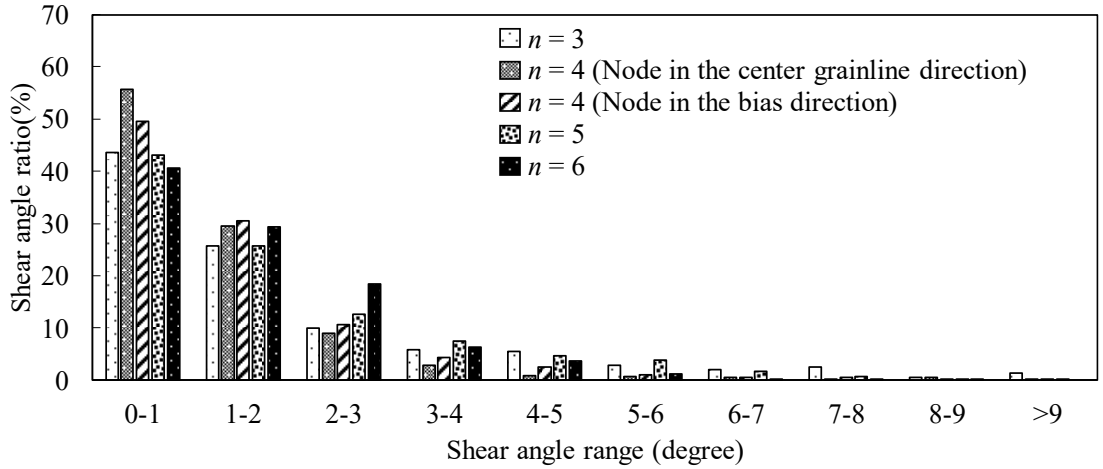

(a) Broadcloth

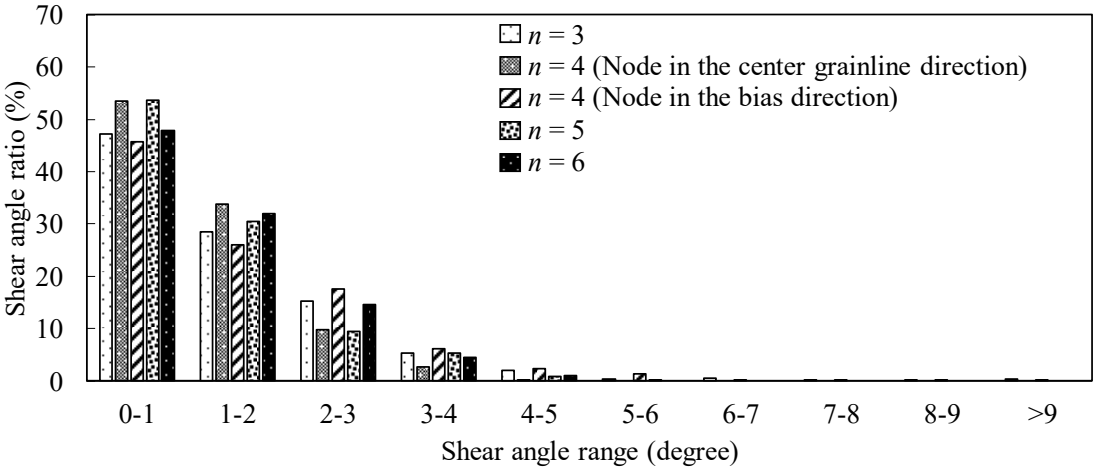

(b) Taffeta

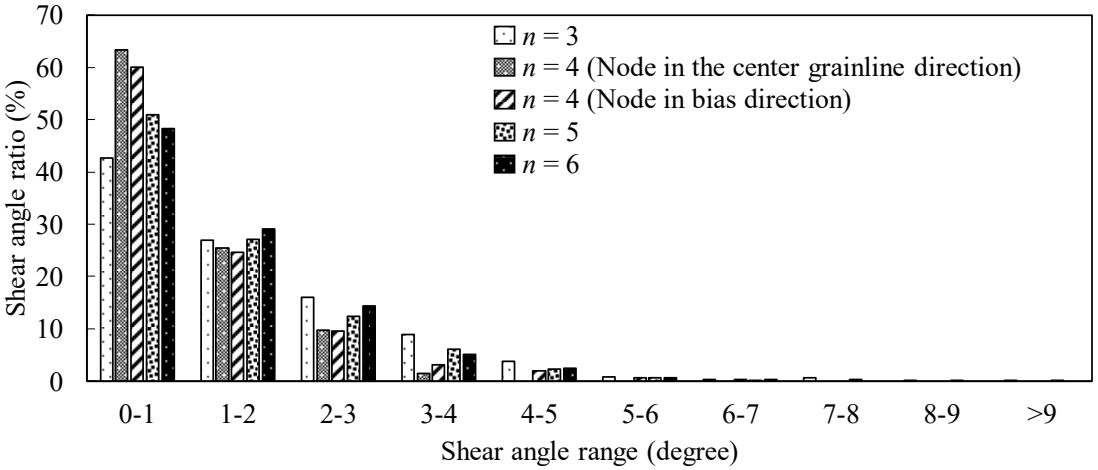

(c) Satin

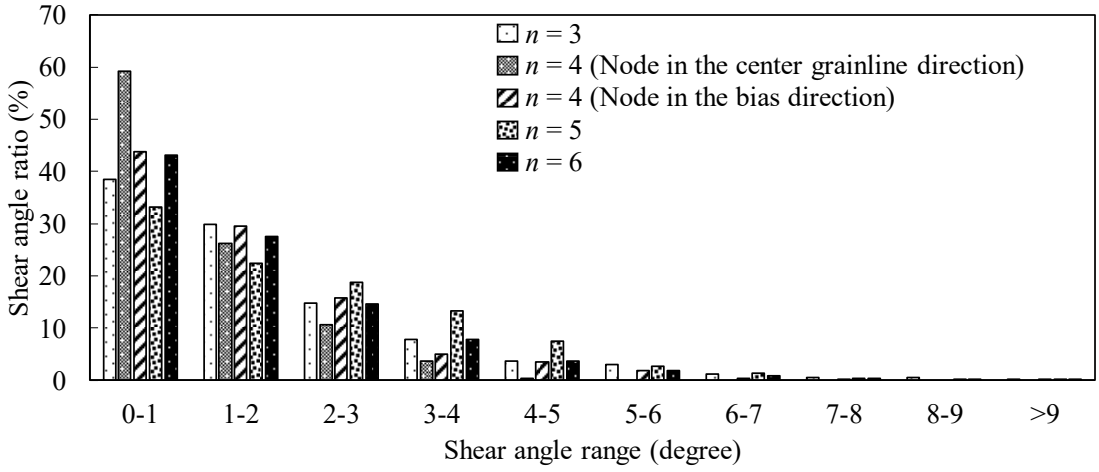

(d) Denim

Figure 4.11 Shear distributions for different samples

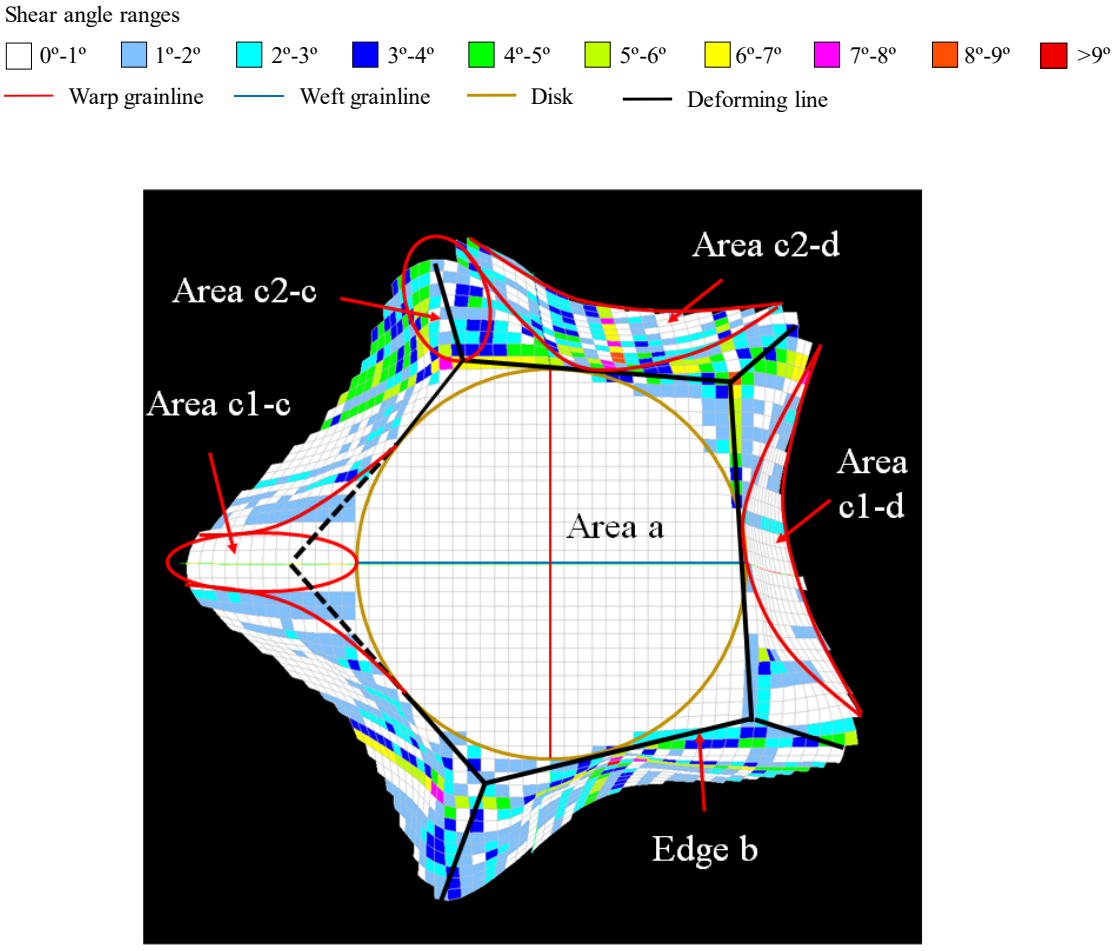

Figure 4.12 Areas for bending and shear deformation in drape

4.5.2 Effects of mechanical properties on local shear deformation

To clarify the relationship between shear deformation and mechanical properties, the relationships between the obtained shear angles, and bending rigidity and shear stiffness of fabrics were investigated. Yang et al. [34] and many researchers have shown that the mechanical parameter $(B/w)^{1/3}$ is a fundamental parameter related to the drape test. Niwa and Seto[5] added the mechanical parameter $(G/w)^{1/3}$ to investigate the relationship between the drape test and mechanical properties from the analogy of $(B/w)^{1/3}$. Thus, the relationships between the shear angle ratio for shear angle >3 º to $(G/w)^{1/3}$ in Figure 4.13, and to $(B/w)^{1/3}$ in Figure 4.14, respectively, were investigated. For G and B, the mean values of the shear stiffness and bending rigidity of the sample fabrics shown in Table 4.1 were used. The regression equations and corresponding coefficients of determination of the shear angle ratio for shear angle >3 º to $(G/w)^{1/3}$ and $(B/w)^{1/3}$ are shown in Table 4.2. Figure 4.13, for n = 3, 5, and 6, shows that the higher the shear stiffness, the lower the shear angle ratio for shear angle >3 º. This means that fabrics with high shear stiffness were less deformed by large shear angles. However, for n = 4, irrespective of the node positions and the center grainline direction, no apparent relationship between the shear angle ratio for shear angle >3 º and shear rigidity was observed. This is because drape shapes can be formed without large shear deformation and are less related to the shear stiffness. It could be more related to the bending rigidity. As shown in Figure 4.14, irrespective of n, the higher the bending rigidity, the lower the shear angle ratio for shear angle >3º. Therefore, it is clarified that local shear deformation in drape is affected by not only the shear stiffness, but also the bending rigidity.

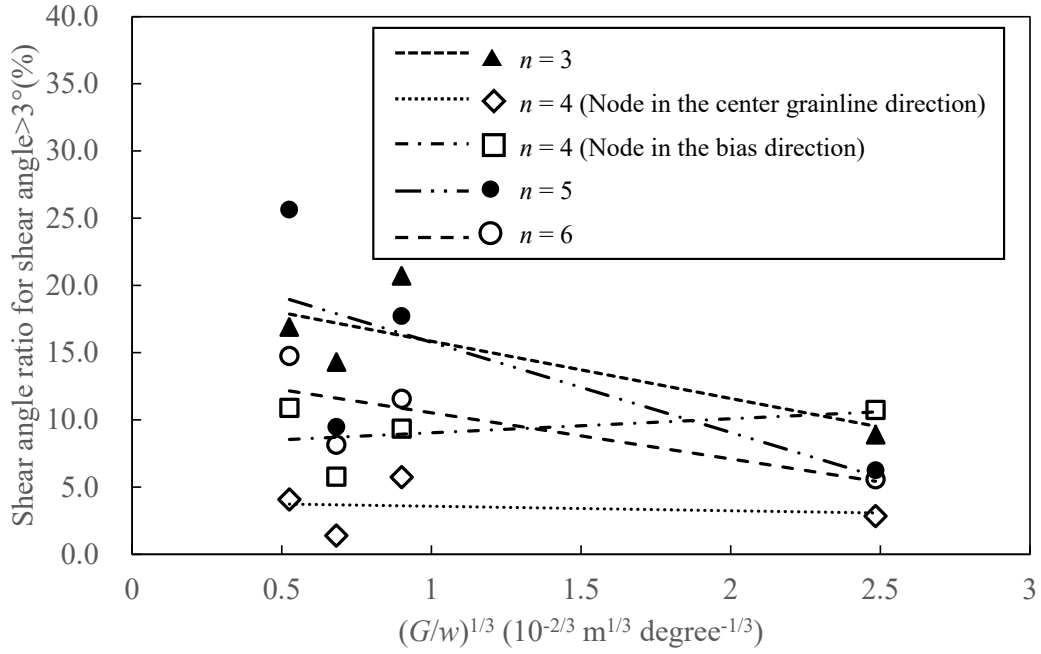

Figure 4.13 Relationships between the shear angle ratio for shear angle >3 º and $(G/w)^{1/3}$

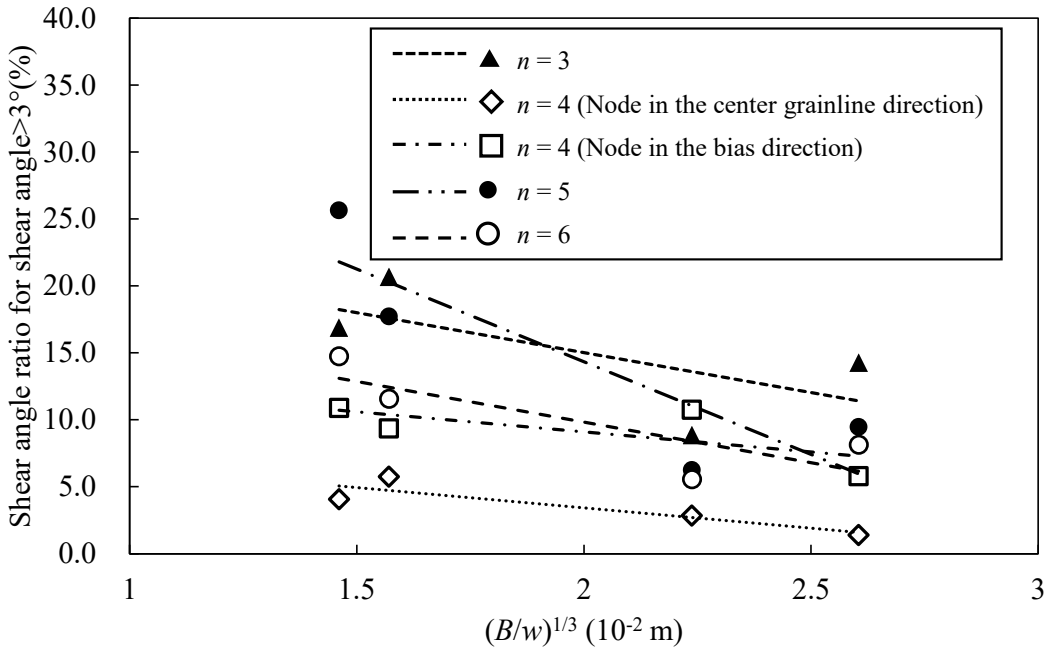

Figure 4.14 Relationships between the shear angle ratio for shear angle >3 º and $(B/w)^{1/3}$

Table 4.2 Regression equations and coefficients of determination for Shear angle ratio for shear angle >3 ºand mechanical parameters

Relationships / Number of nodes	Shear angle ratio for shear angle >3 º (y) and $(G/w)^{1/3}$ (x)		Shear angle ratio for shear angle >3 º (y) and $(B/w)^{1/3}$ (x)	
	Regression equation	Coefficient of determination	Regression equation	Coefficient of determination
n = 3	y = -4.26x + 20.10	0.60	y =-5.96x + 27.0	0.43
n = 4 (Node in the center grainline direction)	y = -0.334x + 3.90	0.027	y = -3.02x + 9.47	0.80
n = 4 (Node in the bias direction)	y = 1.05x + 8.00	0.16	y = -3.00x + 15.1	0.32
n = 5	y = -6.70x + 22.5	0.45	y = -13.8x + 42.0	0.75
n = 6	y = -3.43x + 14.0	0.60	y = -6.06x + 21.9	0.68

4.6 Conclusion

I investigated the relationship between the local shear angles in drapes, the node numbers, and mechanical properties of fabric by measuring the local shear angles in FRL drape tests for four different fabrics with three to six nodes using the proposed method. The findings are summarized below:

- Place and type of deformation in drape

FRL drape can be characterized by three areas, except for the flat areas of the support disks:

1) Areas along the center grainlines with zero or small shear angles within 3º, which could result from single curvature bending.

2) Areas along the bias directions with relatively large shear angles over 3º, which could result from double curvature bending.

3) Polygon edges connected with tangents of the support disk in the FRL drape test with a relatively larger shear angle than the surroundings, which could result from both bending and shear deformations, such as folding and wrinkles.

- Relationship between the shear angle and the node position relative to the center grainlines

Node areas along the center grainline had smaller shear angles than the nodes in the bias direction. Therefore, I found that local shear deformation in drape is affected by the relative position of the node to the center grainline of fabric, regardless of the node numbers.

- Relationship between shear deformation and mechanical properties

When n was 3, 5, and 6, the shear angles were related to both the shear stiffness and bending rigidity. Fabric with high shear stiffness and high bending rigidity form drape without large shear angles. However, when n was 4, the large shear angles occurred with small bending rigidity, regardless of the shear stiffness. Thus, the bending rigidity indirectly affects shear deformation in drape.

Consequently, using the proposed method, I successfully measured local shear deformation in FRL drape of woven fabrics, which has not been measured yet. I also clarified the effects of the node positions relative to the center grainlines, and the mechanical properties of fabric on local shear deformation. The advantage of the proposed method is that by tracing the loci of the two center grainlines, the shear deformation of the entire surface can be measured. The method provides a new means for analyzing the complicated deformation of woven fabrics. However, because the method is based on the assumption that fabric does not stretch along the yarn direction, for fabric that can stretch regardless of shear deformation, such as knitted fabric, the method cannot be applied.

The results of the present study deepen the understanding of the shear deformation of woven fabric in drape, by clarifying the relationship among local shear deformation, the node position relative to the center grainlines, and the mechanical properties of fabric in drape. These results will help to verify the simulation of woven fabric behavior considering shear deformation.

References

1. Chu CC, Cummings CL and Teixeira NA. Mechanics of elastic performance of textile materials: Part V: A study of the factors affecting the drape of fabrics—the development of a drape meter. *Textile Research Journal* 1950; 20: 539-548.

2. Chu CC, Platt MM and Hamburger WJ. Investigation of the factors affecting the drapeability of fabrics. *Textile Research Journal* 1960; 30: 66-67.

3. Cusick GE. 46—the Dependence of Fabric Drape on Bending and Shear Stiffness. *Journal of the Textile Institute Transactions* 1965; 56: T596-T606. DOI: 10.1080/19447026508662319.

4. Morooka H and Niwa M. Relation between drape coefficients and mechanical properties of fabrics. *Journal of the Textile Machinery Society of Japan* 1976; 22: 67-73.

5. Niwa M and Seto F. Relationship between Drapability and Mechanical Properties of Fabrics. *Sen'i Kikai Gakkaishi* 1986; 39: T161-T168.

6. Nagai S, Suda N and Inagaki K. Applicability of the Evaluation Method of Isotropic Sheets Drapability to That of Textile Fabrics. *J Jpn Res Assoc Text End-Uses* 2008; 49: 413-420.

7. Hearle JWS, Grosberg P and Backer S. *Structural mechanics of fibers, yarns, and fabrics Volume 1*. Wiley-Interscience, 1969.

8. Cusick GE. *A study of fabric drape*. The University of Manchester, Manchester, 1962.

9. Imaoka H, Okabe H, Tomiha T, et al. Prediction of three-dimensional shapes of garments from two-dimensional paper patterns. *Sen'i Gakkaishi* 1989; 45: 420-426.

10. Kang TJ and Yu WR. Drape Simulation of Woven Fabric by Using the Finite-element Method. *Journal of the Textile Institute* 1995; 86: 635-648. DOI: 10.1080/00405009508659040.

11. Teng J, Chen S and Hu J. A finite-volume method for deformation analysis of woven fabrics. *International Journal for Numerical Methods in Engineering* 1999; 46: 2061-2098.

12. Hu J, Chen S-F and Teng JG. Numerical Drape Behavior of Circular Fabric Sheets Over Circular Pedestals. *Textile Research Journal* 2000; 70: 593-603. DOI: 10.1177/004051750007000706.

13. Lafleur B, Magnenat-Thalmann N and Thalmann D. Cloth animation with self-collision detection. *Modeling in computer graphics*. Springer, 1991, pp.179-187.

14. Breen DE, House DH and Wozny MJ. A particle-based model for simulating the draping behavior of woven cloth. *Textile Research Journal* 1994; 64: 663-685.

15. Mitsui S, Komai D, Dai X, et al. Particle Model Reflecting Non-linearity and

Anisotropy of the Mechanical Properties of Cloth and Its Collision and Repulsion Mechanism. *The Journal of the Institute of Image Information and Television Engineers* 2000; 54: 1762-1770. DOI: 10.3169/itej.54.1762.

16. Dai X, Furukawa T, Mitsui S, et al. Drape formation based on geometric constraints and its application to skirt modelling. *International Journal of Clothing Science and Technology* 2001; 13: 23-37. DOI: 10.1108/09556220110384842.

17. Dai X, Li Y and Zhang X. Simulating anisotropic woven fabric deformation with a new particle model. *Textile research journal* 2003; 73: 1091-1099.

18. Mack C and Taylor H. 39—the fitting of woven cloth to surfaces. *Journal of the Textile institute Transactions* 1956; 47: T477-T488.

19. Shinohara A and Uchida S. The Surface Fitness of Textile Fabrics. *Journal of the Textile Machinery Society of Japan - Transactions* - 1966; 19: T17-T23. DOI: 10.4188/transjtmsj1965b.19.T17.

20. Moriguchi S and Sato K. Nunoji No Kikagaku (Geometry of Fabrics). *Suugaku Seminaa* 1972; 8: 55-59.

21. Heisey F, Brown P and Johnson RF. Three-Dimensional Pattern Drafting:Part I : Projection. *Textile Research Journal* 1990; 60: 690-696. DOI: 10.1177/004051759006001110.

22. Heisey F, Brown P and Johnson RF. Three-Dimensional Pattern Drafting:Part II: Garment Modeling. *Textile Research Journal* 1990; 60: 731-737. DOI: 10.1177/004051759006001206.

23. Van Der Weeën F. Algorithms for draping fabrics on doubly-curved surfaces. *International journal for numerical methods in engineering* 1991; 31: 1415-1426.

24. Potluri P, Sharma S and Ramgulam R. Comprehensive drape modelling for moulding 3D textile preforms. *Composites Part A: Applied science and manufacturing* 2001; 32: 1415-1424.

25. Vanclooster K, Lomov SV and Verpoest I. Experimental validation of forming simulations of fabric reinforced polymers using an unsymmetrical mould configuration. *Composites Part A: Applied Science and Manufacturing* 2009; 40: 530-539.

26. Cho Y, Komatsu T, Inui S, et al. Individual Pattern Making Using Computerized Draping Method for Clothing. *Textile Research Journal* 2006; 76: 646-654. DOI: 10.1177/0040517506066966.

27. Mohammed U, Lekakou C and Bader M. Experimental studies and analysis of the draping of woven fabrics. *Composites Part A: Applied science and manufacturing* 2000; 31: 1409-1420.

28. Kim K, Suzuki T and Takatera M. Measurements and prediction of fabric surface fitting ability under low tension. *Textile Research Journal* 2018; 88: 1413-1425. DOI: 10.1177/0040517517700201.

29. May-Plumlee T, Eischen J, Kenkare N, et al. Evaluating 3D Drape Simulations: Methods and Metrics. In: *International Textile Design and Engineering Conference (INTEDEC)* 2003.

30. Kenkare N, Lamar TAM, Pandurangan P, et al. Enhancing accuracy of drape simulation. Part I: Investigation of drape variability via 3D scanning. *Journal of the Textile Institute* 2008; 99: 211-218. DOI: 10.1080/00405000701489222.

31. Pandurangan P, Eischen J, Kenkare N, et al. Enhancing accuracy of drape simulation. Part II: Optimized drape simulation using industry-specific software. *Journal of the Textile Institute* 2008; 99: 219-226. DOI: 10.1080/00405000701489198.

32. Yang L, Kim K and Takatera M. Measurement of Fabric Shear in Drape Using Three-dimensional Scanning. In: *Textile Bioengineering and Informatics Symposium* Suzhou, China, 8-11 September 2019, pp.303-309. TBIS.

33. Bigliani R and Eischen JW. Collision Detection in Cloth Modeling. In: House; DH and Breen DE (eds) *Cloth Modeling and Animation*. Wellesiey, USA: A. K. Peters, Ltd, 2000, pp.199-205.

34. Yang L, Kim K and Takatera M. Effect of the fabric dimension on limits of the drape coefficient. *Textile Research Journal* 2020; 90: 442-459. DOI: 10.1177/0040517519868175.

35. Artec Studio 9 User's Guide / Manual, http://builds.artec-group.com/users_guide/Manual-9.2.0-EN.pdf (accessed April 2 2020).

Chapter 5

Conclusion

Chapter 5 Conclusion

Geometrical effects caused by fabric dimension and mechanical issues of bending and shear deformation on drape have been discussed in the presented study.

To clarify the geometrical effects, fabric drapes under various conditions of fabric and support disk radii were numerically analyzed considering the bending rigidity for infinite and zero shear stiffness. In the theoretical upper-limit calculation of infinite shear stiffness, unlike traditional method using a strip cantilever, a segment cantilever was used in this study. In the theoretical lower-limit calculation of zero shear stiffness, strip cantilevers of equal length in all radial directions were used. The two theoretical limits were verified with eight kinds of woven fabrics and one sheet, with different combination of fabric radii and disk radii. It is found that the DCs of samples are between the two theoretical limits although there are variations for even the same K or K'. The variations might be due to depressions between adjacent nodes or the presence of double-curvature deformation due to lower shear stiffness. The effects of dimensions in the drape test considering bending rigidity for infinite and zero shear stiffness are thus clarified theoretically and experimentally.

To investigate the local shear deformation in drape, by measuring the local shear angles, the relationship between the local shear angles and the node numbers and the mechanical was clarified. It is found that the FRL drape can be characterized by three areas, except for the flat areas of the support disks: 1) areas along the center grainlines with zero or small shear angles within 3º, which could result from single curvature bending, 2) areas in the bias directions with relatively large shear angles over 3º, which could result from double curvature bending, and 3) polygon edges connected by tangents of the support disk with relatively larger shear angles than their surroundings, which could result from both bending and shear deformation, such as folding and wrinkles.

By investigating the relationships between areas with large shear angles and the bending rigidity/shear stiffness, it is also clarified that the bending rigidity indirectly affects the local shear deformation of drape has been clarified.

This study demonstrated the geometrical and mechanical effects on drape, which had not been clarified until now. The results could be helpful for drape simulation in both views of the drape shape and deformation of fabrics.

In future studies, it could be interesting to develop a numerical model for drape prediction with parameters not only the bending rigidity but also the shear stiffness under the conditions of various fabric lengths. This study also shows a research interest to compare the deformation between simulation and actual fabric or garment, which could lead to the improvement for a more accurate apparel simulation system.

Published papers

This dissertation is based on the following papers:

1. Yang Liu, Kim KyoungOk and Takatera Masayuki. Effect of the fabric dimension on limits of the drape coefficient. Textile Research Journal 2020; 90(3-4): 442-459.

2. Yang Liu, Kim KyoungOk and Takatera Masayuki. Measurement of Local Shear Deformation in Fabric Drape Using Three-dimensional Scanning. Textile Research Journal. Epub ahead of print October 12, 2020. DOI: 10.1177/0040517520963347.

Acknowledgements

It has been ten years since I started my study at university: four years for undergraduate education at Donghua University and six years for graduate study at Shinshu University. Ten years ago, with a good yearning for university life, I stepped into the door of the university. At that time, I never thought that I would stay on the academic path for such a long time.

I am very grateful to myself for making the decision to study in Japan and grateful to the people who have taken good care of me over the decade, Loudi-Shanghai-Tokyo-Ueda-World. After seeing this vast world, I nowadays have grown from a teenager who only knew to solve questions of the gaokao to a person who understands the knowledge of textile/clothing/information technology and masters three foreign languages.

Among all the people who helped me in my Ph.D. study, firstly, I would like to express my deep respect and special thanks to my supervisor Prof. Masayuki Takatera, and Assoc. Prof. KyoungOk Kim. They provided me the golden opportunity to conduct the project. They shared their pearls of wisdom with me and gave me generous support and guidance to accomplish my dissertation. Especially for Prof. Takatera, not only as a supervisor, but he is also a great mentor on the road of my life. It is no exaggeration to say he could be my father in Japan.

I owe my deep gratitude to the rest of my thesis committee: Prof. Shigeru Inui, Prof. Limin Bao (Shinshu University), Prof. Sachiko Sukigara (Kyoto Institute of Technology), and Prof. Jintu Fan (The Hong Kong Polytechnic University) for their insightful comments and advice. Thanks to Dr. Xiaogang Chen (The University of Manchester) for accepting me as a visiting student to study at UoM. During my visiting time, he taught me the knowledge about the Finite Element Method, shared his precious opinion on my study, and led me to experience the culture of the UK.

I am thankful for and fortunate enough to receive support in the form of a Grant-in-Aid for the Shinshu University Advanced Leading Graduate Program from the Ministry of Education, Culture, Sports, Science, and Technology (MEXT), Japan, which helped me

complete my study and work. I extend my sincere thanks to all staff of the Advanced Leading Graduate Program of Shinshu University for their constant encouragement and support.

I will not forget my colleagues at Takatera and Kim Laboratory and my friends, for their generous assistance and warm encouragement in every aspect of my life.

Special thanks to Dr. Tsuyoshi Otani for giving me a strict direction to train my business mind and sharing his opinion on fashion engineering with me, which is very helpful for me to start my new life in the coming future.

To finish, I express my greatest gratitude to my beloved family for their understanding and generous support, without which it would be impossible for me to study in Japan. Unfortunately, my beloved grandfather could not witness the completion of my Ph.D. study. But I believe that he should be happy in heaven for my achievements today.

Thanks to the past decade, and now I am ready to meet the next decade. All achievements remain in the past, tomorrow is another day.

Liu Yang

2020.12.15